SPATIAL AND TEMPORAL VARIATIONS OF WATER AND NUTRIENT FLUXES WITHIN A STEEP-SLOPED AGRICULTURAL CATCHMENT

CM Orchard

Submitted in fulfilment of the requirements
for the degree of Master of Science

Supervisor: Professor V Chaplot

School of Bioresources Engineering and Environmental Hydrology
University of KwaZulu-Natal
Pietermaritzburg
March 2012

ABSTRACT

A proper understanding of the spatial and temporal variations of runoff and nutrient fluxes are critical in understanding catchment hydrology. Runoff and nutrient fluxes may exhibit large variations both spatially and temporally, but this issue has largely been overlooked in the existing literature. The present study intends to respond to two main research objectives: (a) improve the understanding of the spatial and temporal variations (*i.e.* the dynamics) of overland flow (OF) and its factors of control and (b) quantify the evolution of runoff, nutrient and sediment fluxes from hillslope crest to catchment outlet.

The research study was undertaken in a 1000 ha agricultural catchment of the Drakensberg foothills in the Bergville District, KwaZulu-Natal, South Africa under rangeland, small scale agriculture and commercial agriculture. The first objective was to evaluate the dynamics of OF during four rainfall seasons (2007 to 2011) by using 1×1m² microplots (n=15) located at five landscape positions within the rangeland upper part of the catchment. Automatic tipping buckets linked to a datalogger were used to estimate the delay between the start of the rain and the start of OF, which corresponded to the time of runoff initiation (TRI). Multivariate analysis was applied to the OF data and the information on selected environmental factors (rainfall characteristics, selected soil physical properties, soil water content and soil surface conditions). Nested scales of 1 and 10 m^2 plots, and 23, 100 and 1000 ha catchments equipped with buckets for plots and conventional H-flumes for catchments, were used to quantify the downstream evolution of water and nutrient (C, NO_3^- and P) fluxes. The fluxes were compared with data from the shallow and deep groundwater (GW) collected from piezometers and boreholes, respectively. This allowed for the determination of the mixing sources at the three catchment outlets, using stable isotopes of water (to differentiate between old and new water) and silica concentrations to identify soil water (SW) contributions.

The average OF rate varied 2.3-fold across the Potshini Catchment (from 15% footslope to 35% backslope), while the average TRI varied by a 10.6-fold factor (between 0.6 minutes in the bottomland and 6.4 minutes at the footslope position). TRI temporal variations correlated the most with the duration of rainfall (Pearson *r* coefficient of 0.8) and the cumulative amount of rainfall after the onset of the rainy season (r=-0.47), while TRI spatial variations were significantly controlled by soil crusting (-0.97<r<-0.77). Water fluxes were found to increase

from the microplot scale (208 l/m^2) to the runoff plot scale (350 l/m^2, delivery ratio of 1.68). The scale ratios calculated for the period of 2010-2011 show that there was a steady decrease in the delivery of water from the hillslope scale to the catchment scale. Cumulative water fluxes were found to be 316 l/m^2 at the 23 ha catchment and 284 l/m^2 at the 100 ha catchment (delivery ratios of 0.90 and 0.89 respectively). Water fluxes decreased sharply to 198 l/m^2 at the 1000 ha catchment outlets (delivery ratio of 0.70). Runoff at the 23 ha catchment outlet was sourced from the mixing of GW (average of 63%), OF (22%) and SW (15%.) At the 100 ha outlet, GW contributions decreased to 50%, while OF contributions remained constant at 22% and SW contributions increased to 28%. The main contributor at the 1000 ha catchment was GW (55%) followed by SW (37%) and OF (8%). During the strongest rainfall event of the study period, OF contributed 97% to total runoff at the 23 ha catchment outlet, whilst at the 100 ha catchment, OF and SW both contributed 50% each. Groundwater in all cases was the major contributor to runoff at the 1000 ha catchment outlet. Both dissolved organic Carbon (DOC) and particulate organic Carbon (POC) increased from the microplot (8.44 and 25.51 g/m^2 for DOC and POC) to the plot scale (14.92 and 26.91 g/m^2). Lower yields occurred at the 23 ha catchment than on the hillslope (5.03 g/m^2 and 8.18 g/m^2). From the 23 and 100 ha catchment outlets, POC sharply decreased to 0.06 g/m^2, while DOC increased considerably to 9.58 g/m^2. This pointed to the decomposition of POC, which not only releases CO_2 to the atmosphere but also adds DOC to runoff. At the 1000 ha catchment, POC yields were minimal due to a lack of eroded sediments whilst DOC decreased slightly (6.42 g/m^2). These results yield a better understanding of the processes of water, nutrient and Carbon movements within landscapes.

A further understanding of the processes leading to changes of nutrient and carbon fluxes needs to be performed in order to link this study with the overall ecosystem functioning of a landscape.

ACKNOWLEDGEMENTS

I would like to express my gratitude to the following individuals who have all contributed in the compilation of this thesis. Your contributions are greatly appreciated.

My Supervisor, Professor Vincent Chaplot, and Co-Supervisor, Professor Simon Lorentz, for their continued guidance and support throughout the research process. I have learnt a great deal and have grown individually under such expert tutelage.

Thanks must be extended to the Water Research Commission (WRC), the former School of Bioresources and Environmental Engineering (BEEH) and the Institut de Recherche pour le Développement (IRD) for funding and allowing the research undertaken in this thesis.

Professor Graham Jewitt for his comments and corrections on the earlier versions of the document.

Mr. Cobus Pretorius and Mr. Jean-Louis Janeau for technical assistance when conducting field and laboratory work.

Mrs. Sharon Rees for her assistance in proof-reading and grammar corrections, as part of compiling this dissertation.

The Potshini Community for allowing this research to be performed on their land. Their hospitality is greatly appreciated.

PREFACE

The work described in this dissertation was carried out in the School of Bioresources Engineering and Environmental Hydrology, University of KwaZulu-Natal, Pietermaritzburg, from January 2009 to December 2011, under the supervision of Professor V. Chaplot.

This study represents original work by the author and has not otherwise been submitted in any form for any degree or diploma to any tertiary institution. Where use has been made of the work of others, it has been duly acknowledged in the text.

Author: Mr. C.M. Orchard Date

Supervisor: Prof. V.A.M Chaplot Date

PLAGIARISM DECLARATION

I, …….....…… declare that

1. The research reported in this dissertation, except where otherwise indicated, is my original work.
2. This dissertation has not been submitted for any degree or examination at any other university.
3. This dissertation does not contain other persons' data, pictures, graphs or other information, unless specifically acknowledged as being sourced from other persons.
4. This dissertation does not contain other persons' writing, unless specifically acknowledged as being sourced from other researchers. Where other written sources have been quoted, then:
    a. Their words have been re-written but the general information attributed to them has been referenced.
    b. Where their exact words have been used, then their writing has been placed in italics and inside quotation marks, and referenced.
5. This thesis does not contain text, graphics or tables copied and pasted from the internet, unless specifically acknowledged, and the source being detailed in the dissertation and References sections.

Signed: ……..

TABLE OF CONTENTS

LIST OF FIGURES

LIST OF TABLES

1. INTRODUCTION

1.1 Spatial and Temporal Variations of Overland Flow

Understanding spatial and temporal variations of water and nutrient fluxes in landscapes is essential for improved land management. In the past few decades, many experimental studies have been conducted to better understand rainfall-runoff processes. Although, there have been many hydrologic studies performed worldwide for improved understanding of hydrologic processes, there is still a need to develop methods to characterise runoff generation mechanisms occurring over hillslopes. This will ultimately lead to a better understanding of the way in which a catchment generates flow and how this impacts on the transport of nutrients and sediments.

Classically, there are two mechanisms describing overland flow generation (Horton, 1933; Hewlett and Hibbert, 1967):

a) Hortonian flow (generated when rainfall intensity exceeds infiltration capacity of the soil);
b) Saturation excess surface runoff (generated when the perched water table rises, saturating the whole soil profile and ultimately creating a seepage face at the soil surface).

Whilst these mechanisms have been used to classify overland flow generation throughout the world, there is still a lack of knowledge in terms of the spatial and temporal variations of overland flow and its factors of control (Sen *et al.*, 2010; Van de Giesen *et al.*, 2011). It is this gap that this thesis seeks to address.

Surface areas within a catchment respond differently to rainfall and it cannot be assumed that overland flow generated within a landscape is uniform. Overland flow generation is a highly non-uniform and spatially-variable process compounded by a large degree of temporal variation (Bergkamp, 1998; Cammeraat, 2001). The interaction between the static characteristics, such as topography, soil and land cover and dynamic characteristics, such as rainfall event characteristics, soil surface conditions, antecedent soil moisture conditions,

infiltration rates, soil hydraulic properties and the depth to water table, all affect the overland flow generated within a catchment (Casenave and Valentin, 1992; Hernandez *et al*., 2003).

This complex interaction between many controlling factors has been the subject of many research studies. Williams and Bonell (1988), in tropical Australia, found that soil infiltration and surface storage were highly spatially variable. Joel *et al.* (2002) found that the overland flow was generated as a result of several interrelated factors, such as soil hydraulic conductivity, surface depressions, initial soil water content, slope length, crack development and crusts and seal formation on the soil surface. These factors that affect the generation of overland flow vary spatially *e.g.* Hortonian flow occurs when the rainfall intensity is greater than the infiltration rate of the soil. In contrast, saturation excess overland flow occurs typically in areas where saturation occurs (*i.e.* bottomlands and seepage faces) (Sen, 2009; Van de Giesen *et al.*, 2011).

As a result, overland flow will vary spatially. In a study conducted in north-eastern Tunisia (Mekki *et al.*, 2006), found that overland flow varied spatially within a catchment largely as a result of the spatial variations of the soil surface conditions that occurred within the catchment. The spatial variations of overland flow have been found in many other studies conducted throughout the world. Of particular interest was the work of Mekki *et al.* (2006) who found that overland flow had large spatial and temporal variations.

Overland flow is likely to change with increasing area, resulting in a scaling effect. This scaling effect has been found to be significant. In the study of plots of different lengths in West Africa (Côte d'Ivoire, Ghana, and Burkina Faso), van de Giesen *et al*. (2011) showed that longer plots had much lower annual runoff than shorter ones. Furthermore, the scale effect for overland flow was shown to be highly varied in time as due to rainfall conditions. This strongly suggests that overland flow does have a high degree of spatial and temporal variations. However, the literature, has so far, not given reasons for such variations in overland flow.

Overland flow occurs when rainfall is partitioned at the soil surface into either soil infiltration or overland flow. Consequently, it is important to investigate the soil surface characteristics (environmental factors) which control the generation of overland flow. In four different studies, which investigated the effect of soil surface characteristics on overland flow

generation, it was found that an increase in groundcover was found to enhance infiltration and ultimately decrease the amount of overland flow generated (Bartley *et al*., 2006; Bautista *et al*., 2007; Sanjari *et al*., 2009; Podwojewski *et al*., 2011). Results from a study conducted in New South Wales, Australia, support this as a multi-factored model was derived, incorporating rainfall, maximum rainfall intensity and the percentage of the soil surface covered by vegetation, which explained 41% of overland flow depth (Murphy *et al*., 2004). Such behaviour and response will largely be caused by the increase in organic matter found in the soil surface, which decreases the soil bulk density. The decrease in bulk density will result in a greater amount of infiltration occurring. Soil surface coverage by vegetation has been found to have an inverse relationship, with the generation of overland flow. Sanjari *et al*. (2009) stressed that the linkages between the soil surface characteristics and the generation of overland flow is a multi-factor relationship. This multi-factor relationship is between the different overland flow generation mechanisms and a catchment's physical characteristics. Bergkamp (1998) states that effective infiltration rates on grassland hillslopes vary with rainfall intensity and flow depth, due to the interaction between rainfall, runoff, and vegetated micro-topography. Environmental factors vary both in time and space and, as such, they will affect the spatial and temporal variations of overland flow generation.

Soil surface crusting has been found to play a leading role in the volumes of overland flow generated. Soil surface crusts cause a decrease in infiltration and promote overland flow (Bautista *et al*., 2007). In a study conducted in the Potshini Catchment, South Africa, under an artificial rainfall simulation, Podwojewski *et al.* (2011) found that crusting was linked to the rate at which overland flow was generated. It was found that infiltration was controlled by soil surface crusting (Podwojewski *et al.*, 2011). Furthermore, the initial infiltration rate was found to vary due to the spatial variations of the soil surface crusts. The final infiltration rates of the study site were not found to have as high values as the initial infiltration rate. The initial infiltration can be viewed as an important factor on the temporal scale response of a spatially heterogeneous catchment. In addition, using studies from semi-arid and arid Africa, Casenave and Valentin (1992) indicated that surface crusts significantly decreased water infiltration in soils. From the nine main types of soil surface crusts they identified only three types of soil surface crusts: (a) structural (rough surface made of coalescing partially slaked aggregates), (b) erosion (smooth surface made of a single seal of fine cemented particles) and (c) sedimentary (laminated with layers of different texture) within their study site. This can be

further investigated in a study focussing on the spatial and temporal variations of overland flow under natural rainfall conditions and the controlling factors of overland flow generation.

1.2 Runoff Connectivity at the Catchment Scale

The studies and literature listed above investigated the spatial and temporal variations of water and nutrient fluxes from the plot to the hillslope scale. While much research has been done at the hillslope scale, the changes in fluxes at the catchment level (i.e. hydrological connectivity) (Bracken and Croke, 2007) and their factors of control have received less attention.

Hydrological connectivity has had a great deal of research conducted on it throughout the world (McGlynn *et al.*, 2002; McGlynn *et al.*, 2003; McGlynn and McDonnell, 2003a; McGlynn and McDonnell, 2003b; McNamara *et al.*, 2005; Ocampo *et al.*, 2006; Latron and Gallart, 2008; Wenninger *et al*., 2008; James and Roulet, 2009; McGuire and McDonnell; 2010; Chaplot and Poesen, 2012). Hydrological connectivity has been described as the movement of water from one part of a catchment to another, which results in runoff being generated (Bracken and Croke, 2007). Hydrological connectivity is inextricably linked to landscape connectivity, as the landscape plays an important role in the generation of runoff within the catchment. Hydrological connectivity has been found to be controlled by the interaction of many factors and occurs over all scales (Bracken and Croke, 2007).

In a study in the area of Dartmoor, United Kingdom, Meyles *et al.* (2003) and Meyles *et al.* (2006), used a nested scale approach to investigate the impact of grazing on hydrological processes. They found that the runoff response of the catchment was linked to the soil moisture conditions of the catchment. An interesting finding was that the catchment was found to have two behaviours depending on the state of wetness of the catchment. Similar results were found by several different studies from throughout the world. In a similar study, Sidle *et al.* (1995) found that, with an increase in the antecedent precipitation index (API) the soils increased in water content and the hillslopes studied started to contribute to catchment flow.

In another study, conducted by Detty and McGuire (2010) in New Hampshire State, USA, insights into hydrological connectivity was achieved by monitoring the groundwater

fluctuations within the catchment in relation to catchment response. This was achieved by, using piezometers and soil moisture variations along the hillslope (use of soil moisture sensors). The hillslope was found to be hydrologically connected to the riparian area when soil saturation occurred.

Furthermore, Detty and McGuire (2010) found that the bottom portion of the hillslope (the Footslope) consistently contributed to flow during the wet season. The threshold amount of soil water required for runoff to be generated was found to be 315 mm. Related to this is a study conducted by Hopp and McDonnell (2009), in which virtual experiments were used to better understand the hydrological connectivity at the hillslope scale in a catchment located close to Atlanta, Georgia. Simulations of the model found that at the hillslope scale, hydrological connectivity was controlled by soil characteristics such as texture and depth, the amount of water stored in fractured bedrock and the topography of the hillslope. Similar results were found in many studies where catchment connectivity was found to be controlled by the integration of soil macropores, fractured bedrock, topography of the hillslope and the temporal variations in the dynamic behaviour of the groundwater (Ocampo *et al.*, 2006; Iwagami *et al*., 2010; Fujimoto *et al*., 2011).

The storage of water within the catchment bedrock was found to be a major controlling factor of catchment connectivity. McGlynn *et al.* (2002) showed that the bedrock water plays an important role, the stored water being displaced by new rain water. The role of the catchment antecedent moisture conditions were found to be significant. Subsurface runoff response increased as macropore flow and soil saturation increased. Subsurface flow was found to have occurred when the percentage of soil saturation was at 95 percent in Georgia, USA (Hopp and McDonnell, 2009). Cerdan *et al.* (2004) found that the rainfall required for runoff to be generated within a catchment was three times greater than the amount of rainfall which resulted in overland flow being generated at the plot scale. Similar results were found by Cammeraat (2004) in a study conducted in the southeast part of Spain. It was found that from the plot scale to the catchment scale, the amount of rainfall required to generate runoff increased (with an event average of 20mm for catchment scale versus 10mm for plot scale). The finding that the amount of runoff producing rainfall events was found to be higher at the plot scale than at the catchment scale was particularly interesting (Cammeraat, 2004). In a study conducted by McGlynn and McDonnell (2003b), in which stable isotopes were used to perform hydrograph separations to quantify the relative contributions from the hillslope and

riparian areas to catchment runoff in the MaiMai Catchment. It was found that the hillslope response was related to the storm duration and amount. For a rainfall event of 27 mm (a small event for the study area), it was calculated that the hillslope contributed between 2 and 16 percent of the catchment runoff (McGlynn and McDonnell, 2003b). For a large event (70mm), it was determined that the hillslope generated flow contributed between 47 to 55 percent of the measured catchment runoff for selected events (McGlynn and McDonnell, 2003b). This points to a catchment wetting up and reducing the soil moisture deficit before runoff is generated and measured within a stream channel. A reason for this is the establishment of a shallow groundwater table within a hillslope during rainfall events (Sidle *et al.*, 1995; Ocampo *et al.*, 2006; Latron and Gallart, 2008). These examples emphasise the role that the antecedent moisture condition plays in the hydrological connectivity of a catchment.

Generally for hydrological connectivity to occur, the antecedent moisture condition of a catchment needs to be high. When a catchment is dry, it can be assumed that there will be little to no hydrological connectivity. Any runoff generated during dry periods will be overland flow in areas where infiltration is limited. Such hydrological responses within a catchment have high spatial variations (Cammeraat, 2004).

In support of this is a study conducted by Li *et al.* (2008) who used a rainfall simulation in the Tengger Desert, China, to investigate the effect that the linkages between crusted areas and vegetated areas along a hillslope have on runoff, sedimentation and specific nutrient losses. It was found that, on crusted areas, 53 percent of rainfall was converted to overland flow. However, the spatial arrangement of crusts in relation to the vegetation patches was found to be important, as vegetation patches were found to be a sink for infiltration and deposition along the slope (Li *et al.*, 2008). The decrease in crusted areas along the slope was found to decrease the amount of connectivity along the slope, which ultimately decreased the amount of sediments and nutrients lost from the system (Li *et al.*, 2008). Related to this is a study conducted by Bergkamp (1998) in southeast Spain, where a nested scale approach in connection with a rainfall simulation experiment was used to understand the generation of runoff, specifically overland flow, and how it was affected by selected environmental factors. It was found that the spatial distribution and arrangement of vegetation and soil surface characteristics was key to the hydrological connectivity between fine scales, such as plots and the broader scales (hillslope and catchment) (Bergkamp, 1998). Bergkamp (1998) stressed that the runoff response of a catchment cannot be directly related to the overland flow

generated on the slopes. However, one cannot solely look at one particular portion of a catchment, as a catchment is a complex system and not a sum of its individual fields (Cerdan *et al.*, 2004).

For hydrological connectivity to occur at the catchment scale, there needs to be an intense storm and or a storm of long duration (Sidle *et al*., 1995; McGlynn *et al.* 2004; Bracken and Croke, 2007; Detty and McGuire, 2010). In contrast to this, at the hillslope scale the rainfall event can be of a short duration for connectivity to occur. At the hillslope scale and during dry periods, it has been found by many authors that the response of a catchment is patchy with any runoff response being found to be localised (Jencso *et al.*, 2009; Detty and McGuire 2010). Van de Giesen *et al.* (2005) found that the decrease in slope length resulted in the increase in runoff generated per unit area.

The presence of dams within a catchment can result in the hydrological connectivity of a catchment being reduced (Bracken and Croke, 2007). Overland flow generated on hillslopes will only be directly connected to a stream if (1) the mechanism which generated the overland flow was saturation excess in an area which is directly connected to a stream and (2) overland flow generated in areas which are severely degraded such as animal or foot pathways which direct water towards the stream. Therefore, the spatial arrangement of the factors of control within a catchment is key for hydrological connectivity to occur.

The scale at which hydrological processes occur is often a major driver of any hydrological study. In a study conducted in the Loam belt of Northern France, Cerdan *et al.* (2004) monitored the difference in the hydrological responses of a catchment from the plot scale to the catchment scale. The land use and soils of the study area were similar with the difference in hydrological response between the different scales being investigated. Cerdan *et al.* (2004) found that there was a decrease in the amount of runoff generated from the plot scale to the catchment scale (19.95% for plots, compared to 0.49% for a 1100 ha catchment). This shows that different processes occur at different scales (Zehe and Bloschl, 2004). This ultimately results in there being a large degree of uncertainty and variability in any predictions relating to the hydrology of an area. Zehe and Bloschl (2004) stress that “there will always be a smaller-scale component of hydrologic variability”. This largely relates to the fact that the environment will have a large degree of small-scale variations.

Increased hydrologic connectivity has an impact on the transport and loss of nutrients from a catchment (Jencso *et al.*, 2009). In an integrated study looking at hydrological connectivity and the export dynamics of dissolved organic carbon (DOC) in the MaiMai Catchment in New Zealand, McGlynn and McDonnell (2003a) found that there was a flushing of DOC during rainfall events. Subsequently, it was found that the DOC concentration at the outlet of a catchment was similar in concentration to the hillslope which was the major contributor to catchment runoff. It was found that the DOC concentration in the groundwater of the MaiMai Catchment was four times lower than the event water generated in the hillslopes (McGlynn and McDonnell, 2003a). This indicated that the export of DOC happened within soil macropores and that soil organic carbon was easily dissolvable or that DOC was easily transportable, once hydrological connectivity has been established. It was found that the export of DOC was controlled by the physical characteristics of the catchment.

Catchment scale observations supported by hillslope observations of internal hydrological and nutrient state variables have made significant advances in monitoring nutrient losses at the catchment scale (Ocampo *et al.*, 2006). Ocampo *et al.* (2006) further stress that the hydrological processes occurring within a landscape need to be investigated to better understand the link between nutrient losses and the movement of water. Consequently, the hydrological connectivity of a catchment will impact upon the transfer of nitrates which have been accumulating within the upland areas of the catchment. These nitrates will only be transported once the catchment has been wetted up and connectivity has been established throughout the whole catchment (Ocampo *et al.*, 2006).

A holistic monitoring scheme of hydrological processes, such as catchment runoff is required. Bloschl and Sivapalan (1995) suggested that scale should be viewed from one of two viewpoints: process scale (the operational scale of natural processes) and observation scale (the scale at which processes are observed). However, individual processes monitoring schemes require the understanding of the non-linearity of each individual process. To determine the response of a system to a rainfall event, the quantification of the system's hydrological and erosional behaviour is needed (Cammeraat, 2004) and this dictates the monitoring and sampling strategy. This integrates the various processes, which have different spatial and temporal scales of operation (Heathwaite and Johnes, 1996).

To overcome the issue of selecting the right scale and sampling strategy to determine the system's hydrological and erosional behaviour, it is advantageous to use nested scales within the catchment (Bergkamp, 1998; Cammeraat, 2004). The use of nested scales involves the use of point measurements (e.g. 1 m^2) through to catchment level (e.g. 23 ha catchment), sub-catchment (e.g. 100 has) and, finally, a first order catchment (e.g. 1000 has). At these nested scales, it is important to sample regularly and uniformly to integrate the various processes occurring within the system. The use of nested scales will generate more data and will ultimately result in the greater understanding of the runoff generation process (Bergkamp, 1998).

This literature review stresses the need for a better understanding of the spatial and temporal variations of overland flow and runoff connectivity within a catchment.

1.3 Research Objectives

The main objectives to be investigated in this study were:

a) To investigate the spatial and temporal variations of overland flow and its factors of control at the hillslope level;
b) To quantify the evolution of runoff, nutrient and sediment fluxes within a catchment.

To meet the first objective, a survey of the spatial and temporal variations of overland flow in a catchment was performed. Furthermore, the investigation related the spatial and temporal variations of the overland flow response to certain environmental factors found within the catchment. It was important to understand the environmental factors' spatial variations and how these affected overland flow generation. The first aim of this research was to determine and further understand the spatial and temporal variations of overland flow. To achieve this aim, runoff microplots installed at different locations along a typical hillslope catena were used. The hillslope was located within an agricultural catchment of which the main land use was livestock grazing. This methodology can be utilised to gain information on the spatial variations of overland flow and infiltration. Of particular importance was the determination of the variable, Time to Runoff Initiation (TRI), which was the delay of microplot response (soil surface response) with respect to a rainfall event. The TRI variable can give an indication of how the soil surface of a hillslope with varying soil surface conditions responded to a rainfall event.

The second objective of this study was to involve the observation of water, nutrient and sediment fluxes at different scales: (a) Spatially, from microplot, plot and catchment scales; and (b) temporally, from a rainfall event to inter and intra season variations. These will be complemented by observations of the soil water and groundwater dynamics within the catchment, as a way to better understand catchment hydrology. Associated with the generation of runoff within the catchment (the main aim of this study), is the water quality, specifically the organic carbon and sediment fluxes. An initial understanding of the factors of control on the hydrological connectivity was also attempted.

1.4 Aims of Overall Research Project

Numerous studies have looked at the impact of commercial agricultural areas on water, nutrient and sediment fluxes. The project aims to focus on the effects of rural smallholder agricultural areas on water, nutrient and sediment fluxes. Such a focus has been lacking in research within South Africa. The research project aims to: (a) define and quantify nutrient and organic carbon fluxes in a small-scale agricultural catchment; and (b) to scale up the water, nutrient and organic carbon fluxes from the 1 m^2 and 10 m^2 microplots and plots to the 1000 ha watershed through nested catchments of 23 ha and 100 ha.

1.5 Background of Project and Expected Benefits

This study forms part of a larger ongoing investigation (WRC K5/1904//1) monitoring nutrient and organic carbon fluxes from rural smallholder agriculture in the Potshini Catchment, KwaZulu-Natal, South Africa. The project is funded by the Water Research Commission (WRC). The WRC project is an expansion of an initial investigation which evaluated the spatial variation of interrill erosion occurring on the hillslopes of the catchment. Additional water, nutrient and sediment fluxes were monitored at different nested scales to determine the impacts that different land uses have on the water quality of receiving streams. This is important for the Potshini community as the first investigation revealed that overgrazing results in greater volumes of water being generated on slopes associated with a decrease in the infiltration of water into soils. From a social perspective, this study will be beneficial for the stakeholders of the Potshini community, as knowledge about the local river's water quality will help manage any problems associated with poor water quality.

Ultimately, the improvement of water quality will reduce the potential health effects associated with polluted water.

1.6 Dissertation Structure

The dissertation is organized in five chapters as follows. A review of the literature is contained in the Introduction of the first chapter. Chapter 2 presents the materials and methods, focussing on field data collection, laboratory analysis and specific data treatments. The results of the main findings are presented in Chapter 3. Chapter 4 covers the discussion of the results and the conclusion is to be found in Chapter 5, which looks at perspectives for future research.

2. MATERIALS AND METHODS

2.2 The Characteristics of the Study Site

The Potshini Catchment is located within the KwaZulu-Natal province, South Africa (Figure 2.1). The area that this study is concerned with is a 1000 ha catchment (longitude: 29.36°; latitude: 28.82°) located in the upper Thukela Basin (30,000km²) near the town of Bergville.

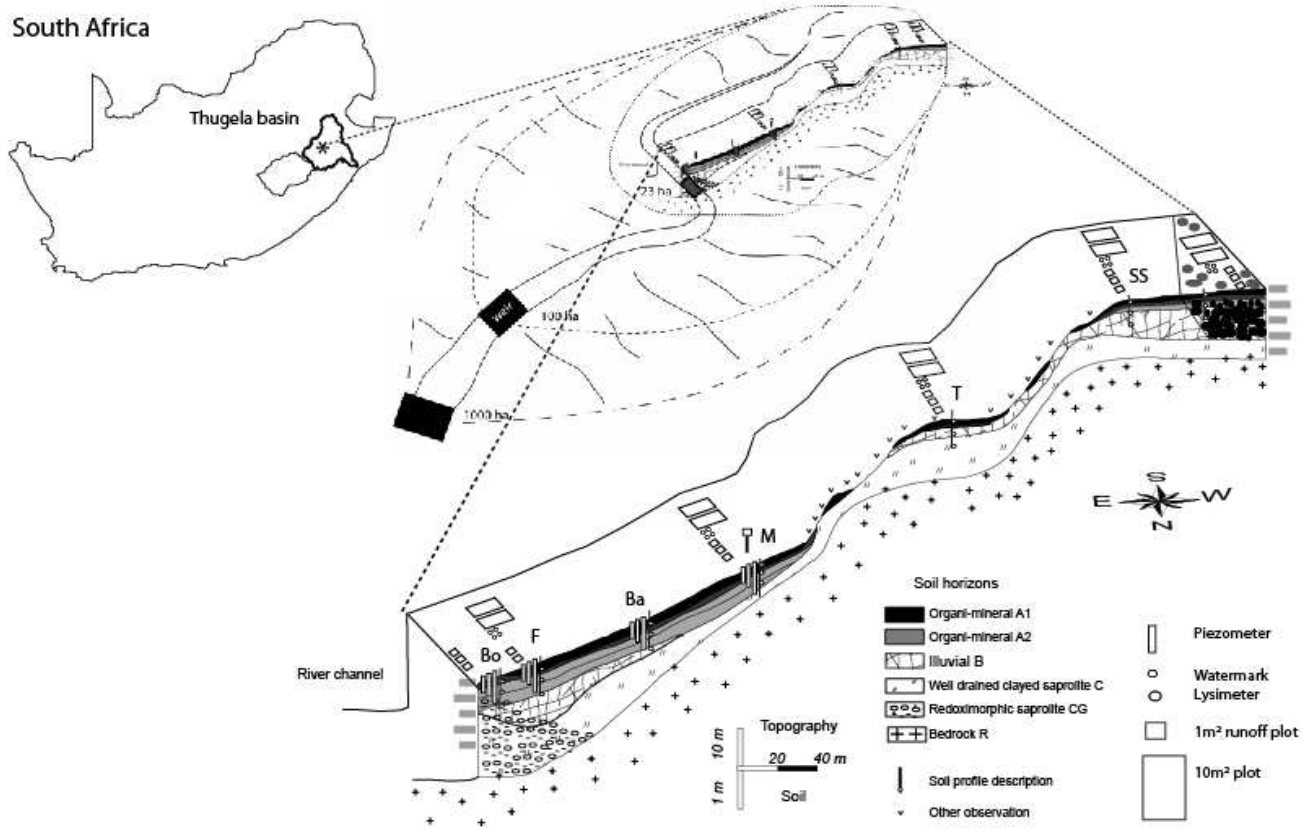

Figure 2.1 Experimental setup and location of the Potshini Catchment

The climate in the area is sub-tropical, humid and with a strongly seasonal summer rainfall pattern (October–March) (Schulze, 1997). The nearest government-maintained weather station located 10 km to the east of the study site in the town of Bergville, had a mean annual precipitation of 684 mm per annum over the past 30 years, with a potential evaporation of 1600 mm per annum and a mean annual temperature of 13°C (Schulze, 1997), and with frosts that are common in winter.

At the Potshini study site, altitude ranges from 1080 to 1455 masl. The relief is relatively gentle with a mean slope gradient of about 15.7%, but with steep slopes of 50-70% found in the upper part of the catchment, whereas in the vicinity of the catchment outlet and on the plateau, the topography is relatively flat all the way to the 1000 ha catchment outlet.

Soils are formed from the Karoo Supergroup and Beaufort Group parent materials (Figure 2.2, Table 2.1). The geology exhibits a horizontal, alternating succession of fine-grained sandstone, shale, siltstone and mudstone (King, 2002).

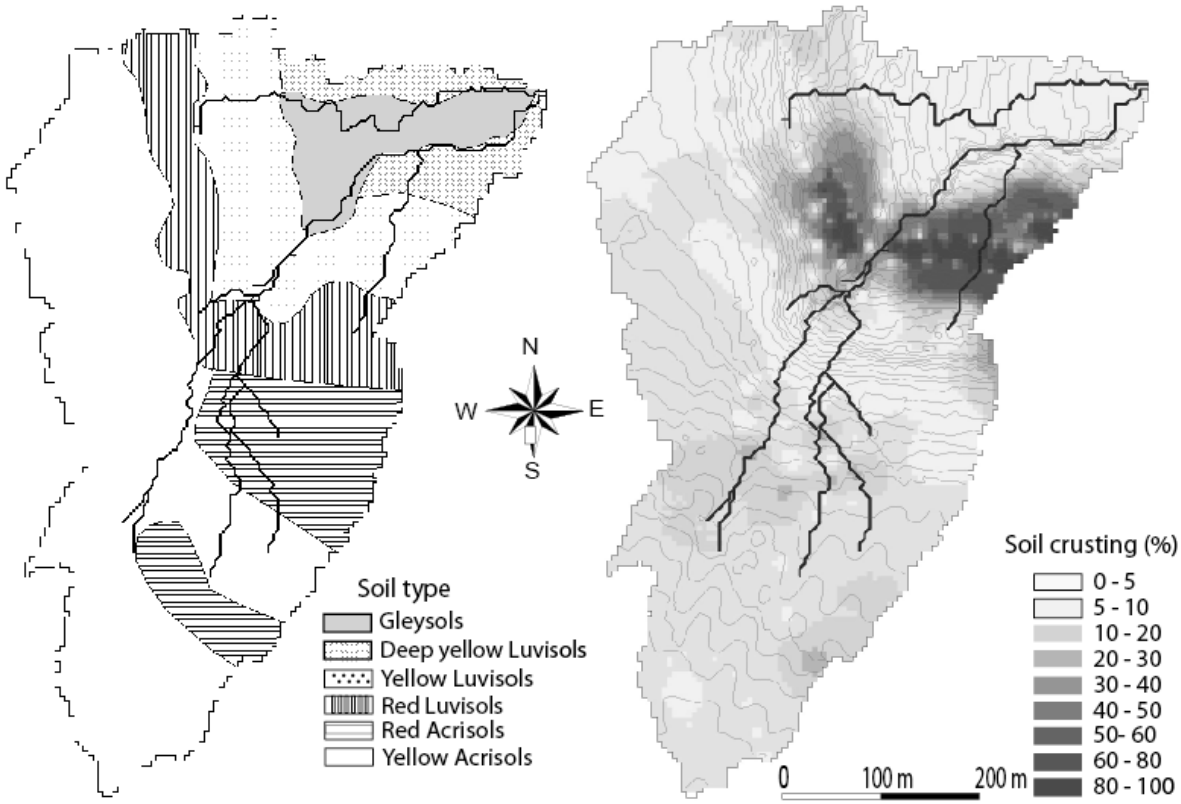

Figure 2.2 Spatial distribution of soil types and of soil surface crusting within the 23 ha catchment. Kriged maps interpolated, using 200 georeferenced field observations

A main dyke from the Karoo Dolerite is intruded in these horizontal layers in the upper portion of the catchment, giving specific weathering features of rounded boulders. Soils developed from sandstones and dolerites are Acrisols (ISSS Working Group, 1998) and Inanda soil form (Soil Classification Working Group, 1991). Within hillslopes, deep Acrisols (~2 m) characterize the footslope and Gleysols the bottomland. Bottomlands (Bo) exhibit

features of waterlogging, such as a surface dark grey A horizon, enriched in organic matter. At the footslope (F) position, the soils are well-drained. The midslope (M) position exhibits a similar soil profile, but much shallower. The soils at the terrace (T) and the shoulder (SD) have developed from dolerites. Finally, the soils found at the other shoulder location (SS) are derived from sandstones and are yellow in colour.

Table 2.1 Location label, Slope position, Soil type, proportion of the soil surface covered by crusting (Crust), proportion of the soil surface covered by vegetation (Cov), mean slope gradient (Slope), soil clay content and soil bulk density (ρb) at the different plot locations. Three plot replicates are located at each site: bottomland (Bo); footslope (F); midslope (M); terrace (T); shoulder under dolerite (SD); and shoulder under sandstone (SS). (n = 18)

n	Label	Slope position	Soil type	Crust	Cov	Slope	Clay	ρ_b
				----------%----------				g/cm^3
1	SS	Crest	Yellow Acrisols	15	85	19	30.5	1.12
2	SD	Crest	Red Acrisols	8	92	18	53.9	1.02
3	T	Terrace	Red Luvisols	5	95	23	39.8	1.13
4	M	Midslope	Yellow Luvisols	50	50	26	27.4	1.32
5	F	Footslope	Deep Yellow Luvisols	2	98	25	27.8	1.24
6	Bo	Bottomland	Gleysol	1	99	6	27.8	0.96

The land use of the catchment is predominantly grazed grassland. Cattle are seen as an important cultural asset and in good times, community members, both those living in the catchment and those who work and live in the major cities, invest in cattle, leading to increasing herd sizes. This, combined with the highly acidic low productive soils, rapidly leads to overgrazing, with a decreasing proportion of soil surface coverage by the vegetation and an associated increase in bare soils. Microplots have been installed in areas of the catchment that have different degrees of overgrazing intensities present, as well as other specific environmental factors. The installation of the microplots in areas of varying environmental factors allows for the use of two specific statistical techniques, a Principal Component Analysis (PCA) and a correlation matrix, to better understand the specific contribution that an environmental factor has on the spatial and temporal variations of overland flow generation within the research catchment.

The PCA and correlation matrix is derived using the statistical program, STATISTICA, which has an option to generate these analyses of the data.

There are three main embedded scales (as shown in Figure 2.1), which correspond to the three main land uses in the area. The land use of the 23 ha steep-sloped catchment (the smallest catchment surface area) is communal pasture for the local community. The land use within the 100 ha catchment is predominantly small-scale agriculture where maize (*Zea mays*) and small cash crops are grown for domestic consumption. From the 100 ha outlet to the 1000 ha catchment outlet, the land use changes to commercial agriculture, where irrigation takes place. Two dams, which store water for irrigation, are located upstream of the monitoring site of the 1000 ha catchment outlet.

2.3 The Experimental Methods

2.3.1 Rainfall measurements

Rainfall data were obtained from an automatic rain gauge located at the midslope position location of a hillslope located within the catchment. The rain gauge was calibrated to measure 0.2 mm per tip and was connected to a HOBO event logger that measured the exact time and date of each tip recorded by the tipping bucket. For the purpose of this study, it was assumed that the rainfall characteristics do not vary spatially within the catchment and that the rainfall is uniform and spatially distributed. Specific rainfall characteristics are to be used for this study and obtained from the data collected at the rain gauges within the catchment. These include the cumulative rainfall since the onset of the rainy season (RainC); three-days prior rainfall amount (PreRain-3); event duration (Dur); event average rainfall intensity (I); and the maximum event six-minute rainfall intensity ($Max_{6min}I$). These rainfall characteristics were used to determine their role in the spatial and temporal variations of OF generation. In addition, a manual rain gauge was present at the footslope position of the hillslope. This rain gauge was used to manually record the amount of rainfall for each rainfall event and was used to validate the rainfall amount recorded by the automatic rain gauge.

2.3.2 The nested scales used for water and nutrient fluxes evaluation

There are four main embedded/nested scales within the Potshini Catchment, (Figure 2.1).

a) Microplots and plots (7 monitoring nests installed along a hillslope where overland flow plots, soil water tension monitoring equipment installed at different depths and piezometers are located at each site. An automatic rain gauge was installed at the footslope location of the hillslope)
b) 23 ha catchment (monitored hillslope is located within the 23 ha catchment. An H Flume is installed, from which flow height is recorded by a data logger. An automatic water sampler is also located at the outlet of this catchment)
c) 100 ha catchment (23 ha feeds into this catchment. A H-Flume is located at the outlet of this catchment to monitor flow, which is logged by a data logger. An automatic water sampler is coupled with the data logger to take water samples)
d) 1000 ha catchment (outlet of the greater Potshini Catchment. Flow heights are monitored and logged, using a pressure transducer and a data logger). It is important to state that there are two dams located and used on a commercial farm for storage of water for agricultural use.

2.3.3 Microplots

Eighteen 1m x 1m overland flow microplots were installed within the catchment (Figure. 2.3). The microplots were installed at six different topographical positions or sites, with different soil types and intensities of overgrazing present.

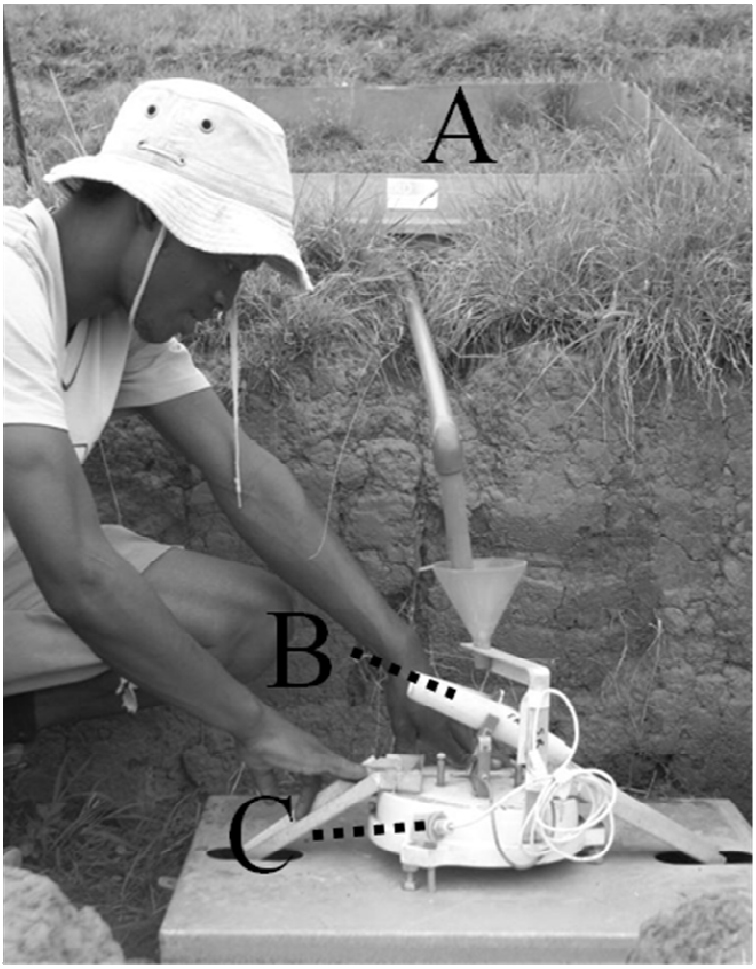

Figure 2.3 Example of a $1m^2$ microplot with its metallic frame inserted into the soil (A). View on the collection pipe which directs overland flow to a tipping bucket (B) aimed at recording the temporal variations of overland flow. The time of the tip is recorded by a HOBO® Event Logger©

The metal borders surrounding the micro-plots were inserted to a depth of 0.1 m in the soil. The microplots were installed parallel to the slope direction (as shown in Figure 2.3). This allowed for any overland flow that was generated to be directed down the slope and into the gutter of the microplot. The gutter was designed to channel and concentrate water into the bottom of the gutter. The gutter feeds into the outlet of the microplot. This outlet was connected to a pipe, which fed into a modified tipping bucket system. Finally, after the tipping bucket mechanism, the water generated by overland flow was collected in a bucket that was installed in the subsurface. After each rainfall event, the total overland flow volume (R) from each microplot replicate (Figure 2.3) was measured with a measuring cylinder. The precision was ±10 ml for total runoff volumes between 10 and 2000 ml and ±10 ml at higher runoff volumes.

At each location, the tipping bucket mechanism was connected to a HOBO event-logger (Pendant logger). The tipping bucket mechanism was designed to measure 40 ml for each tip. In addition, the specific time at which the tip occurred, was logged. This was to ensure that the exact temporal response of each individual microplot location (in terms of overland flow) was measured after the onset of a rainfall event. In addition, the intensity of the overland flow could be calculated.

2.3.4 Plots

Ten 5×2m² runoff plots were installed adjacent to the microplots with only two replicates per position (Figure 2.1). The metal borders surrounding both the microplots and runoff plots were inserted in the soil to a depth of 0.1m. All plots were installed parallel to the slope direction. This allowed for any overland flow that was generated to be directed down the slope and into the gutter of the plot. The gutter was designed to channel and concentrate water into the bottom of the gutter. The gutter fed into the outlet of the plot. This outlet was connected to a pipe, which fed into a tipping bucket system. Finally, after the tipping bucket mechanism, the water generated by overland flow collected in a bucket. At each location, the tipping bucket mechanism was connected to a HOBO event-logger (Pendant logger). The tipping bucket mechanism was designed to measure 2 litres for the 5m x 2m runoff plots. In addition, the specific time at which the tip occurred, was logged. This was to ensure that the exact temporal response of each individual microplot location (in terms of overland flow) was measured after the onset of a rainfall event. In addition, the intensity of the overland flow was calculated.

2.3.5 Catchment monitoring

Conventional H flumes coupled to ISCO 6712 and 3700 series automatic samplers were installed at the outlets of the 23 and 100 ha catchments, respectively. The H flume at the 100 ha catchment outlet was built in 2006, whilst the flume located at the 23 ha catchment was built in 2009. The height of flow at both catchment outlets were logged by a datalogger and were converted to runoff using site specific rating curves derived for each monitored site. The automatic water samplers were used to quantify catchment runoff water quality (in terms of nutrients and soil losses) during base flow periods and on the rising and falling limb of a

hydrograph during rainstorm events. At both the catchment and catchment scales sediment and water samples were collected using automatic samplers during rainfall events and manual sampling in between events when visiting the field site.

At the 1000 ha catchment outlet, a pressure transducer together with a HOBO data logger were installed, under a culvert bridge approximately 4km downstream from the monitored 100 ha catchment outlet. Particulate nutrient and sediment loads were not monitored at this site due to the existence of small upstream reservoirs, which in turn, trap the sediment load in the stream. The pressure transducer was calibrated by subjecting it to pressure from a gradually increasing height of water from 0 to 1000 mm while recording the output voltage signal from the transducer. A similar exercise was done for a decreasing water column. The calibration equation for the pressure transducer is as indicated in Equation 2.1:

$$H = 13.5307564 + 0.45355129 \times V \tag{2.1}$$

where H is the stream flow depth (mm) and V is voltage output from the pressure transducer (mV). Velocity transect surveys, at different discharges, were carried out across the culvert bridge using a propeller current meter. The concrete culvert bridge had a regular rectangular shape and hence made it easier to apply the Manning's open channel flow equation and subsequent development of the rating curve. Equation 2.2 shows the established rating curve at the culvert bridge.

$$Q = 8.267 \times H^{1.6403} \tag{2.2}$$

where Q is flow rate in m3/s and H is the stream flow depth (m).

2.4 Spatial and Temporal Variations of Overland Flow

The installation of the microplots at different locations and in conjunction with a tipping bucket connected to a data-logger, was done to account for the spatial and temporal variations of overland flow in the catchment. Eight representative runoff events were selected for detailed study of the temporal and spatial variations of overland flow. These events have been chosen, as all plot locations recorded overland flow and thus were assumed to be representative of events when overland flow was generated within the catchment. Figure 2.4 shows the selected runoff events for the microplots.

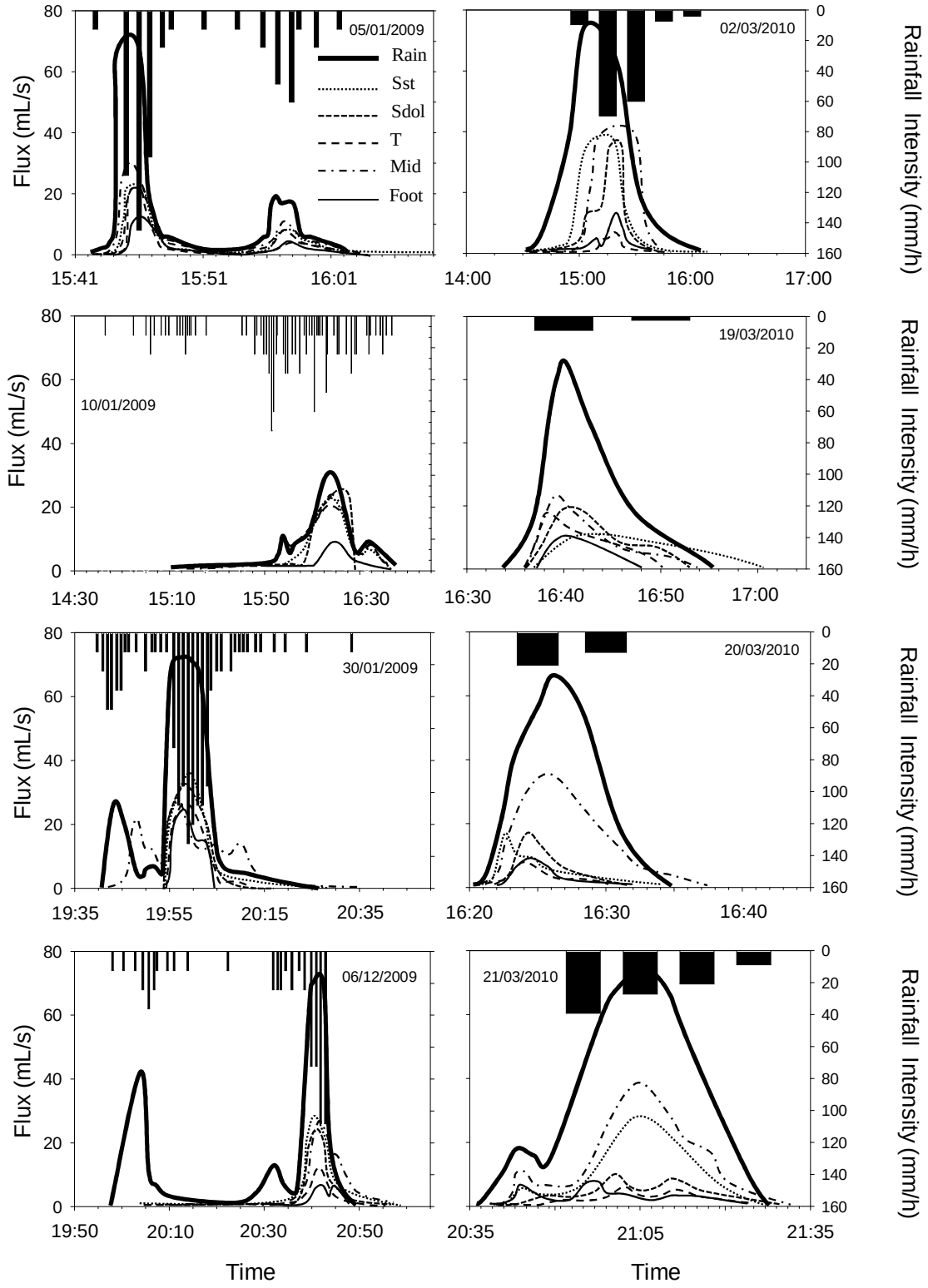

Figure 2.4 Overland flow response at the five microplot locations, for eight representative events selected from among the 90 events of the 2007-2010 period

The lag between the onset of rainfall and the start of the overland flow in each microplot can be derived from the curves and was used to estimate the Time to Runoff Initiation (TRI) (calculated using Equation 2.3);

$$TRI = T_{rain} - T_{plot} \tag{2.3}$$

The TRI can be defined as the difference in the time of the first tip of the microplot to the measured tip of the rainfall that generated the overland flow. The time of the rainfall is labelled as time zero (T_{rain}) and T_{plot} is the time, at which the microplot responded to the rainfall.

TRI is a key index to describe the spatial variation of overland flow generated within a catchment. From the experimental setup of this study, TRI was estimated for different areas within the catchment. This allowed for a better understanding of the spatial variations of overland flow. In addition, the TRI of each microplot location for a specific rainfall event was ranked to qualitatively assess the spatial variations of overland flow characteristics.

Three overland flow events were selected to investigate the spatial variations of overland flow, based upon the spatial extent of the soil surface crusting present within the catchment. This was done by plotting each individual location's microplot TRI value versus the microplot soil surface crusting value. From this, a simple linear regression model can be used to predict the TRI in the catchment where there are no microplots.

The events chosen were chosen according the overriding antecedent moisture conditions of the catchment prior to the overland flow events and the characteristics of the rainfall event that caused the overland flow event. The three selection criteria for the three different events were as follows:

a) Catchment saturated, large and intensive rainfall
b) Catchment dry, small rainfall event
c) Catchment saturated after a prolonged period of rainfall in a season with lower than average rainfall

2.5 Runoff Flux Monitoring

Runoff flux data from each of the catchment outlets, as well as the microplot and plot scale allowed for the calculation of the yields of water generated per unit area (in l/m^2). Overland flow generated within the plot and microplot area was manually measured after each rainfall event and was summed up at the end of each rainy season to determine the water generated per unit area (in l/m^2). The amount of water generated per unit area (in l/m^2) for the three catchment outlets was calculated directly from the automatically logged flow data where the time difference (s) between flows was multiplied by the average flux (l/s) to get a volume of water (l). Finally, this volume was then divided by the area of the catchment to obtain l/m^2. The spatial and temporal variations of the water fluxes for the different scales can, therefore, be easily quantified (both inter- and intra-season variability). Such data treatment results in a direct comparison of the different scales' productivity in terms of water movement.

2.6 Water and its Quality at Different Scales

2.6.1 Sediments

The total sediment fluxes corresponded to the mass of suspended sediments (about 200 samples per surface area per year, from 2009 to 2011) in the weir. Their dry weight (g) was evaluated after each rainfall event by drying the aliquot of water in an oven at 110°C. This was then multiplied by the volume of water (l) to get the sediment concentration (g/l). The sediment yields (g/m^2) for each nested scale were then calculated by multiplying the sediment concentration (g/l) by the runoff flux per unit area (l/m^2).

2.6.2 Nutrients

Water samples collected at the different spatial scales were used to assess the quality of the water. Water samples were collected both automatically (by the automatic samplers installed at the 23 ha and 100 ha catchment outlets) and manually (from runoff collecting buckets at the microplots and plots, and grab samples taken at all three catchment outlets during visits to the catchment). In addition, sampling was performed in the soil profile and in the groundwater following classical procedures (Sen *et al.*, 2010). The water quality constituents are the Nitrates-Nitrogen (NO_3-N), Total phosphorus (P), Dissolved Organic Carbon (DOC),

particulate carbon and particulate nitrogen (POC, PON). POC was defined as the fraction of carbon which had been bonded onto soil particles and then subsequently eroded. POC also included any organic matter which had been eroded. DOC was defined as the fraction of Carbon which been dissolved into solution buy rainfall and soil water. Water samples were collected in the field by taking 100mL aliquots and stored in a cooler box on site. Once back at the laboratory, samples were stored in a fridge, which was kept at a constant temperature of 4^{o}C until completion of analysis.

2.6.3 Nitrates (NO_3^-) and total phosphorus measurement

NO_3^- and P concentration in water samples were obtained, using a HACH DR/2000 spectrophotometer (Hach Company 1989). The absorbances of the water samples were read, using a Hach DR2000 spectrophotometer and converted to concentrations (given as mg/l but converted to g/l), using frequently calibrated standard curves. The accuracy of all nutrient analyses were within 10% of the actual concentrations. Concentrations were converted to yields (in g/m^2) by multiplying the concentrations by the runoff flux per unit area (l/m^2).

2.6.4 Dissolved organic carbon

Dissolved organic Carbon (DOC) was determined after sampling, using a Shimadzu TOC-5000 analyzer with an ASI-5000 autosampler and Balston 78-30 high purity total organic carbon (TOC) gas generator. In this technique, the organic solutes were converted to CO2 and the CO2 produced is measured as DOC (in g/l). Concentrations were converted to yields (in g/m^2) by multiplying the concentrations by the runoff flux per unit area (l/m^2).

2.6.5 Particulate carbon and nitrogen

Sediments were dried at 105°C for 24 hours. The sediments were weighed to determine sediment concentration in runoff and ultimately to compute sediment losses. Sediment samples from these aliquots were dried and stored to be further analysed for total soil organic carbon and nitrogen. C and N was estimated, using a LECO CNS-2000 Dumas dry matter combustion analyzer. The output from this analysis Particulate organic carbon (POC) and particulate organic nitrogen (PON) is given as a percentage of total soil analysed. This

percentage can be used to calculate the yields of POC and PON in (g/m^2) by multiplying the sediment yield (in g/m^2) by the percentage of POC and PON.

2.6.6 Tracers and end member mixing analysis

One commonly-used application of stable water isotopes, is aimed at the identification of river flow sources *e.g.* rainwater, overland flow or groundwater flow, with the composite signature in the river being an indicator of the portion of the different sources contribution. The water samples were analyzed for the isotopes of water, δ^2H and $\delta^{18}O$, using the Liquid-Water Isotope Laser Analyzer at the School of Bioresources Engineering and Environmental Hydrology, University of KwaZulu-Natal (Los Gatos Research, 2007). The OA-ICOS technique uses the absorption of a laser beam passing through an evaporated water sample to calculate the isotopic composition of the sample (Los Gatos Research, 2007). The laser scans the isotopes' spectral absorption, so the technique can detect several isotope species simultaneously. Sample measurements were calibrated with five standards, which were iteratively measured after each set of five sample measurements. Each measurement was conducted 6 times to provide a high value precision. Results are presented in δ notation *i.e.* parts-per-million deviations from Vienna Standard Mean Ocean Water (V-SMOW) as δ^2H and $\delta^{18}O$.

The oxygen and deuterium isotope ratios of the water collected at the different water source zones, as well as in shallow to deep aquifers (through the use of existing boreholes), will allow for the understanding of the movement of water through the different pathways in the catchment. Analysis was done on water samples that were automatically collected by the automatic samplers and grab samples at all the nested scales.

The use of isotopes of the different monitored hydrological zones in conjunction with other naturally-occurring tracers, such as Silica, allows for the determination of end member mixing at a catchment's outlet and it's different sources as used by Uhlenbrook and Hoeg (2003). Hydrograph separations, the stable isotopes of water determine the new event water and old water (*i.e.* pre-event water). In addition, the use of silica (determined using a Technicon TRAACS 2000 continuous flow auto-analyzer) in conjunction with the stable isotopes of water, can be used to differentiate between the reactive water (that flowed through the soil

compartment) and the unreactive water (that had minimum soil contact *i.e.* overland flow) (Huth *et al.*, 2004). Such an approach is consistent with the classic technique of three-stage hydrograph separation, as used by Huth *et al*. (2004) and Wenninger *et al.* (2008). The ultimate aim of such an approach is to gain a better understanding of the End Member Mixing of the different runoff sources contributing to the runoff at monitored catchment outlets. The end member mixing analysis of the 23 ha catchment and 100 ha catchment outlets, were determined using Equations 2.4 to 2.6, respectively which were utilised by Huth *et al*. (2004) in a study conducted in a catchment located in the Sierra Nevada, California.

$$Q_n = \frac{Q_s \times (C_s - C_o)}{(C_n - C_o)} \tag{2.4}$$

$$Q_r = \frac{Q_s \times (C_s - C_{unr})}{(C_r - C_{unr})} \tag{2.5}$$

$$Q_{unr} = \frac{Q_s \times (C_s - C_r)}{(C_{unr} - C_r)} \tag{2.6}$$

Where Q_n is the event water flux, Q_s is the discharge when the sample was taken, C_s the concentration of the water at the catchment outlet, C_o the pre-event water (groundwater), C_n the new water *i.e.* rainfall, Q_r the soil water contribution, Q_{unr} the contribution from the unreactive water *i.e.* overland flow, C_{unr} concentration of overland flow from runoff plots, and C_r concentration of soil water which was collected from piezometers. For reactive and unreactive water fractions, the water samples of both the runoff plots and piezometers were analysed for their silica (Si) content as Si has been found to differentiate between reactive water and unreactive water. Additionally, the use of silica has been found to representative of a conservative tracer in other studies conducted in other parts of the world such as Hooper and Shoemaker (1986), Uhlenbrook and Hoeg (2003), Huth *et al*. (2004) and Wenninger *et al* (2008). From Equations 2.4 and 2.5, the amount of water stored within the soil profile can be calculated using Equation 2.7.

$$Q_{nsw} = Q_n - Q_{unr} \tag{2.7}$$

Where Q_{nsw} is the event water generated from the soil profile and interpreted as the contribution of soil water to catchment runoff.

Hydrograph separations and end member mixing analysis are used to better understand the spatial and temporal variations in runoff and nutrient fluxes. Such an approach gives insight into the sources as well as the response of the catchment runoff. An in-depth analysis will not be attempted, as whole research projects are dedicated to hydrograph separations and end member mixing analysis. The end member mixing analysis performed in this study is an initial attempt.

2.7 Controlling Factors of Runoff Generation

2.7.1 Soil surface conditions

The topographic information at the study microplots and plots was derived from a Digital Elevation Model (DEM) with a 5-m resolution and a vertical precision of 0.05 m. It was generated for the purpose of this study from 36,000 data points of altitude. This DEM has been generated with a differential GPS and interpolated by using the inverse distance weighting function of ArcView3.2 (ESRI, 2004). From this, the altitude above sea level of each microplot was extracted, using the DEMAT function of ArcView3.2. The mean slope gradient of the eight cells surrounding each plot was estimated using the same ArcView function.

The proportion of the soil surface crusting and soil surface coverage at the microplots and plots was evaluated by Podwojewski *et al*. (2011). A grid of 100 nodes was placed on each of the 18 microplots, to evaluate the soil surface coverage (Cov).

The proportion of the soil surface covered by the vegetation at each microplot has been characterized visually in the field by qualitative assessment, using a $1m^2$ grid with $100cm^2$ cells, which is a well-documented methods (e.g. Auzet *et al*., 2004). The proportion of the soil surface with crusts has also been considered because of its recognised impact on overland flow generation (e.g. Casenave and Valentin, 1992). Following the field methodology of Casenave and Valentin (1992), the type of crust was recognised in the field using a knife and a magnifying glass and its proportion on the soil surface was evaluated using the $1m^2$ grid. The proportion of each crust type was summed to obtain the proportion of the soil surface with crusts. Additional information of exposed roots was gathered. Over 200 field observations were performed throughout the catchment. Information was obtained at the 15

microplots and at 185 randomly-selected points (at the boundaries between the different crusting percentages), the location of which was captured in the field using the differential GPS with a 0.2 m lateral accuracy. The resultant information is shown in Figure 2.2. GIS layers for the proportion of soil surface coverage and crusting were afterwards interpolated, using ArcMap and ordinary kriging, which is well-adapted for lower sampling densities (McBratney and Webster, 1983).

Core rings were used to sample the plot surface 0-0.05 m soil layer for soil bulk density (ρ_b) estimation at the microplot and plot positions. Three core samples were dried at 105°C for 24 hours to determine ρ_b, expressed as g cm^{-3}. Finally classical soil analysis was used, to estimate soil clay content

2.7.2 Soil water

At each location where the microplots have been installed, nests of Watermark sensors were also installed. The nests consist of three sensors installed at different depths within the soil profile. The depths to which the Watermark sensors were installed were 20, 50 and 100 cm.

The Watermark (Irrometer Company, Riverside, CA) is a granular matrix sensor, used to monitor soil water tension/soil water potential. It consisted of two concentric electrodes placed within a reference matrix material, which is bounded by an artificial covering for protection against deterioration. Movement of water between the soil and the sensor results in changes of electrical resistance between the electrodes within the sensor. The electrical resistance is then converted to soil water tension (in mm), using calibration equations specific to the site. The range of the soil water tension that a Watermark sensor can monitor, is between 0 to -2 bars or 0 to -200 kPa.

To ensure proper functioning, the Watermark sensors were soaked overnight and installed to the desired depth, as above, using an access hole, dug with an auger. The hole was subsequently filled with the excavated soil material to reconstruct the original soil profile and its horizon order. The soil material was firmly stamped during the process, but excessive compaction was avoided. An extensive watering was finally performed to improve the filling of voids and the contact between the Watermark sensors and the soil matrix. The sensors were finally connected to a four-channel HOBO logger, which was programmed to log the

electrical resistance in the sensors every hour. A temperature sensor was placed at a 20 cm depth to record soil temperature. The electrical resistance at the three depths was converted to soil suction, using Equation 2.5, a non-linear equation developed by Shock *et al*. (1998) and currently recommended by the manufacturer.

$$SMP = \frac{4.093 + (3.213 \times mV)}{(1 - (0.009733 \times mV)) - (0.01205 \times Ts)} \tag{2.8}$$

Where *SMP* is the soil matrix potential in kPa, *mV* is the sensor output and *Ts* is the measured soil temperature.

No specific calibration was performed on the sensors, but because it has been reported that the sensors' response may vary across soils and can be poor under wet soil conditions, the Watermarks' readings were compared to additional observations made at piezometers installed nearby the sensors at depths of 20, 50 and 100 cm. The soil water tension for all three depths at each location prior to the overland flow events (*i.e.* the hour before), has been extracted and used to investigate the impact that antecedent moisture conditions have on the generation of overland flow. Soil water tensions of the entire study period have been monitored to link water and nutrient fluxes at different scales with the catchments' state of wetness.

3. RESULTS

3.2 Rainfall Characteristics Over the 2007-2011 Period

The rainfall characteristics over the four-year study period are displayed in Table 3.1.

Table 3.1 General rainfall characteristics of the four hydrological seasons (2007-2011). Cumulative yearly rainfall amount (Cum); minimum, maximum, average event rainfall amount; standard deviation and coefficient of variation of average event rainfall amounts and maximum 6-minutes rainfall intensity of events ($Max_{6min}I$) (n = 52377).

	Cum	Min	Max	Av	StDev	CV	$Max_{6min}I$
	----------mm----------					%	$mm.h^{-1}$
2007-2008	761.9	4.2	30.8	14.7	7.8	53.3	38.4
2008-2009	852.0	0.6	79.6	11.7	15.1	128.2	42.3
2009-2010	627.8	1.0	53.8	7.3	8.1	111.5	36.4
2010-2011	1059	1.2	60.4	16.4	12.3	774.1	32.0
Average	747.2	1.9	54.7	11.2	10.3	97.7	39.0

The rainfall amounts for the three different rainfall seasons are shown in Table 3.1. The total amount of rainfall for each rainfall season was 761.9 mm in 2007-2008; 852 mm in 2008-2009; 627.8 mm in 2009-2010 and 1059 mm in 2010-2011. This indicates that each individual rainfall season was inherently different and, as such had different characteristics of rainfall.

In support of this are the differing event minimum and maximum for each individual season. For 2007-2008, the maximum event depth was 30.8 mm, whilst the event minimum was 4.2 mm; in 2008-2009 the event maximum was 79.6 mm and the event minimum was 0.6 mm; the event maximum for 2009-2010 was 53.8 mm and the event minimum was 1 mm and in 2010-2011 the event maximum was 60.4 mm and the event minimum was 1.2 mm.

The maximum 6-min intensities for events in each specific season were 38.4 $mm.h^{-1}$ in 2007-2008, 90 $mm.h^{-1}$ in 2008-2009; 69.6 $mm.h^{-1}$ for 2009-2010 and 32.0 $mm.h^{-1}$ for 2010-2011.

These specific events intensities corresponded to the maximum event amounts for each season.

The average rainfall amount per event was 14.7 mm in 2007-2008, 11.7 mm in 2008-2009; 7.3 mm in 2009-2010 and 16.4 mm in 2010-2011. The standard deviations and coefficients of variation reported in Table 3.1 indicated that the rainfall season of 2008-2009 showed highly variable rainfalls (Stdev 15.1 mm and CV 128.2 mm). High variations in event total rainfall also occurred in 2009-2010 (Stdev=8.1 mm; CV=111.5 mm). The 2007-2008 season showed smaller variations in event rainfall amounts, with for example, a CV of 53.3 mm, *i.e.* about half of this calculated from the 2008-2009 and 2009-2010 data. The rainfall for the 2010-2011 season showed the highest variations in event rainfall events with a CV of 774.1 mm which was considerably higher than that of the other seasons considered.

3.3 Spatial Variations of Overland Flow

3.3.1 Generalities

General statistics of overland flow at the different plot locations and events and for the three rainy seasons under study are presented in Table 3.2.

Table 3.2 General statistics of overland flow (cumulative litre per square metre) and Time to Runoff Initiation at the different plot locations and events and for the three rainy seasons under study. Three plot replicates are located at each site: bottomland (Bo); footslope (F); midslope (M); terrace (T); shoulder under dolerite (SD); and shoulder under sandstone (SS). A total of 15 plots and 90 events were considered.

	SS	SD	T	M	F	Bo
2007-2008 (n=34)						
Mean	7.0	4.3	3.7	6.6	4.5	40.2
Rank	*2*	*5*	*6*	*3*	*4*	*1*
2008-2009 (n=37)						
Mean	10.6	10.1	10.6	10.7	8.1	58.2
Rank	*3*	*6*	*5*	*3*	*2*	*1*
2009-2010 (n=19)						
Mean	5.2	3.7	4.1	4.8	2.6	30.8
Rank	*3*	*4*	*5*	*2*	*6*	*1*
TRI (min)						
2007 - 2008	4.2	6.6	7.2	6.6	10.8	0.1
2008 - 2009	3.6	5.4	4.2	3	7.2	0.3
2009 - 2010	0.6	0.6	0.6	0.6	1.2	0.2
Average	2.8	4.2	4	3.4	6.4	0.2
TRI (rank)						
2007 - 2008	2	3	5	3	6	1
2008 - 2009	3	5	4	2	6	1
2009 - 2010	2	2	2	2	6	1
Mode	3	4	5	2	6	1

The Overland flow generated differed from plot location to plot location. The average 2007-2008 overland flow was the highest at Bo, then followed by SD, M, SS, T, and F. Bo was ranked first for all seasons. Bo remained ranked first for all seasons with SS, M and F were

the next most productive situations. Reddish shallow and deep Acrisols at T and SD were the least productive microplot locations over the years.

In Table 3.2, it can be also seen that there was a greater within-situation variability at the different locations of the OF generated. For example, F generated its largest event OF mean of 81 litres in 2008-2009; the next productive season was 2007-2008 with a mean of 4.5 litres; and the least productive season was 2009-2010, with a mean of only 2.6 litres generated.

3.4 Time to Runoff Initiation (TRI)

The overland flow response to rainfall for eight representative events selected among the 90 events of the 2007-2010 period, is presented in Figure 2.4. The events chosen exhibited a large range of rainfall characteristics. The highest maximum six-minute rainfall intensity (42.3 mm h^{-1}) occurred on 30 January 2009 and the highest rainfall amount (37.6 mm) was recorded on 2 March 2010. Events were selected to demonstrate antecedent rainfall conditions prior to the rainfall event and, thus, represent antecedent soil moisture conditions. The rainfall characteristics of the eight representative overland flow events selected to graphically investigate the spatial and temporal variations of TRI at the catchment level are shown in Table 3.3. Where Cum is the total rainfall of the event, I the average intensity of the event, $Max_{6min}I$ the maximum six minute intensity, RainC the antecedent rainfall that had bfallen since the onset of the rainy season (1 October) and PreRain-3 the antecedent rainfall 3 days prior to the overland flow producing rainfall event.

Table 3.3 Rainfall characteristics of the eight representative overland flow events selected to graphically investigate the spatial and temporal variations of TRI at the catchment level.

Date	Duration	Cum	I	$Max_{6min}I$	RainC	PreRain-3
	min	mm	-------mm h^{-1}------		--------mm-------	
05-Jan-09	19	10	31.6	39.3	504.6	15.2
10-Jan-09	121	21	10.4	38	517.6	6.0
30-Jan-09	54	23	25.6	42.3	650.6	82.2
06-Dec-09	44	11.4	15.5	36.3	182.4	4.2
02-Mar-10	60	37.6	37.6	20.3	434.0	1.8
19-Mar-10	30	2.8	5.6	19.8	528.4	10.6
20-Mar-10	30	8.4	16.8	22.6	531.4	4.8
21-Mar-10	45	24	32	36.4	544.4	13.2

The event on 06 December 2009 occurred relatively early into the rainy season, therefore it had a low RainC (182.4 mm of cumulative rainfall since onset of season). In contrast, the event of 30 January 2009 occurred later on in the rainy season (RainC=650.6 mm). The cumulative rainfall of the three days prior to the event (PreRain-3) ranged between 1.8 mm on 2 March 2010 and 82.2 mm on 30 January 2009.

The hyetograph for the eight events are displayed in Figure 2.4. The distribution of the rain was either mono-modal or bi-modal. Mono-modal events occurred on the following dates: 02 March 2010. 19 March 2010, 20 March 2010 and 22 March 2010. Bi-modal events occurred on 05 January 2009, 10 January 2009, 30 January 2009 and 06 December 2009. From the curves, it is noticeable that the OF obviously commenced after the rainfall started, the time lag between the two corresponding to TRI. The evolution over time of OF generated at the different locations is mostly asymmetrical and OF peaks appeared to be considerably lower than that of the rainfall (if the curves were exactly the same, then all the event rainfall would have been converted into OF). Out of the 8 events, only 2 events showed OF bi-modal behaviour, whilst OF for the remaining six events was mono-modal. M and SST locations had the highest OF peaks for all events, followed by SD, T and F. The evolution over time of OF for Bo was super-imposed on the rainfall (100% OF) for all the events except on 6 December 2009, during which no OF occurred (100% infiltration). The frequency distribution of TRI, as

shown in Figure 3.1, shows that the majority of TRI of the microplot locations for the selected overland flow events (44 data points out of 48) had a TRI of less than 60 minutes. The majority of microplot locations had a response of less than 20 minutes (32 data points out of 48 were considered).

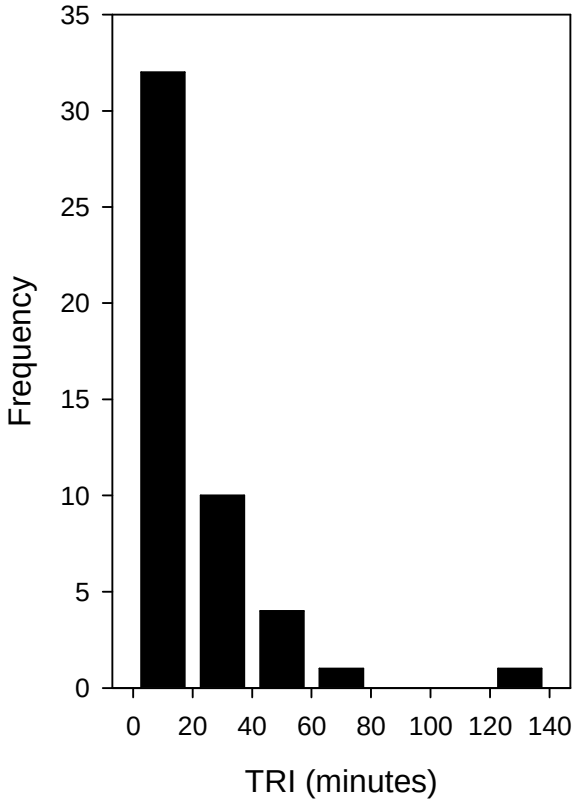

Figure 3.1 Frequency distribution of Time to Runoff Initiation (TRI) for all microplot locations

Average TRI at the different landscape locations and for each of the three rainy seasons are displayed in Table 3.1. Values varied between 0.6 minutes at Bo to 6.4 minutes at F. TRI was the lowest at Bo, followed by M; SS, SD, T, and F. This ranking was consistent across the three rainy seasons. While at Bo, average TRI only varied slightly from year to year, much higher variations have been observed at the other landscape positions. For example, at F, average TRI ranged between 1.2 minutes in 2009-2010 and 10.8 minutes in 2007-2008. Overall, TRI values were the lowest in 2009-2010 and the highest in 2007-2008 (Table 3.1).

3.4.1 Controlling factors of TRI

One-to-one relationships between TRI and the selected environmental factors are displayed in Table 3.4. Due to the unique behaviour of OF in the bottomland (Bo) (i.e., 100% OF when the bottomland water table reaches the soil surface and 0% OF otherwise) two correlation matrices have been generated, one with and one without bottomland plots.

Table 3.4 Correlation matrix between TRI (with and without data from the bottomland) and the selected soil variables and environmental factors: Crust, Cov, Slope, Clay, ρ_b, ER (proportion of soil surface with exposed roots); SWT (soil water tension at depths of 20; 50 and 100 cm); Rain (total event rainfall amount); RainC (cumulative rainfall since the onset of the rainy season); PreRain-3 (3-days prior rainfall amount); Dur (event duration); I: event average rainfall intensity; $Max_{6min}I$ (maximum event 6-min rainfall intensity) (n = 144)

	TRI	
	Hillslope	Bottomland
Crust	-0.08	-0.16
Cov	0.08	0.16
Slope	-0.03	-0.27
Clay	0.06	-0.1
ρ_b	-0.05	-0.19
ER	-0.16	-0.13
SWT_{20}	0.08	-0.13
SWT_{50}	0.10	-0.11
SWT_{100}	0.20	-0.12
Rain	0.41*	-0.08
RainC	-0.47*	-0.35*
PreRain-3	-0.23	-0.08
Dur	0.80*	-0.03
I	-0.17	-0.09
$Max_{6min}I$	-0.15	-0.1

*Marked correlations are significant at $p < 0.05$

When including all locations, TRI significantly correlated with only the cumulative amount of rainfall since the onset of the rainy season (*r*=-0.35). R coefficients were the lowest for Dur (r=-0.03), Rain and PreRain-3 (r=-0.08), and I (r=-0.09). The highest r were found with S (r=-0.27), Cov (r=0.16), Crust (r=-0.16), and ρ_b (r=-0.19). Overall, TRI decreased (i.e., increase of OF response) as mean slope gradient; proportion of the soil surface covered by crusting; exposed roots; percentage soil clay content; soil bulk density, the cumulative amount of rainfall since the onset of the rainy season, the cumulative rainfall three days prior to the event and the average rainfall intensity of the event and the maximum six-minute rainfall intensity of the event, and soil water tensions increased.

Results from the multivariate analysis, a PCA, the two first axes of which explained 47 percent of the entire data variability (Figure 3.2a; which is shown by the horizontal bars located in the top right hand corner of the PCA), revealed a strong correlation between TRI and axis-1 of the PCA, an axis interpreted as a soil and soil surface degradation axis. TRI appeared to be the lowest at high crust, high ρ_b and steep slopes. The second axis, which explained 17% of data variance, correlated with the rainfall characteristics (positive coordinates on axis 2) and the soil water tensions (negative coordinates on axis-2). TRI did not correlate with this axis, which was interpreted as an axis of wetness status of the catchment.

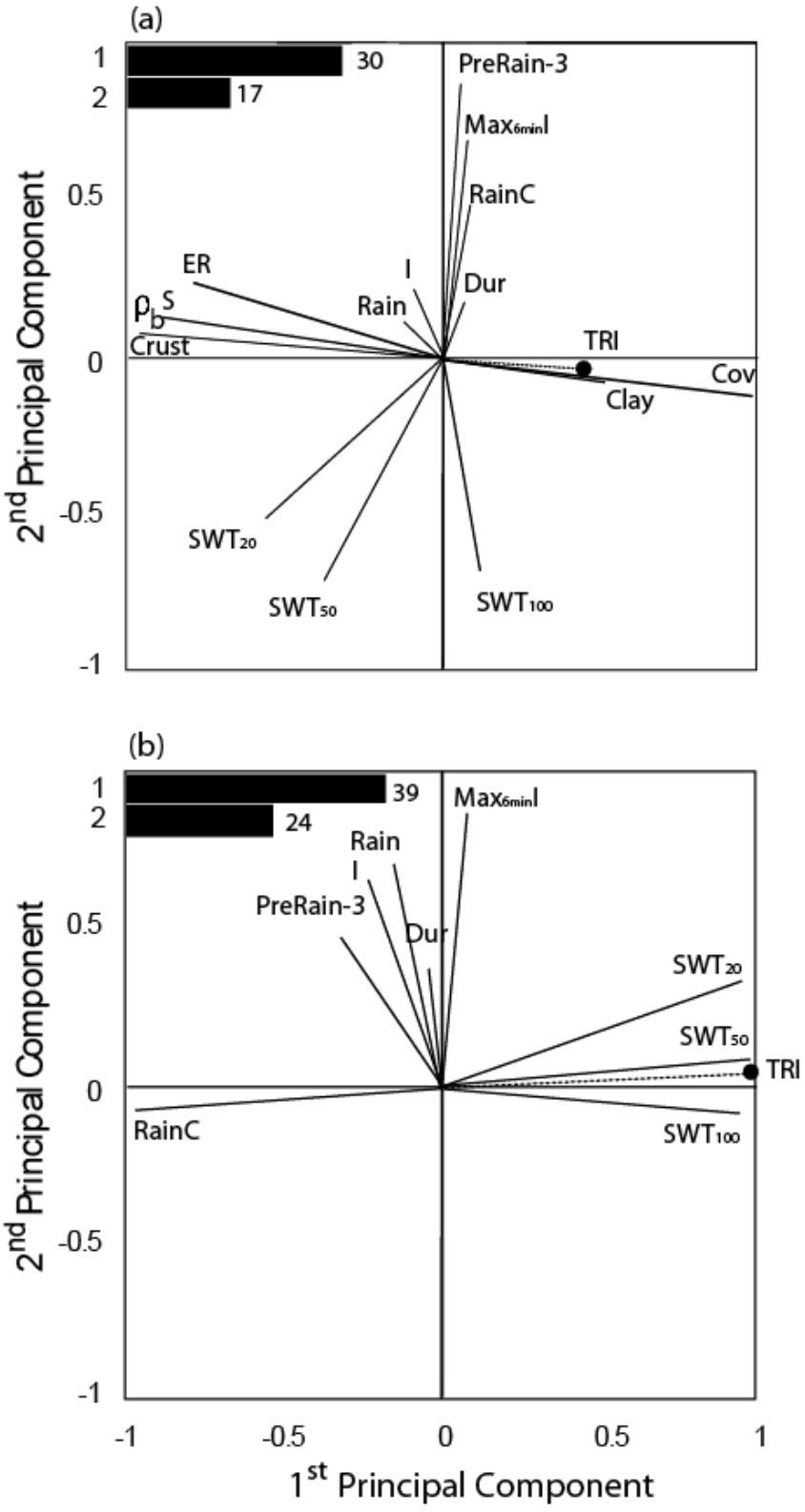

Figure 3.2 Principal Component Analysis of TRI and environmental variables for hillslope (a) and bottomland (b)

A second PCA has been generated, using the data of only the bottomland location, where the excess saturation was expected to control OF generation (Figure 3.2b). This PCA explained

63 percent of the total data variability. The first PCA axis, which accounted for 39% of data variance, correlated the most with soil water content (from 20 to 100 cm depth) and RainC. It can be interpreted as an axis of bottomland soil wetness or water table establishment, soil wetness increasing as cumulative rainfall increased. The second PCA axis contrasts large and intense rainfall events to small and low intensity ones and can thus be interpreted as an axis of rainfall event characteristics. On the PCA, TRI correlated with axis-1, on which it showed a positive coordinate. These results revealed that TRI, in the bottomlands, is primarily controlled by the soil wetness status in relation to excess soil water saturation, in contrast to the characteristics of rainfall events. TRI was shown to be high under dry soil conditions and close to zero when the water table reached the soil surface.

These results highlight that TRI was controlled by the excess soil saturation in the bottomland and by soil surface features elsewhere in the catchment. The strong relationship observed between TRI and soil crusting was used to evaluate the spatial and temporal variations of TRI within the catchment, except bottomlands. In the bottomland, TRI was zero when the soil surface horizon was saturated by water. Using this knowledge, simple regression models between TRI and soil crusting (Equations 3.1 to 3.4) were generated for three selected events and for the entire 2007-2010 period. The models, which explained between 59 and 95% of data variance, were applied to the whole catchment (Figure 3.3), using a map of soil crusting spatial variations generated by Dlamini *et al*. (2011) and interpolated from 200 field observations and a map of bottomland extent generated for this study.

30-Jan-09:	$TRI = -0.259 \times Crust + 15.45$	$r^2 = 0.95$	(3.1)
06-Dec-09:	$TRI = -0.228 \times Crust + 38.26$	$r^2 = 0.72$	(3.2)
21-Mar-10:	$TRI = -0.128 \times Crust + 8.259$	$r^2 = 0.59$	(3.3)
Average:	$\mathbf{TRI = -0.139 \times Crust + 18.87}$	$\mathbf{r^2 = 0.65}$	**(3.4)**

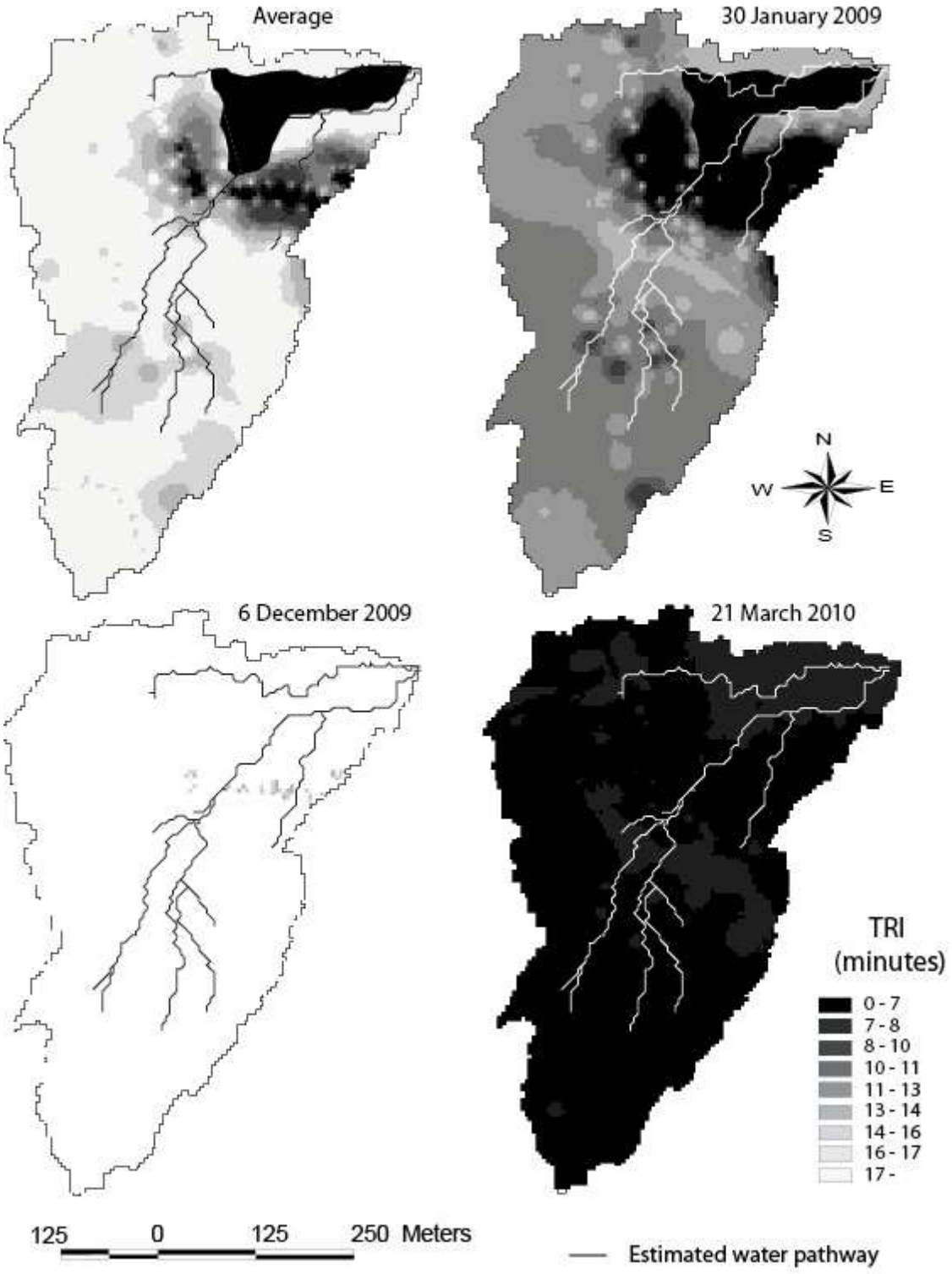

Figure 3.3 Spatial variations of TRI for three rainfall events of the 2007-2010 period. Data estimated at the catchment level, using Equations 3.1 to 3.4

The map of the average 2007-2010 TRI is displayed in Figure 3.3. From the model that explained 65% of data variability, the average TRI was 17.2 min. with values between 4.9 and

18.9 min. The lowest TRI is expected to have occurred in the bottomland, due to saturated soil conditions conditions; and at the midslope position, due to a high degree of crusting. In contrast, TRI is likely to have been the highest (>15 min.) on the steep convex crest and hillslope plateau, and at the footslope under low crusting. The map for the 30th of January 2009 showed similar spatial trends *i.e.* faster OF response to rainfall in the bottomland and midslope than on the hillslope plateau. The model used to generate this map explained 95% of the TRI variance, which was the highest value among the selected events. On that date, TRI varied between 0 and 15.5 min., with an average of 12.3 min. The event of 6th December 2009 was characterized by an average TRI of 35 min. with values between 15 and 38 min, the faster OF response occurring at the midslope position, where the soil surface crusting was the highest. The event of 21st of March 2010 showed the lowest data range (0<TRI<8.2min.), indicating a more uniform OF response to rainfall. This model only explained 58% of TRI variance.

3.5 Water and Nutrient Fluxes at the Different Nested Scales

3.5.1 Runoff at various scales

Data of cumulative water fluxes for the two seasons and for the different scales (1m² for microplots; 5m² for plots; 23 ha catchment; 100 ha catchment; and 1000 ha catchment) are presented in Figure 3.4.

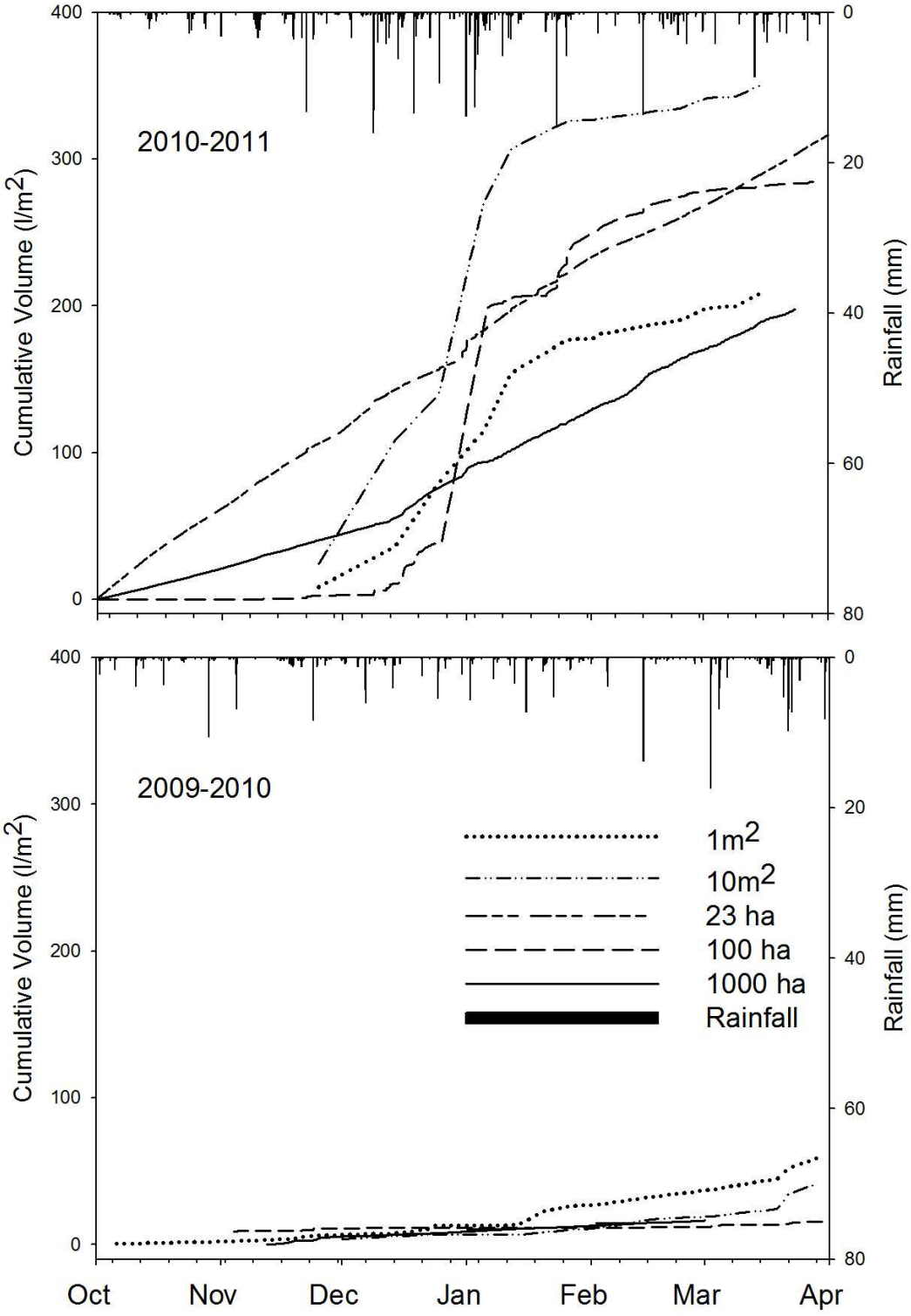

Figure 3.4 Cumulative runoff volume per unit area for the two rainy seasons of the different scales monitored in the research catchment (in l/m^2)

For the first rainy season (2009-2010), the greatest cumulative volume of water generated was observed for microplots (average of 58.6 L m^{-2}, n=15 *vs.* 41.3 L m^{-2} for plots, n=10). The first overland flow event on 1x1m² occurred on 06 October 2009, after there had been 11.2 mm of

rainfall since the start of the rainy season. The first overland flow on 5x2m² plots occurred at the end of November 2009, which corresponded to a cumulative rain since the rainy season onset of 173 mm. Such a result indicated that runoff generation at this scale was more dependent on the antecedent soil moisture status of the soil than on microplots. The average runoff coefficient estimated using an annual rainfall amount of 628 mm was 9.3% on microplots and 6.6% on plots.

The 2010-2011 rainy season exhibited much higher cumulative overland flows at both spatial scales (1×1m and 5m×2m). The increase was from 58.6 to 208.0 $L.m^{-2}$ for microplots and from 41.3 to 350.0 $L.m^{-2}$ for plots. The resulting runoff coefficients for this wetter year (1059.2 mm of cumulative rain) were 19.6% for microplots and 33.0% on plots.

The first overland flow event in 2010-2011 occurred on 25 November 2010, which corresponded to an antecedent rainfall of 201.6mm since the onset of the rainy season. The general trend for this season was for the 10m² plots to produce more overland flow than the microplots. The plots were the most productive out of all the monitored scales within the catchment. The $1m^2$ microplots were the fourth most productive scale. The 10m² plots appear to be more sensitive to rainfall as a result of the steepness of the cumulative curve, while microplots show a more gradual increase of cumulative flux over time.

The 23 ha catchment showed a relatively constant flow over time, as exhibited by a linear shape for the line of cumulative fluxes. The seasonal cumulative flux was 316 $L.m^{-2}$ in 2010-2011 (the first rainy season at which the catchment was instrumented), which made it the second most productive scale (with a runoff coefficient of 29.8% in relation to annual rainfall). The existence of constant flows (the presence of low flows during dry periods together with slight flow increases during rainfall events) points to the existence of a water source from the subsurface, which acts as a buffer between overland flow generated on the slopes and the catchment runoff of the river network.

At 100 ha, the cumulative flux was 16.66 $L.m^{-2}$ (this corresponded to a runoff coefficient of 2.6%) for the period 2009-2011. The first recorded change in water flux at the 100 ha catchment occurred after there had been 74mm of rainfall recorded in total since the onset of the rainy season. There was minimal flow throughout the rainy season, which is indicative of the impact that the quantity of rainfall has on the hydrological response of the 100 ha

catchment. There was a greater amount of rainfall in the month of March 2010 and the flux of water at the 100 ha catchment did increase.

The 100 ha catchment initially displayed a slow response to rainfall for the period 2010-2011. It appeared that the hydrological response of this catchment outlet was dependent on the antecedent moisture status of the catchment. The first monitored flow at the 100 ha catchment occurred on 10 November 2010. The amount of rainfall that had occurred since the start of the rainy season (01 October 2010) totalled 133.4mm. Once this rainfall amount had fallen, there was consistent low flow occurring at the 100 ha scale through to the middle of December 2010. From the middle of December 2010, there was a sudden increase in the amount of cumulative flow. This coincided with a period of high rainfall amounts. From this period, the 100 ha catchment produced large quantities of flow until the start of January 2011. In a period from the middle of February to the middle of March 2011, the 100 ha catchment produced more flux than the 23 ha catchment. This period again coincided with a period of high rainfall and pointed to the flux at this scale being antecedent soil moisture content driven, where large amounts of flux occurred when the catchment was wet. The 100 ha catchment was the third most responsive monitored scale for this study period (284 $l.m^{-2}$). This cumulative flux value corresponded to a runoff coefficient of 26.8%.

At the 1000 ha catchment outlet, the cumulative runoff flux was 16.25 L m^2 in 2009-2010 and 197.6 L m^2 y^{-1} in 2010-2011. These cumulative flux values corresponded to runoff generation ratios (calculated in terms of the total seasonal rainfall amounts) of 2.6 (2009-2010) and 18.7% (2010-2011) respectively. The yearly fluxes were ranked last among the study scales, but fluxes appeared second in 2010-2011 at the early stages of the rainy season. It was interesting to note that during this period, the cumulative flux showed a lower slope than that at the end of the rainy season.

A summary of cumulative seasonal fluxes at the different spatial scales (plotted as a function of longest flow path for each nested scale; determined from the catchment Digital Elevation Model) is presented in Figure 3.5. In order to understand (and explain) the variations in the flux of water at the different scales, the use of the longest flowpath distance of each individual nested scale from the catchment upper limit can be helpful in highlighting the spatial variations in the generation of water flux. As was shown in Figure 3.4, the 2009-2010 rainy

season had fluxes that were significantly lower than the fluxes that were generated in the 2010-2011 rainy season.

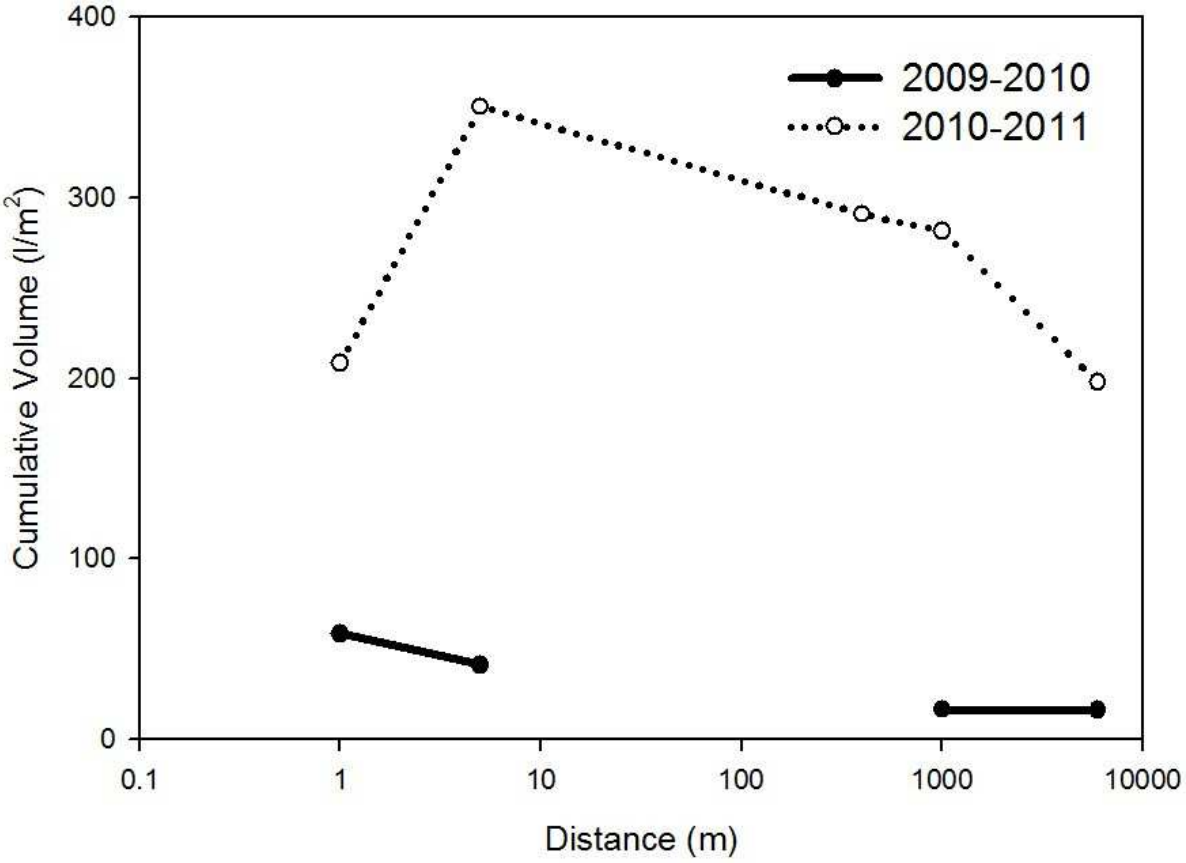

Figure 3.5 Cumulative yearly volumes of the water per unit area as a function of distance from catchment upper limit for the two seasons. One metre corresponds to microplotdata; 5 m to plot; 500 to 23 ha; 1000 m to 100 ha and 5000 m to 1000 ha

In 2009-2010, the $1m^2$ microplots generated the most water per unit area out of the scales. With an increase in the distance from the catchment limit, there was a decrease in the amount of water per unit area generated at the nested scales with the $10m^2$ runoff plots (5m distance) generating the second highest amount of water, followed by the 100 ha catchment outlet (1000m distance) and finally, the 1000 ha catchment outlet (6000m distance). Since there was no data available for the 23 ha catchment outlet (400m distance), one can assume that the amount of water generated at this catchment outlet would be between the amount of water generated at $10m^2$ runoff plots and the 100 ha catchment outlet.

The rainy season of 2010-2011 showed a significantly higher amount of runoff generated at the nested scales. In contrast to the 2009-2010 rainy season, the $1m^2$ microplots did not generate the highest flux of the nested scales. A greater quantity of flux was generated at the $10m^2$ runoff plots (5m distance; the greatest amount of flux generated), the 23 ha catchment outlet (400 m distance; second highest amount of flux generated) and the 100 ha catchment outlet (1000 m distance; third highest amount of flux generated), than at the $1\ m^2$ (1m distance; fourth highest amount of flux generated). This change in behaviour could be a result of there being a methodological error associated with the $1m^2$ microplots where there was preferential infiltration at the metal borders of the microplot perimeter. The decrease from 5m to 1000m is linear, indicating that there was possibly a constant decrease in the amount of water being delivered to each site (*i.e.* infiltration and/or evaporation). The least productive scale was that of the 1000 ha catchment outlet (6000 m distance). The cumulative flux at both the $1m^2$ microplot scale and the 1000 ha catchment outlet was similar. The decrease in flux between the distances of 1000 m and 6000 m (100 ha catchment and 1000 ha catchment outlets, respectively) could be pointing to higher infiltration (along the stream channel) and evaporation (as a result of the storage dams located between the two catchment outlets). The use of environmental tracers, such as the stable isotopes of water, could be a useful tool to support such an issue.

3.5.2 Variations of sediment yields at the different spatial scales

The cumulative sediment yields for two different rainy seasons (2009-2010 and 2010-2011) are presented in Figure 3.6. At first glance, it is noticeable that the two seasons were inherently different, with the 2010-2011 rainy season having considerably higher sediment yields (at all observation scales) than the 2009-2010 rainy season.

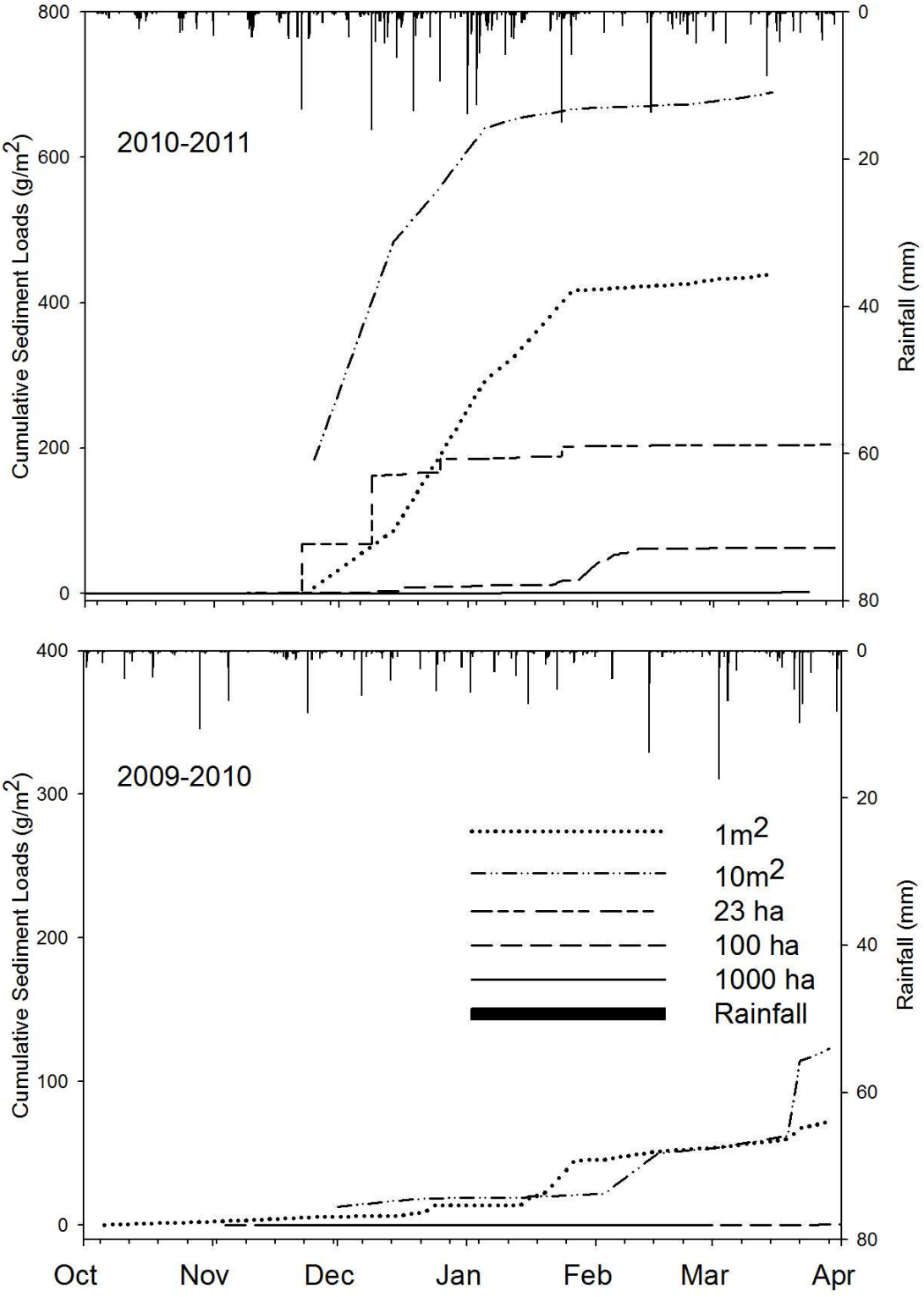

Figure 3.6 Cumulative sediment loads for the two seasons of the different scales monitored in the research catchment (in g/m^2)

With regards to the 2009-2010 season, all scales showed a slow accumulation of sediment yields. The first scale that showed any response was that of the 1m^2 microplots. The next

scale that responded was that of the 100 ha catchment outlet, followed by the 1000 ha catchment outlet, and finally, the $10m^2$ runoff plots. The $10m^2$ runoff plots showed the highest sediment loads for any specific event (*i.e.* the $10m^2$ runoff plot curve had the steepest gradient of any of the observation scales' curves), with the $1\times1m^2$ microplots having the next highest event sediment yield.

The 2009-2010 rainy season accumulated sediment yields for the different scales indicated that the $10m^2$ runoff plots had the highest sediment yield (122.74 g/m^2) followed by the $1m^2$ microplots (72.11 g/m^2), 100 ha catchment outlet (0.83 g/m^2), and finally, the 1000 ha catchment outlet (0.16 g/m^2).

At first, all the observation scales showed little to no accumulated sediment yields. The first scale that showed an increase in accumulated sediment yields was that of the 23 ha catchment outlet. Subsequently, the $5\times2m^2$ runoff plots and $1m^2$ microplots responded at the same time. Both of the hillslope scales showed a gradual increase in sediment yields as a response to erosive rainfall events. At the end of the rainy season, both hillslope scales' curves did taper off. The 100 ha and 1000 ha catchment outlets both exhibited a slow accumulation of sediment yields, with the 100 ha catchment outlet responding before the least responsive observation scale, the 1000 ha catchment outlet. In terms of the greatest event specific sediment yields, the 23 ha catchment exhibited the greatest instantaneous change in sediment yields.

From Figure 3.6, the final accumulated sediment yields for the different scales are shown. The scale with the highest sediment yield was that of the $10m^2$ runoff plots (689.92 g/m^2). The scale with the next highest sediment yield was that of the $1m^2$ microplots (439.86 g/m^2), then the 23 ha catchment outlet (204.97 g/m^2), 100 ha catchment outlet (62.93 g/m^2) and finally the 1000 ha catchment outlet (1.98 g/m^2).

In terms of water fluxes (as presented in Figure 3.5), it appeared that on the hillslope, sediment yields increased with greater surface water flux along the hillslope. The sediment yield transport between the hillslope and the 23 ha catchment appeared to be low, as there was difference in sediment yields between the two. The sediment yield data for the 23 ha and 100 ha catchment outlets indicated that there was low continuity, possibly, due to an increase in sedimentation between the two catchment outlets. The 1000 ha catchment outlet sediment

yield data highlights the influence that the storage dams immediately upstream from the sampling site had on the transport of sediments. All soil particles (sand, silt and clay) would have been deposited within the dams. This would have resulted in the decrease in the sediment yield observed at the 1000 ha catchment outlet.

3.5.3 Nitrate concentrations

Table 3.5 displays the basic statistics of the concentration of dissolved nitrates (NO_3^--N) of the nested scales.

Table 3.5 Basic statistics of the concentrations of the dissolved elements and particulate elements of the nested scales (n = 160)

		$1m^2$	$10m^2$	23 ha	100 ha	1000 ha	Hillslope Piezometers	Boreholes
Dissolved (mg/L)								
NO_3^-	Mean	27.10	29.65	14.46	30.58	9.65	40.74	5.18
	Stdev	26.72	25.59	5.71	30.74	1.13	48.98	5.39
P	Mean	0.56	0.50	0.11	0.19	0.06	1.01	0.07
	Stdev	0.58	0.60	0.04	0.11	0.05	1.18	0.05
DOC	Mean	40.52	42.61	15.90	33.65	32.50	105.31	45.39
	Stdev	52.25	43.30	20.29	31.73	36.79	72.56	49.99
Particulate (g/100g of sediment)								
C	Mean	5.82	3.94	4.30	0.10			
	Stdev	1.48	0.99	0.98	1.35			
N	Mean	0.59	0.35	0.24	0.10			
	Stdev	0.23	0.07	1.23	0.64			

The average nitrate concentration for the different scales had a range of between 9.65 mg/l (1000 ha catchment) and 30.58 mg/l (100 ha catchment). Similar nitrate concentrations were found at the $1m^2$ microplot scale (27.10 mg/l) and the $10m^2$ runoff plot scale (29.65 mg/l). The nitrate concentration of the 23 ha catchment scale (14.46 mg/l) was found to be lower than what was found from both sets of runoff plot scales. Therefore, it was apparent that the nitrate concentration decreased from the runoff plot scale to the 23 ha catchment outlet, from where the concentration increased to the 100 ha catchment and, finally, a decrease to the 1000

ha catchment. There was a great deal of variability of the nitrate concentration, with the 100 ha catchment having the highest standard deviation (30.74 mg/l). The monitored scale with the smallest deviation was the 1000 ha catchment (Stdev = 1.13 mg/l).

In terms of the nitrate concentrations for the monitored groundwater sampling points, it was found that there was a higher mean concentration in the hillslope piezometers (40.74 mg/l) than the groundwater monitoring boreholes (5.18 mg/l). The hillslope piezometers showed a variable total phosphorus concentration (Stdev = 48.98 mg/l), with the boreholes being considerably less variable (Stdev = 0.07 mg/l).

From the mean nitrate concentrations of the different sampling points and scales, it was evident that there were possibly three different behaviours occurring within the catchment. Firstly there appears to be some sort of nitrate depletion from the hillslope (the $1\times1m^2$ microplot scale, the $5\times2m^2$ runoff plot scale and the hillslope piezometers) to the 23 ha catchment. Secondly, it would seem, as if there were other sources contributing to the 100 ha catchment. Thirdly, the 1000 ha catchment had a similar nitrate concentration to the deep groundwater/boreholes.

3.5.4 Total phosphorus concentrations

Table 3.5 shows the basic statistics of the concentration of dissolved total phosphorus of the nested scales. The mean concentration of the total phosphorus for the monitored surface scales has a range between 0.06 mg/l (1000 ha catchment) to 0.56 mg/l ($1m^2$ microplots). This is similar to the behaviour of the nitrate concentration, where there were similar total phosphorus concentrations for both the $1\times1m^2$ microplot scale and the $10m^2$ runoff plot scale (0.5 mg/l). The mean total phosphorus concentration decreased at the 23 ha catchment outlet (0.11 mg/l) and then increased at the 100 ha outlet (0.19 mg/l). Finally, the total phosphorus decreased from the 100 ha catchment outlet to the 1000 ha catchment outlet (0.06 mg/l). The total phosphorus concentration was the most variable at the $10m^2$ runoff plot scale (Stdev = 0.60 mg/l) with the 23 ha catchment outlet being the least variable (Stdev = 0.04 mg/l).

In terms of the concentration of total phosphorus for the monitored groundwater zones, there was a higher concentration for the shallow groundwater (1.01 mg/l for the hillslope piezometers) than the deep groundwater (0.07 mg/l for the boreholes). There were

fluctuations in the measured total phosphorus concentration for the Hillslope piezometers (Stdev = 1.18 mg/l), with the borehole total phosphorus being less variable (Stdev = 0.05 mg/l).

3.5.5 Dissolved organic carbon concentrations

Table 3.5 displays the basic statistics of the concentration of DOC at the different nested scales. The mean DOC concentration ranged from 15.90 mg/l (23 ha catchment outlet) to 42.61 mg/l ($5\times2m^2$ runoff plots) for the surface hydrological process zones monitored. The $1m^2$ microplots had a mean DOC concentration that was slightly lower than that of the $10m^2$ runoff plots (40.52 mg/l). From the 23 ha catchment outlet, the mean DOC concentration was found to have increased at the 100 ha catchment outlet (33.65 mg/l), possibly as a result of additions coming from elsewhere in the landscape. The mean concentration of DOC at the 1000 ha catchment outlet was 32.50 mg/l, which was only slightly lower than that of the mean DOC concentration at the 100 ha catchment outlet. The standard deviations of the different sampling sites indicated highly variable DOC concentrations, with the Stdev varying between 31.73 mg/l (100 ha catchment outlet) and 52.25 mg/l ($1\times1m^2$ microplots).

The mean DOC concentration for the two different subsurface monitoring zones showed that the hillslope piezometers had a higher mean DOC concentration (105.31 mg/l) than the boreholes (45.39 mg/l). It was found that the mean DOC concentration was more variable in the hillslope piezometers (Stdev = 72.56 mg/l) than in the monitored boreholes (49.99 mg/l).

3.5.6 Nitrate loads

The cumulative nitrate loads for the different scales for the period of October 2010 to April 2011 is shown in Figure 3.7. From Figure 3.7, it is noticeable that the nitrate loads at the different monitored scales are inherently different. The curves show that for all scales, there was a consistent and steady yield of nitrates coming from these scales. However, the 100 ha catchment outlet showed the greatest change in nitrate loads *i.e.* the greatest instantaneous change in cumulative nitrate loads.

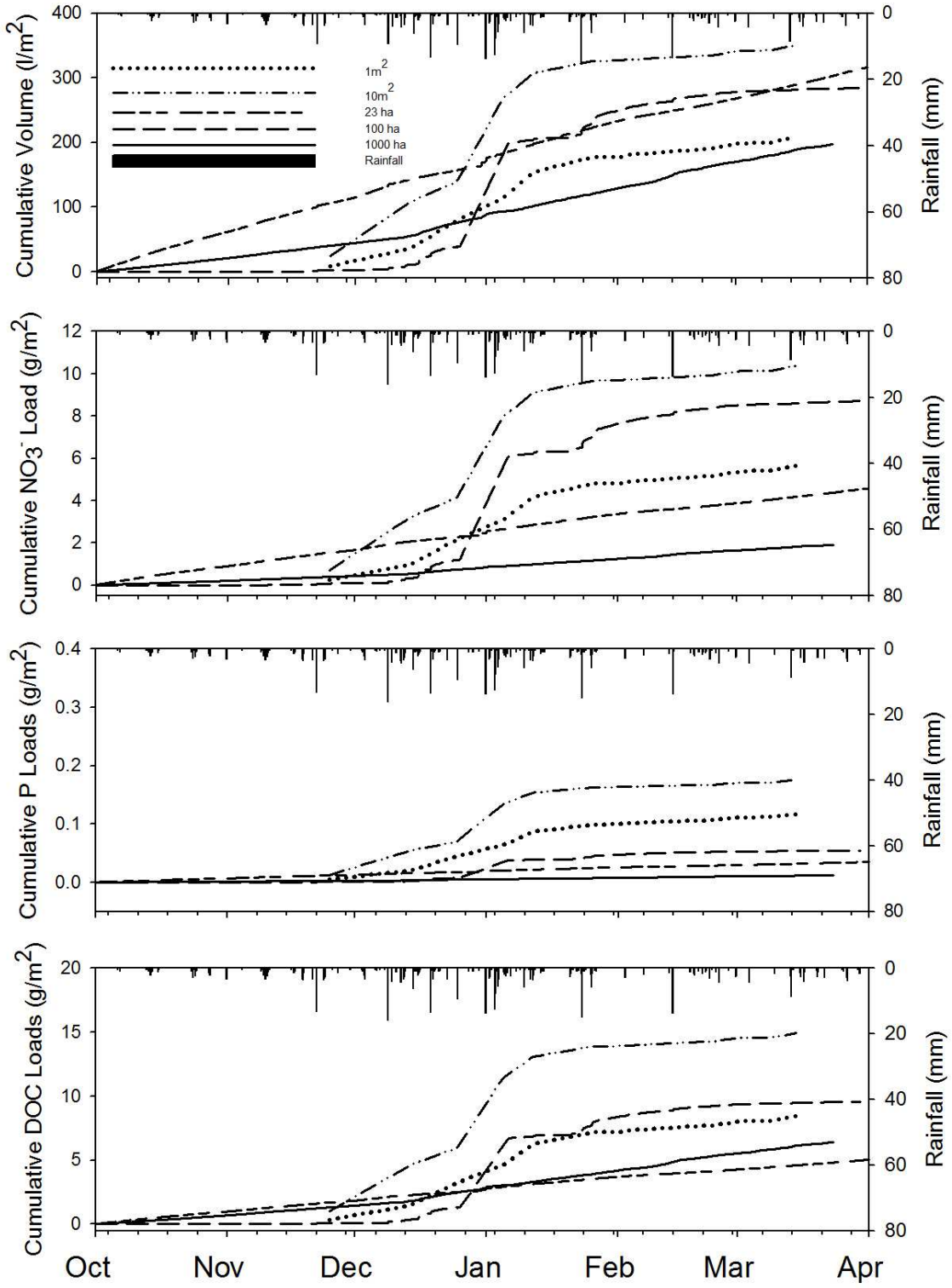

Figure 3.7 Cumulative Dissolved Nutrient Loads (in g/m^2) of the different nested scales for the 2010-2011 rainfall season

The range of the cumulative nitrate loads for the different monitored scales was between 0.04 g/m^2 (1000 ha catchment outlet) and 10.38 g/m^2 (5×2m^2 runoff plots). The scale with the second highest nitrate yield was the 100 ha catchment outlet (8.7 g/m^2), followed by the

$1\times1m^2$ microplots (5.65 g/m^2) and the scale with the fourth highest nitrate yield was the 23 ha catchment (4.57 g/m^2).

From the curves plotted, it was noticeable that the monitored scales located on the hillslope had different yields. It appears that there could be a link between the nitrate loads occurring as overland flow over long distances. However, the nitrate loads for the 23 ha catchment outlet were lower than that of both the microplot and plot scales. From the 23 ha catchment outlet to the 100 ha catchment outlet, the nitrate loads increased, indicating that there have been some additions of nitrate from the landscape between the two monitored scales to the streamflow. Further along the stream, the nitrate load decreases to the 1000 ha catchment outlet. The influence of the two small storage dams located upstream from the sampling point may have had an impact on the nitrate loads calculated at the 1000 ha catchment. The dams would impact the nitrate by storing and impeding the transport of the Nitrates further downstream.

3.5.7 Dissolved organic carbon loads

The cumulative DOC loads (g/m^2) of all monitored scales for the 2010-2011 rainy season are shown in Figure 3.7. The yields of the three catchments did not initially vary. However, due to the consistent flow occurring at the 23 and 1000 ha catchment outlets, there was a consistent load of DOC at these two catchment outlets. The 100 ha catchment outlet only started transporting DOC loads when some flow occurred, but the 100 ha catchment outlet was the monitored scale that exhibited the steepest cumulative curve. The hillslope scales ($1\times1m^2$ microplots and the $5\times2m^2$ runoff plots) were the last scales to respond, with the 5mx2m runoff plots being more responsive than the 1mx1m microplots.

In terms of the final cumulative DOC load values for the different scales, the $5\times2m^2$ runoff plots had the highest DOC yield (14.92 g/m^2). This was then followed by the 100 ha catchment outlet (9.58 g/m^2), $1\times1m^2$ microplots (8.44 g/m^2), the 1000 ha catchment outlet (6.42 g/m^2) and finally the 23 ha catchment outlet (5.03 g/m^2).

The different accumulated yields for the monitored scales located on the hillslope could be attributed to the greater overland flow response of the $5\times2m^2$ runoff plots. There was a decrease in the DOC load from the hillslope to the 23 ha catchment outlet. In contrast, there was an increase in the DOC load from the 23 ha catchment outlet to the 100 ha catchment

outlet. There was increase in the DOC load from the 100 ha catchment outlet to the 1000 ha catchment outlet.

3.5.8 Total phosphorus loads

Figure 3.7 shows the cumulative total phosphorus loads of the different nested scales for the 2010-2011 rainy season. The cumulative total phosphorus load (g/m^2) curves for all five monitored scales within the Potshini Catchment, indicate that the Total phosphorus loads did not initially vary. However, the first observation scale to have a response (an increase in curve gradient), in terms of total phosphorus yield, was that if the $10m^2$ runoff plots. The next scale to exhibit a change in its load of total phosphorus was that of the $1m^2$ microplots, followed by the 100 ha catchment outlet, the 23 ha catchment outlet, and finally, the 1000 ha catchment outlet.

The final cumulative total phosphorus yields showed that the order of the highest yields was as follows: $10m^2$ runoff plots (0.18 g/m^2), $1m^2$ microplots (0.12 g/m^2), 100 ha catchment outlet (0.05 g/m^2), 23 ha catchment outlet, and finally, the 1000 ha catchment outlet (0.01 g/m^2). There were similar loads for the monitored scales at the hillslope scale, with the $10m^2$ runoff plots (larger scale) having a slightly greater Total phosphorus yield of 0.18 g/m^2 than the $1m^2$ microplot scale (0.12 g/m^2). When comparing the hillslope scale to the 23 ha catchment outlet, the catchment loads decreased from the hillslope. However, the loads increased from the 23 ha catchment outlet to the 100 ha catchment outlet. This indicated that there were additions to the system between the two observation scales. The 1000 ha indicated that there was a net loss in the total phosphorus load, which could be caused by retardation and storage within the storage dams located immediately upstream of the observation scale.

3.5.9 Particulate organic carbon loads

In Table 3.5, the mean particulate organic Carbon (POC) concentrations for the different scales are shown. The scale with the highest mean particulate C were those of the $1m^2$ microplots (5.8 g C/100g sediment). The scales with the next highest amount of mean particulate C was that of the 23 ha catchment outlet (4.30 g C/100g sediment) followed by the $10m^2$ runoff plots (3.94 g C/100g sediment), and finally, the 100 ha catchment outlet (0.10 g C/100g sediment). The nested scale with the most variable particulate C was that of the $1m^2$

microplots (Stdev = 1.48 g C/100g sediment) and the least variable nested scale was the 23 ha catchment outlet (Stdev = 0.98 g C/100g sediment).

Figure 3.8 displays the yields of particulate nutrients for all the nested scales monitored. In terms of the particulate C yields, there was a high spatial variability. At the hillslope scale, the $5\times2m^2$ runoff plots had a higher particulate C yield (26.91 g/m^2) than the $1m^2$ microplots (25.51 g/m^2). The particulate C yield decreased from the hillslope to the 23 ha catchment outlet (8.18 g/m^2) and decreased even further to the 100 ha catchment outlet (0.06 g/m^2).

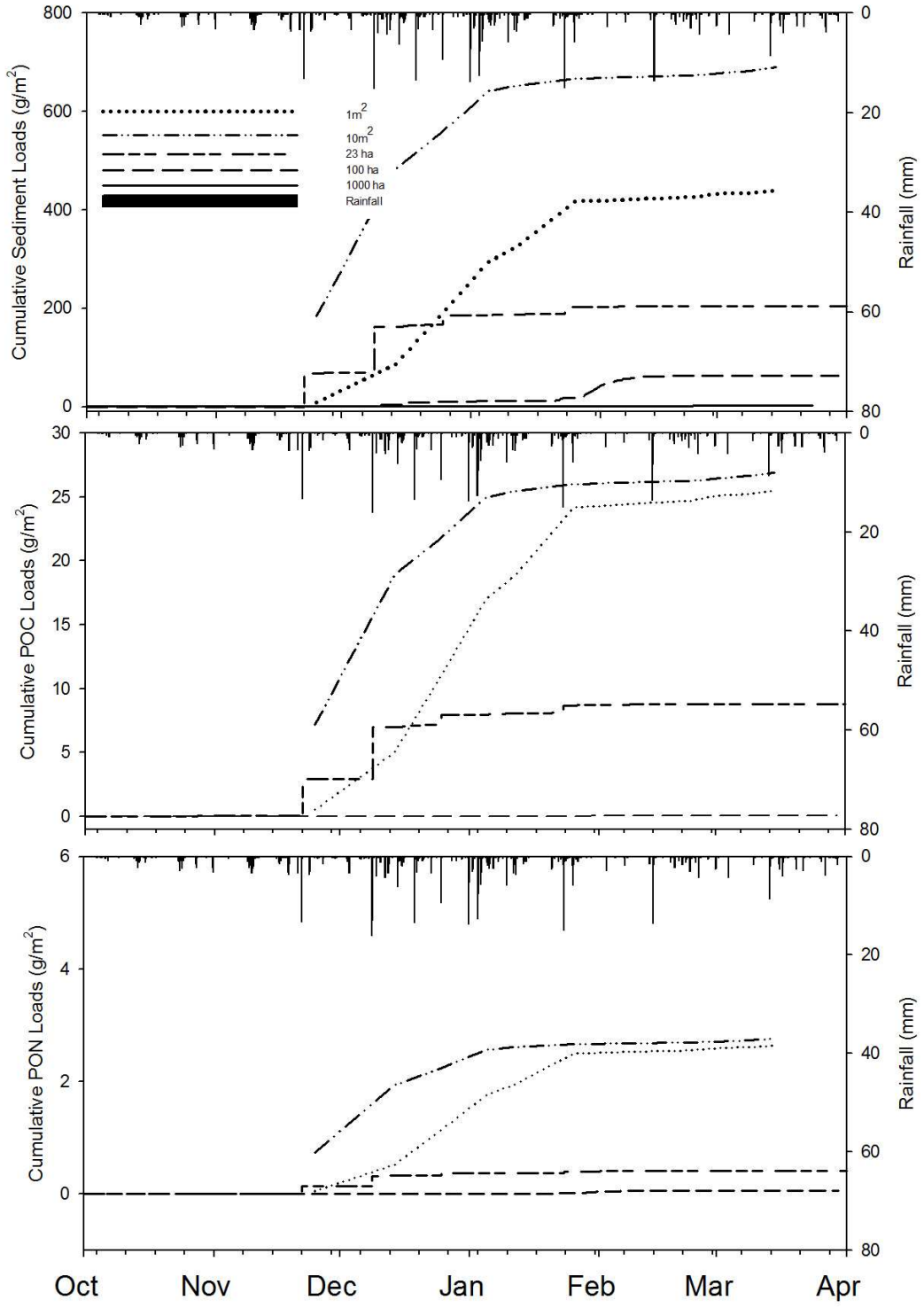

Figure 3.8 Sediment Loads and selected particulate nutrient loads of the different scales monitored for the 2010-2011 season

3.5.10 Particulate organic nitrogen loads

Table 3.5 lists the different scales' mean particulate organic nitrogen (PON) values per 100 grams of sediment. The scales with the highest composition of PON was the 1 m^2 microplots (0.59 g N/100g sediment). The scale with the next highest PON composition was that of the 10 m^2 runoff plots (0.35 g N/100g sediment), then the 23 ha catchment outlet (0.24 g N/100g sediment) and then, finally, the 100 ha catchment outlet (0.10 g N/100g sediment). The scales were found to have variable PON compositions, with the 23 ha catchment outlet being the most variable (Stdev = 1.23 g N/100g sediment) and the 5×2m^2 runoff plots being the least variable (Stdev = 0.07 g N/100g sediment).

Figure 3.8 shows the PON yields for all of the different nested scales. There was a distinct spatial variability in the loads of PON. The nested scale with the highest particulate N yield was that of the 10m^2 runoff plots (2.76 g/m^2). The nested scale with the second highest PON yield was that of the 1m^2 microplots (2.64 g/m^2). Following the 1m^2 microplots, the 23 ha catchment outlet was the third highest PON yield (0.41 g/m^2). Finally, the nested scale with the fourth and lowest PON yield was that of the 100 ha catchment outlet (0.06 g/m^2).

3.6 Isotopic and Tracer Data

The concentration of selected dissolved elements as a function of distance from the catchment upper limit are displayed in Figure 3.9.

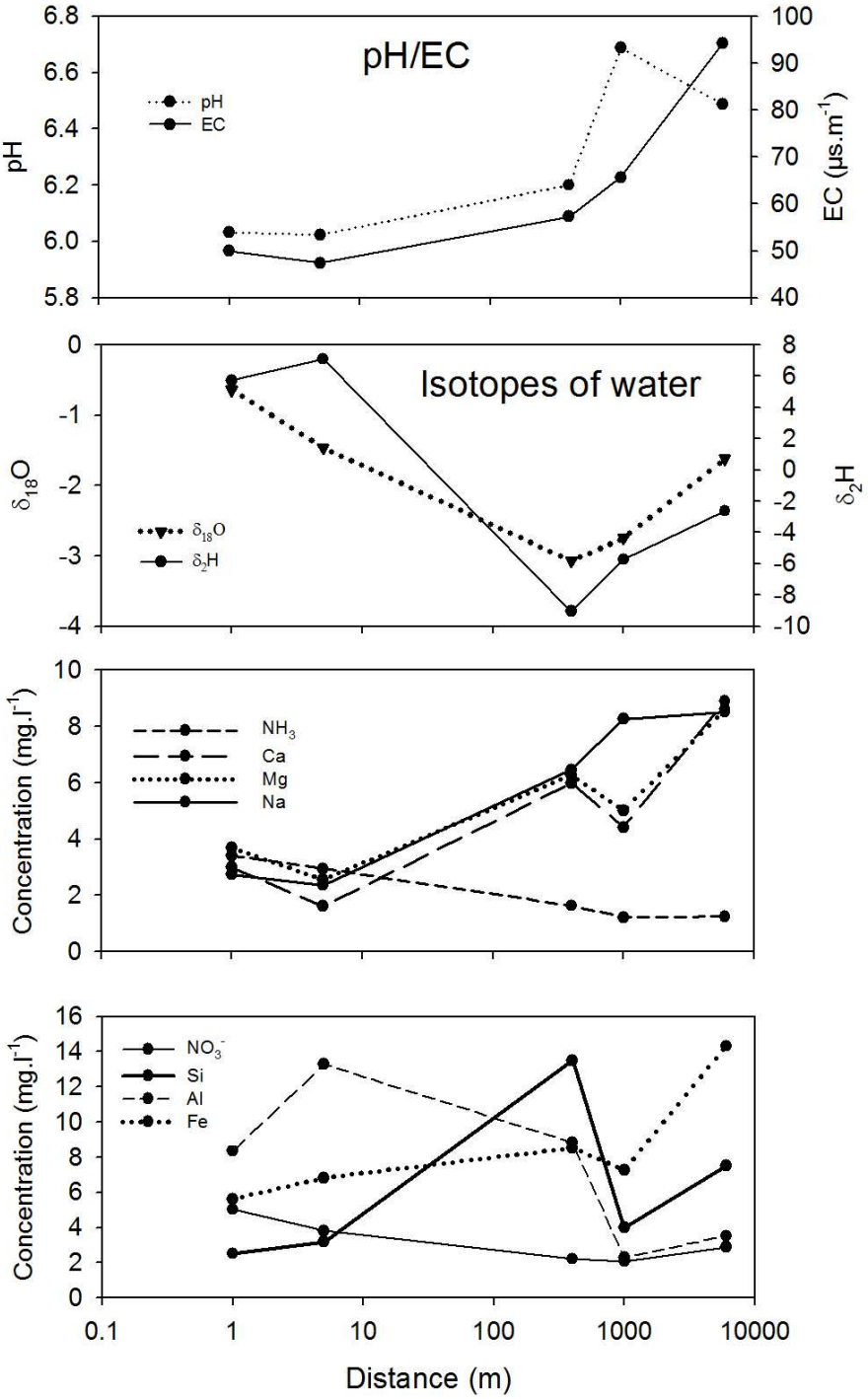

Figure 3.9 Concentration of selected dissolved elements as a function of distance from catchment upper limit

Water collected from microplots (Distance of 1m), plots and the 23 ha catchment outlet (distance=600m) were enriched in N-NH_3, N-NO_3^-, Al, and depleted in Na, Si, Mg, Ca. The 23 ha catchment outlet water showed a higher concentration in Si, Fe, Ca, Mg, Na than the hillslope runoff, but showed similar concentrations as water sampled from the piezometers.

The deep groundwater (25 meters depth) was depleted in most of the measured elements, such as, both N species, Fe, Mg and Al, but enriched in Na (24mg/L). The water from the 100 ha catchment outlet exhibited a depletion in these elements, except Na, which was found in much higher concentrations than at the other spatial scales. The 1000 ha catchment outlet showed enrichment in all elements, especially Ca, Mg, Fe and Si, while N and Na concentrations remained in the same order, as found at 100 ha catchment outlet. Figure 3.9 displayed the evolution of isotopes from the hillslope to the 1000 ha catchment outlet. The general pattern within the landscape was for both isotopes to be depleted from 1m² to 23 ha catchment outlet and to afterwards increase to the 1000 ha catchment outlet.

Both stable isotopes ($\delta^{18}O$ and deuterium) showed similar patterns of fluctuation among the seasons, implying that the travel-time distributions of both tracers have similar shapes (Figure 3.9). Small plots runoff and shallow groundwater of the hillslope tracked the rainfall signature closely. Important variations were observed from one event to another with values ranging from $\delta_{18}O$ 0.71 to -3.90‰, δ_2H 26.85 to -14.95‰ for rain and -2.63 to -6.44‰, δ_2H 38.92 to -30.86‰ for plots; while 23 ha, 100 ha and 1000 ha outlets and groundwater remained constant with $\delta_{18}O$ mean values of -3.26, -2.60, -1.62, -3.73‰ and δ_2H of -8.79, -5.38, -2.63, -14.37‰ respectively.

The use of single elements, individually, does not allow adequate insights into the mixing occurring within a catchment. The use of water isotopes in conjunction with chemical elements in Equations 2.4 to 2.6 allowed end member mixing analysis for the period from 22 February to 1 April 2011 and for all 3 monitored catchments to be performed.

The mean contributions of the three selected water sources (Overland Flow, Soil Water, Groundwater) are presented in Table 3.6. This gives an indication and insight into the spatial variations of the runoff generated at the different scales.

Table 3.6 The mean contribution of the three main water sources for the three catchment scales

	23 ha	100 ha	1000 ha
	----------%		----------
Overland Flow	22	22	8
Soil Water	15	28	37
Groundwater	63	50	55

The results presented are an initial attempt (*i.e.* the first time that this technique has been performed in this specific catchment) at performing general estimates of the sources contributing to runoff at the three monitored catchment outlets. Groundwater contributed the most to runoff fluxes at all the three nested catchments. The mean groundwater contribution was 63% at the 23 ha catchment outlet, 50% at the 100 ha catchment outlet and 55% at the 1000 ha catchment outlet. The mean soil water contribution to catchment runoff increased from 15% at the 23 ha catchment outlet to 28% at the 100 ha catchment outlet, and to 37% at the 1000 ha catchment outlet. Overland flow contribution was almost stable at 22% at the 23 ha catchment outlet and 22% at the 100 ha catchment outlet, but highly decreased to 8% at the 1000 ha catchment outlet. From these results, there was a general trend for soil water contributions to increase with the increase in catchment size. The relative overland flow contribution was similar at the 23 ha catchment and 100 ha catchment outlets, but was much lower at 1000 ha catchment outlet. Groundwater was the major contributor at all scales.

The evolution over time of the contribution of the three water compartments at the 23 ha catchment outlet and the 100 ha catchment outlet are displayed in Figures 3.10 and 3.11, respectively. On 22 February 2011 the antecedent cumulative precipitation was 22.8 mm and 31.2 mm for the previous 3 and 7 days, respectively, which can be considered as a rainy period. A dry spell occurred between the 3rd to the 15th of March, followed by a wet period. As discussed earlier, the calculation of the mixing of sources at the 1000 ha catchment outlet showed that the largest contribution to catchment runoff was that of groundwater during both events and periods of low flow. This approach allowed for an insight into the temporal variations of the sources of runoff at the catchment outlets in conjunction with the spatial variations of catchment runoff at different scales.

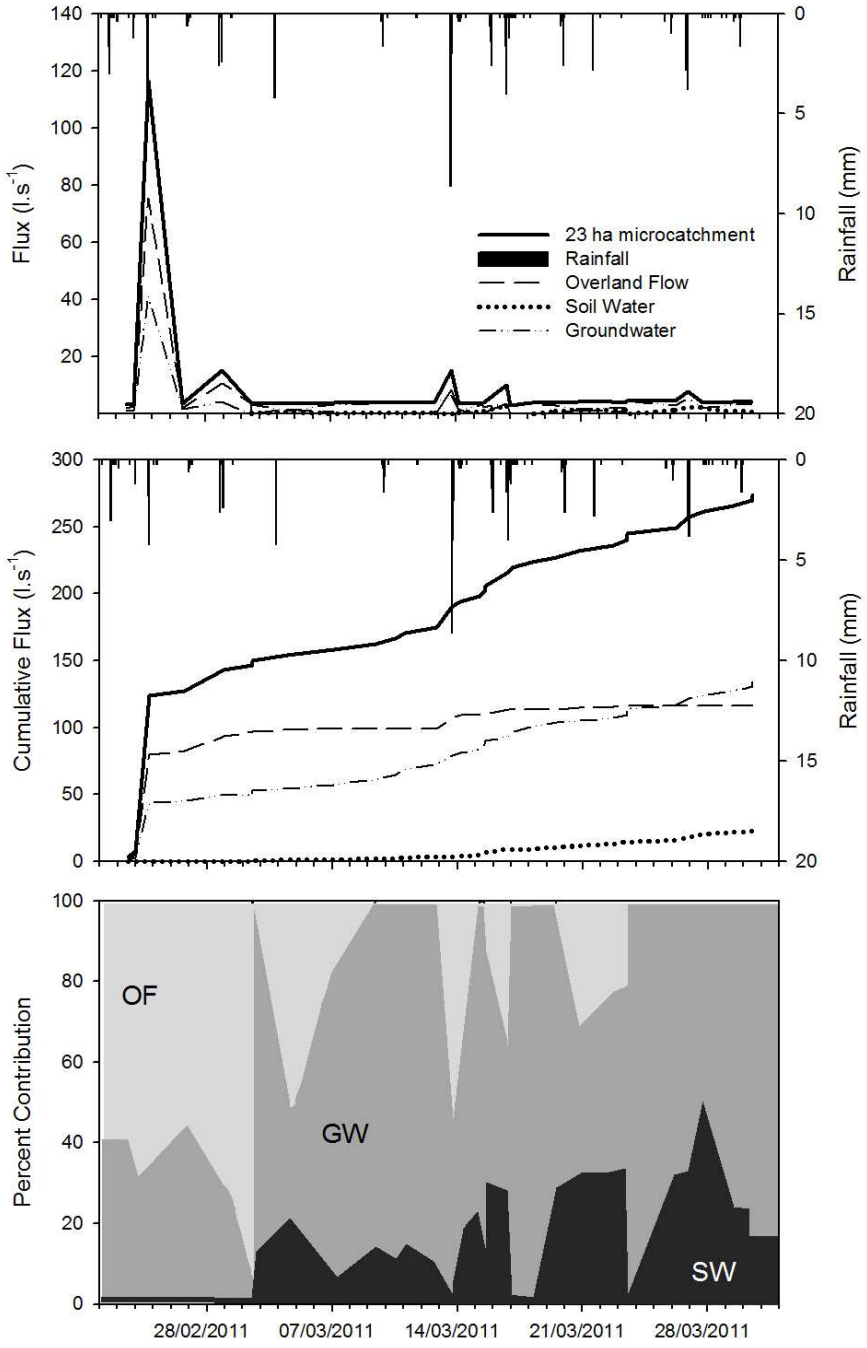

Figure 3.10 Mixing of the sources contributing to catchment runoff at the 23 ha catchment outlet

Overland flow was, with 60%, the highest contributor at the 23 ha catchment to runoff during the initial rainfall event on 25 February 2011. It increased to 97% on 2 March 2011. Over time, the OF contributions decreased, which coincided with increased contributions from soil water. OF contribution was 0% during the dry spell of the first half of March and towards the end of the period. Soil water, that initially contributed nothing to the catchment runoff,

increased over time with a peak at 51% on 27 March 2011. A reason for the low initial contribution of soil water is that the water from the first rains is stored in the soil profile, rather than moving through it. Once the soil moisture deficit was satisfied, soil water contributions increased. However, soil water started contributing on 2 March 2011, after which soil moisture consistently contributed water to catchment runoff. Groundwater contributions at the catchment outlet were 100%, the highest during periods of low flow when there was no rainfall. Groundwater still contributed to catchment flow during events, but the contribution was low (the lowest event contribution being 2.5%).

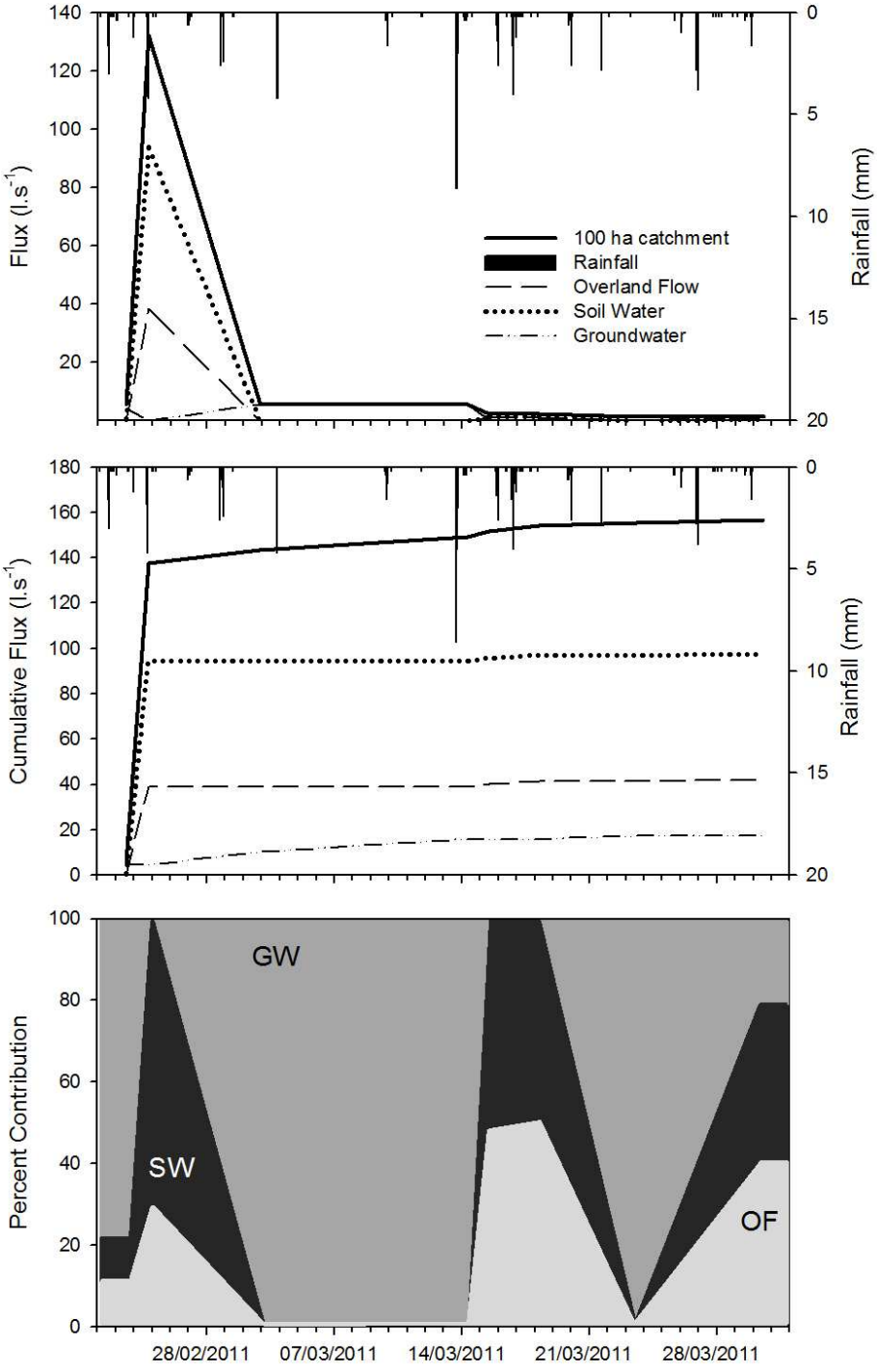

Figure 3.11 Mixing of the sources contributing to catchment runoff at the 100 ha catchment outlet

The mixing of the sources contributing to catchment runoff at the 100 ha catchment are shown in Figure 3.11. Soil water had the greatest contribution (40%) to catchment runoff at the initial storm, followed by OF (30%) and groundwater (30%). Groundwater contribution

was 100% during periods of low flow. For two out of the three distinct events of the period for the 100 ha catchment outlet, soil water and overland flow contributed similar amounts of water to the catchment runoff (50% contributions from each of soil water and overland flow). The event which occurred on 24 February 2011 had a 71% contribution from soil water and 21% from overland flow. It was found that soil water and overland flow only contributed to catchment runoff during events.

4. DISCUSSION

4.2 Spatial and Temporal Variations of Overland Flow and Controlling Factors

4.2.1 Spatial variations of total OF

As expected, it was found that the amount of OF generated varied within seasons in response to variations in rainfall characteristics (Bartley *et al*., 2006; Bautista *et al*., 2007). For any given rainfall, OF response was found to be highly variable within the catchment. Since OF is primarily controlled by the response of the soil surface to rainfall, any variations in rainfall characteristics will cause a large degree of variability in the overland flow that is produced by a rainfall event. The highest volume of OF was generated at the bottomland position, followed by the midslope, whilst the lowest was observed at the footslope. The link between total OF and selected environmental factors of control shows that higher OF generated at the midslope can be explained by the higher occurrence of soil crusting (Dlamini *et al.*, 2011). These results also confirm previous observations by Chaplot *et al.* (2007), where soil crusting was found to mainly control OF in the sloping lands of south-east Asia. Similar results where the soil surface features controlled OF were found by Descheemaeker *et al.* (2006) in a study conducted in the Ethiopian Highlands. The present study confirms the major effect that soil surface conditions such as crusting has on OF volumes. What could be considered here as new is the fact that the impact of soil surface conditions may vary over time and especially as a function of the soil water status. Indeed, field observations of water fluxes at the different scales show that unless the soil profile was saturated by water, there was little connectivity between the different landscape compartments. Fluxes were found to be higher when the catchment was wet and whatever the soil surface conditions (*i.e.* the condition of the soil surface with respect to crusting, and percentage of the soil surface covered by vegetation), soils were producing similar amounts of OF. There is indeed a need to investigate the threshold value of soil water saturation where OF diminishes. It is the author's belief that when the soil is dry, crusting is likely to play a major role, while when soils wet up, the crusting impact on OF is likely to diminish.

4.2.2 Temporal variations of overland flow

In addition to the spatial variation across the landscape of total OF, were variations of time to runoff initiation (TRI) with a three year average ranging from 0.2 to 6.4 minutes. TRI was found to be the lowest in the bottomlands and the highest at the footslope. This order of response was identical to that of total OF, meaning that the locations that produce the largest amount of OF also showed the fastest OF generation. TRI was highly spatially variable and this confirms several studies focussed on soil infiltration and OF generation. At a nearby site under soil and land use conditions but with a greater range of soil crusting, Podwojewski *et al.* (2011) using a rainfall simulator found large variations in OF response to rainfall. TRI estimated from the infiltration curves of a 30 $mm.h^{-1}$ rainfall event ranged from less than two minutes to about five minutes. This TRI range is in accordance with the results that were found in the present study. Similar results were found in the study by Devaurs and Gifford (1984) in the rangelands of Idaho, USA (0.6 <TRI<24 min.). The following part of the discussion investigates the reasons of such high variations in TRI.

The results showed that within hillslopes, bottomlands exhibited a unique behaviour in respect to TRI. The bottomlands, with a full surface coverage by vegetation and little to no crusting, showed infiltration coefficients of either 100 or 0 percent *i.e.* a TRI of 0 seconds or no response at all (infinity). The multivariate analysis performed on the data from this slope position, revealed that cumulative rainfall and soil water tension were the only controlling factors of TRI. TRI was found to be greater early in the rainy season because of dry soil conditions (low cumulative rainfall and high soil water tensions). After a certain cumulative rainfall threshold necessary for the entire soil profile of the bottomland location to become saturated, TRI was found to be 0 sec., indicating instantaneous response to rainfall regardless of the characteristics of the event.

The rest of the hillslope exhibited a different behaviour. The multivariate analysis indicated that TRI was primarily controlled by soil and soil surface characteristics, rather than the soil water status and rainfall conditions. Among the soil surface characteristics, coverage and crusting have been shown to play an important role, with TRI decreasing as soil surface crusting increases. Ben-Hur *et al.* (1985) similarly found that soil crusting has a large influence on the infiltration process and hence overland flow. Podwojewski *et al.* (2011) explained that the differences in overland flow response can be a result of the different soil

surface coverage and crusting, where areas with low soil surface coverage by vegetation and high crusting were found to have a faster response. Soil surface features impact overland flow through changes in soil porosity. The transport of water through the soil takes place in the pore spaces between soil particles and soil aggregates. Soil crusts are the surface layers of soils, which are harder and less permeable than the underlying soil. Soil crusts are formed by disaggregating compound soil particles (sand, silt, clay), which reduces soil porosity of different particle sizes (Dexter and Richard, 2009), thus explaining the link between soil crusting and soil infiltration by water. Greater TRI values at higher vegetation coverage values can be explained, according to Dexter (1988), by features such as plant roots and associated biopores. Miyata *et al.* (2010) suggested that the difference in infiltration along a slope can be explained by the rapid infiltration related to macropore flow. From these results, areas with a high degree of excess soil saturation or areas with a large degree of soil surface degradation will generate OF quickly and will therefore have a low TRI.

Soil characteristics were shown to be key in the control of TRI over the area. The different soil types found within the catchment, whilst similar, displayed different TRI characteristics, as shown in a box plot of TRI, as a function of soil types found in the study catchment (Figure 4.1).

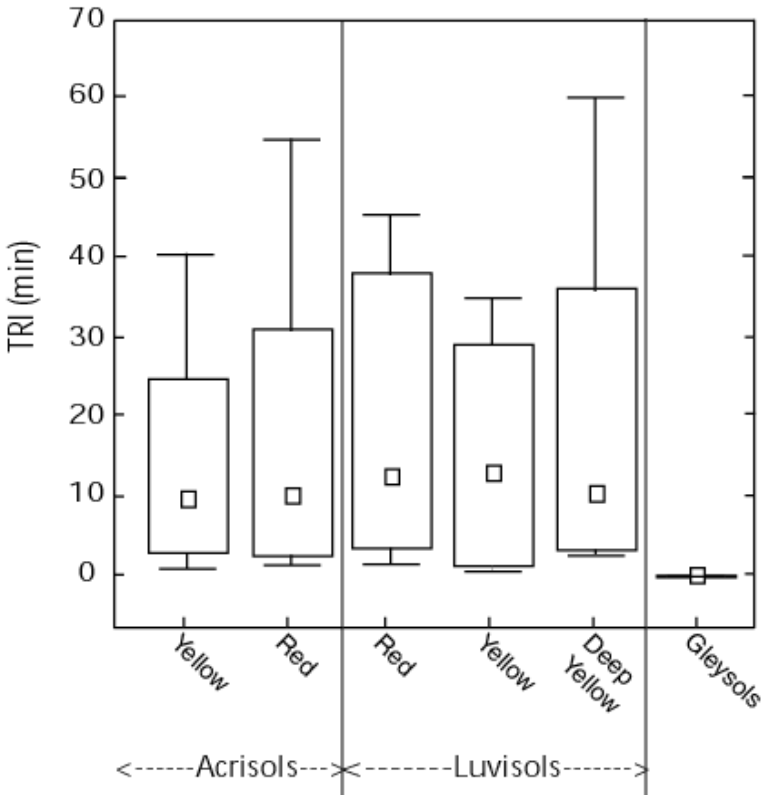

Figure 4.1 TRI as a function of soil types found in the study catchment

The quickest response and lowest TRI values in the catchment were Gleysols, followed by Acrisols with the greatest delay in OF generation occurring in Luvisols found within the catchment. With the use of this finding, the ranking of each of the 6 soil types', found within the catchment, response to three rainfall events and the study based averagw has been ranked (Figure 4.2).

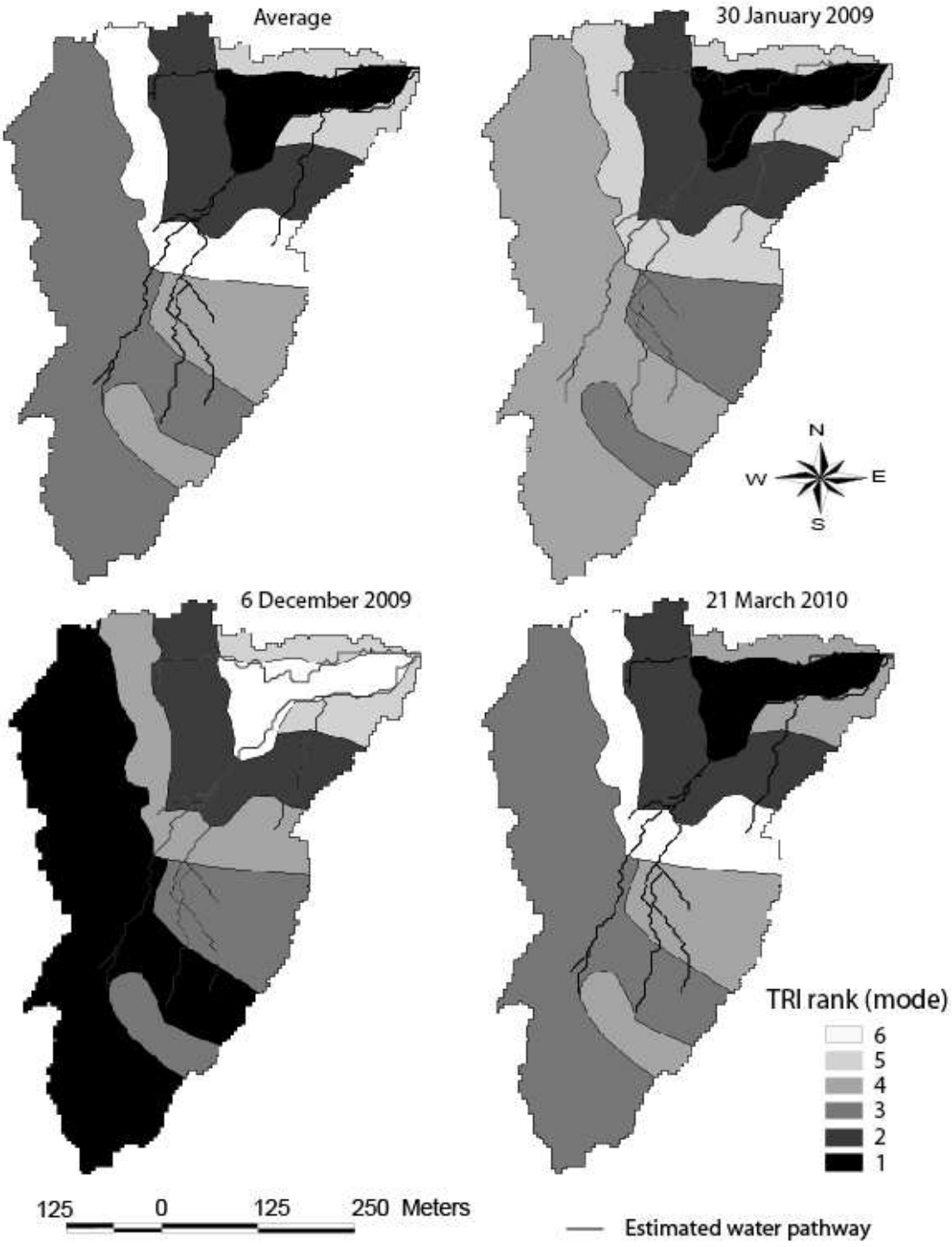

Figure 4.2 TRI ranking for three rainfall events of the 2007-2010 period

Such an approach allows for predictive modelling and assumptions to be made in different catchments in terms of OF response to rainfall. However, some considerations need to be made. As the highest and lowest TRI values were found in the soil types with the lowest soil clay content, soil clay content cannot be the sole explanatory variable for the differences in soil type response. Wakindiki and Ben-Hur (2002) suggested that clay mineralogy and aggregate stability can play an important role in the control of overland flow highlighting the need to further investigate the soil type effect on TRI. Moreover, TRI was shown to increase as soil clay content increased confirming the previous work conducted by Van Es *et al.* (1991) which contradicted the previous results of Williams *et al.* (1981). The positive correlation between clay content and TRI might be explained by the presence of stable aggregates, which as reported by Dlamini *et al.* (2011), decreases soil disaggregation therefore allowing for high infiltration rates and delayed overland flow generation.

This study has added to the previous knowledge in the sense that it allowed to rank the importance of the different factors that control TRI, with soil surface conditions playing a major role, followed by soil characteristics. Soil water content becomes predominant when soils get waterlogged. This, not only occurs in the bottomlands during the wet season, but further up hillslopes, as a soil profile increases in saturation. These results seem to indicate that OF within the area is of two types *i.e.* saturation excess (in the bottomland) and Hortonian (on the rest of the hillslope). Again, it would be prudent to investigate the ranking between such factors of control, before and after the soils get wet.

A final aspect to be discussed, is the generation of a predictive tool for TRI spatio-temporal variations. According to the linear regression models derived, crusting was able to explain over half of the variations for all rainfall events, as illustrated by the strong linear relationships. Therefore, in areas with a high proportion of the soil surface covered by crusts, the models will predict that the TRI will be low. A limitation to this approach is the exclusion, within these models, of the saturated areas within the catchment (*i.e.* Bottomlands) and thus, will be potentially responsive to rainfall events. Consequently, since the results used to derive these simple models were obtained from only 6 microplot locations some caution needs to be taken. Extrapolating the results from relatively few $1m^2$ micro-plots to an entire catchment should be performed with caution.

4.3 Changes in Water Quantity and Quality Across the Scales

Delivery ratios of the fluxes of runoff, selected nutrients and sediments yields (calculated from the end of the 2010-2011 rainy season) can be calculated by using the data from Figures 3.7 and 3.8, respectively. The scale ratio was defined as the ratio of water and nutrients transported and measured from one observation scale to the next. Therefore, for example, a scale ratio of 1for runoff would indicate that there was the same amount of water generated per unit area from one scale to the next. Scale ratios greater than 1 indicated that more water or nutrients were measured at the downstream scale than the upstream scale. Scale ratios less than 1 indicated that the water nutrients per unit area decreased form one scale to the next. Subsequently, Figure 4.3 shows a summary of the runoff, DOC, POC, nitrates and sediment yields observed at the nested spatial scales ranging from 1 m^2 to the 1000 ha catchment outlet of the 2010-2011 rainy season. Please note that the plot scale refers to the 10 m^2 runoff plot

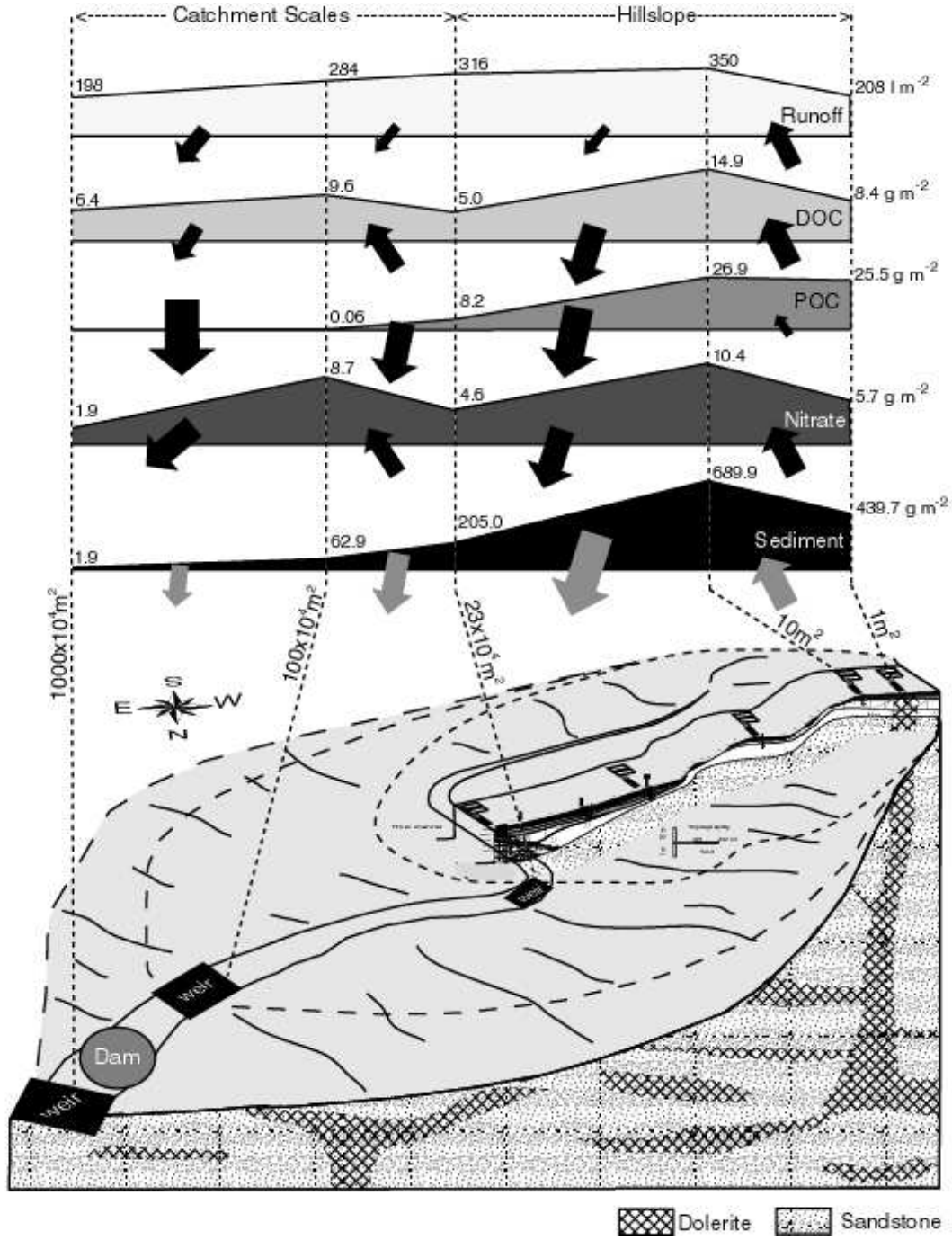

Figure 4.3 Runoff, DOC, POC, Nitrates and sediment yields observed at the nested spatial scales ranging from 1 m² to 1000 ha for the 2010-2011 rainy season

The scale ratio between the microplot and plot scales was 1.68. The scale ratio was 0.90 between plot and 23 ha catchment outlet (*i.e.* the water flux at the 23 ha catchment outlet was 10% lower than that of the plot level); 0.89 between the 23 ha catchment and 100 ha catchment outlets; and decreased sharply to 0.70 between the 100 and 1000 ha catchment outlets. The scale ratios for the period of 2010-2011 calculated showed that there was a steady decrease in the delivery of water from the hillslope scale (*i.e.* overland flow measured at the

plot scale) to the catchment scale. The scale ratio calculated from plot to hillslope was considerably higher than other scale ratios from other regions in the world. Among the few studies available, Chaplot and Poesen (2012) found the delivery ratio between plots and catchment was 0.04, meaning that the catchment yearly flux of water was only 4% of plots' yearly flux. Conversely, the scale ratio calculated from the hillslope to the 23 ha catchment outlet of 0.9 was considerably lower than the ratio of 21.7 obtained in Laos by the same authors. Chaplot and Poesen (2012) state that the lower deliveries (of their study) at the catchment outlet compared to the plot level was likely to come from the infiltration of water on the lower portions of slopes, which are later re-introduced within the catchment. This behaviour has been shown in other studies under different environmental conditions (Cammeraat, 2004; Bracken and Croke, 2007). The increase of the runoff delivery from the hillslope to the catchment level by a factor 21.7 in Laos (Chaplot and Poesen, 2012) was likely due to the contribution of saturation overland flow at the foot of the hillslopes (originating as hillslope seepage). This was observed at the same site in Laos by Vigiak *et al*. (2008).

The results (*i.e.* a 0.9 delivery ratio between the plot and 23 ha catchment scales) tended to show a continuity of overland flow from plot to the 23 ha catchment outlet. However, there might be either a continuity of overland flow or the infiltration of overland flow on hillslopes, subsurface downslope water movements and seepage into the river channel. Those two hypotheses could be valid but runoff data alone cannot be used to support one or the other. The tracer data and end member mixing analysis highlighted the fact that sub-surface water contributions increased at both the 23 ha catchment and 100 ha catchment outlets, as the soil moisture status increased. Field observations identified that infiltration, followed by, wetting up of the soil profile and further seepage into the river channel is a dominant process as shown by the many seepage faces observed along river banks (*e.g.* Figure 4.4).

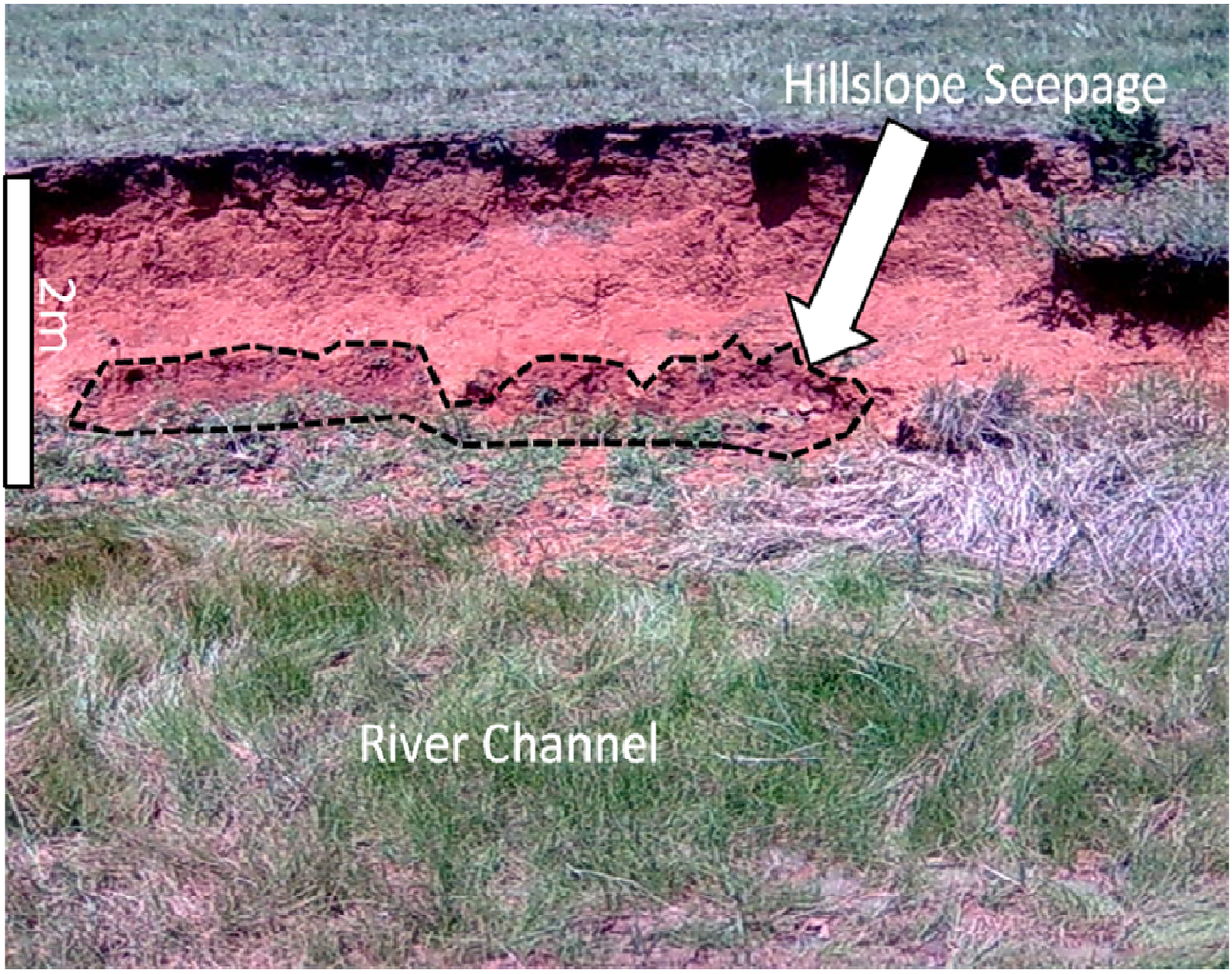

Figure 4.4 Example of hillslope seepage (presented as the darker shade red at the bottom of the channel bank) into the river channel 20 m upstream of the 23 ha catchment outlet (photo taken on 10 February 2010)

Water fluxes subsequently decreased from the 23 ha catchment to the 100 ha catchment outlets by a ratio of 0.89. There might be different processes operating between these monitored scales. From the ratio of 0.89, there could be a relatively low loss of runoff fluxes, by either evaporation or seepage. Other hypotheses such as high losses and gains during the downstream movement of runoff cannot be discarded. Considering the presence of a dense vegetation within the stream channel from the 23 ha catchment to 100 ha catchment outlets, it is the author's belief that evaporation can explain the 10% loss of water volumes per unit area. The differences in fluxes, however, could be the result of errors in the estimation of water fluxes when using weirs or flumes. Continuous calibration of fluxes at monitored scales using complementary methods such as on-site calibration have shown, however, that errors, at least for low flows, are in the order of a few percent (data not presented here).

There was a large decrease of water fluxes per unit area from the 100 ha catchment outlet to the 1000 ha catchment outlet. This could be explained by the presence of the 2 large dams, in-between these nested scales, which is used as storage for irrigation on a commercial farm. Besides water evaporating in the river channel, abstractions from the storage dams for irrigation and the evaporation of water from the dams will decrease the streamflow.

Note that in this evaluation, the data of the 10 m^2 plots were used rather the data of the 1 m^2 microplots as the data representing the water generated on the hillslopes as a methodological error was identified after the research was conducted. The 1 m^2 microplots had a higher density of border perimeter bordering the plot which would cause preferential infiltration to occur and which, ultimately, decrease the amount of overland flow. However, an increase in the runoff generated between the 1 m^2 microplots and the 10 m^2 plots could be a consequence of a greater connection between different surface depressions, which would lead to lower greater connectivity of the overland flow generating areas (Hopp and McDonnell, 2009).

The delivery ratios for sediments was 1.57 between microplot and plot scales; 0.30 between the plot and 23 ha catchment; 0.31 between the 23 ha catchment and the 100 ha catchment; and 0.03 between the 100 ha catchment and the 1000 ha catchment. The ratio between the plot scale and the 23 ha catchment outlet of 0.30 was significantly higher than the range of between 0.01 and 0.1 which has been reported in various studies (Trimble, 1983; Starr *et al.*, 2001; Beven *et al.*, 2005; Rommens *et al.*, 2005; de Vente *et al.*, 2007; Parsons *et al.*, 2006; Walling *et al.*, 2006). The present discussion will not attempt to explain the sources of the eroded sediment at the various nested scales. This has been done in the same Potshini research Catchment by Oakes (2012). Oakes (2012) found that 73% of the sediments lost from the 23 ha catchment originated from the deep soil horizons of the gully banks. This points out that most of the exported sediments do not come from interrill erosion processes on hillslopes but from the collapse of gully banks, which is a continuous process, that has been observed throughout the catchment (Chaplot *et al.*, 2010). Subsequently, it seems that most of the eroded sediments originating from the hillslope are deposited (most likely at footslope positions) before reaching the river system. In response to this trend the recalculated delivery ratio, based on the results from Oakes (2012), is closer to 0.08 than 0.3; which corresponds to the upper range of available studies cited above. There were two other places in the landscape where sediments were deposited further downstream: (1) the river channel due to the decrease

in the mean slope gradient from the 23 ha to the 1000 ha outlets one and (2) the presence of two dams immediately upstream from the 1000 ha catchment outlet.

The selected nutrients were Dissolved Organic Carbon (DOC), Particulate Organic Carbon (POC) and Nitrate (NO_3^-). The sediment delivery ratio between microplots and plots was 1.57. It was 0.30 between plots and the 23 ha catchment and 0.31 between the 23 and 100 ha catchments. The scale ratios of DOC between the overland flow generated on the hillslopes at the plot scale (10 m^2) and the 23 ha catchment was 0.34 *i.e.* the DOC yields at the catchment was 46 percent lower than that of the DOC yields from the plot scale. The delivery ratio between the 23 ha and 100 ha catchments increased sharply to 1.90; and decreased between the 100 ha and 1000 ha catchments to 0.67. The delivery ratio of POC between the microplots and plots was 1.05, which showed that there was more POC transported from the plots than the microplots. A reason for such behaviour can be explained by the different erosion and transport mechanisms occurring at the larger plot scale. Within longer plots there is a combination of both interrill and rill erosional processes, which leads to greater transport of soil particles and entire soil aggregates as shown by Oakes (2012) in the Potshini Catchment. The delivery ratio ratio decreased to 0.30 between the plot and 23 ha catchment outlet; and to 0.01 between the 23 ha and 100 ha catchments. The scale ratio for POC between the 100 and 1000 ha catchment outlets was close to zero since the sediment fluxes at the 1000 ha catchment were minimal.

The NO_3^- delivery ratio was 1.84 between the microplot and plot scales. It sharply decreased to 0.44 between the plot and 23 ha catchment; the delivery ratio between the 23 and 100 ha catchment outlets subsequently increased to 1.90; and finally decreased to 0.22 at the 1000 has.

For both the dissolved nutrients, DOC and NO_3^-, the delivery ratios had similar trends occurring within the landscape. The trend was for the delivery ratio to decrease between the plot and 23 ha catchment (which ranged between 0.34 for microplots and plots; and 0.44 between the plots and the 23 ha catchment); a steep increase between the 23 ha catchment and the 100 ha catchment (exactly 1.90); and a sudden decrease between the 100 ha catchment and 1000 ha catchment, which ranged of 0.67 and 0.22. The decreases from plot scale to the 23 ha catchment can be explained by the associated decrease in delivery ratios of runoff, which can result in differing nutrient yields. This document did not intend to find explanatory

reasons on the variations of nutrient and carbon fluxes across scales. This being said, the increase in both DOC and NO_3^- between the 23 ha catchment and the 100 ha catchment, is likely to come from the decomposition of organic matter, which releases not only CO_2 to the atmosphere, but as well NO_3^- to the water. In addition, the decay of the micro-organisms involved in OM decomposition increases DOC content in the water (Mchunu *et al.*, 2011). Aitkenhead *et al.* (1999) found that the increase in DOC concentration in streams correlated to the amount of wetlands occurring within a catchment. Indeed, the river channel from our 23 ha catchment to the 100 ha outlet is braided into a myriad of connected wetlands. Furthermore, these additions can come from the small-scale agriculture in this area of the catchment. Fertilizers (both inorganic and organic) are used to supplement the natural soil fertility. Such practises are done to increase crop yields. The use of specific tracers such as Ur or Zn, which are present in inorganic fertilisers could allow insights into this issue. The subsequent downstream decrease of nitrate levels may be a result of either an input of water to the river which has a lower nitrate concentration (dilution) or the consumption of nitrate within the river channel. Two sources of water contributing to runoff may play a role: (a) the deep groundwater (sampled from boreholes), and b) water sourced from the hillslopes of the catchment. The first two compartments are likely to have lower nitrate concentrations (Cirmo and McDonnell, 1997) and specifically nitrate concentrations (Grimaldi and Chaplot, 2000). In addition, chemical denitrification in deep groundwater can take place in the presence of iron species which are in contact with geological materials (Koelle *et al.*, 1985; Postma *et al.*, 1991). The decrease in nutrients between the 100 ha and 1000 ha catchments can be explained by the discontinuity in runoff resulting from the dams located the 2 monitored scales, which are utilised on the commercial farm. Any dissolved nutrients in the catchment flow will be impounded by these dams.

The behaviour of the particulate Carbon delivery ratios between the microplot and plot scales showed there being an increase in the amount of particulate Carbon. This is possibly, due to more advanced erosion processes, occurring at the plot scale. This is supported by the sediment delivery ratios between the different scales. The steady decrease in the delivery ratios the plot scale to the 100 ha catchment points to the depletion of particulate Carbon, due to deposition along the hillslope and stream channel or the decomposition of the bonded Carbon by micro-organisms. Low carbon delivery ratios from the plot scale to the 1000 ha catchment outlet, pointed to the decomposition of DOC and possibly POC. POC could as well be deposited within the catchment. Specific studies on organic carbon fluxes at catchment

level are to our knowledge very rare. These results are in concordance with those of Chaplot and Poesen (2012) on POC delivery ratios, which is one of the few papers on the scale issue for eroded organic carbon. Wang *et al.* (2010) in a study conducted in the Belgian Loess belt found that detached POC from the soil did not decompose, but rather was re-deposited within the catchment boundary or further transported downstream in catchment runoff. Such a conclusion was based on the stability of the isotopic signatures and ratios across different spatial scales of C^{13} and C^{12}. Wang *et al.* (2010) based these conclusions on there being no decomposition occurring within the catchment and also does not take into consideration the changes of the ^{13}C isotope, which may be increased by the inputs from the water erosion of organic matter, which can be composed of high $^{13}C/^{12}C$ ratios. Such conclusions seem quite speculative and not applicable for this study. In the case of this study, the decrease in the POC fluxes in conjunction, with the C^{13} ratios staying constant between the 23 ha and 100 ha catchment outlets as found by Juarez (2010), tends to show that decomposition of POC is significant within this catchment. This process, will increase the fluxes of DOC and NO_3^- between the 23 ha catchment and 100 ha catchment.

There needs to be further research and investigation into the behaviour of nutrients, such as DOC, POC and NO_3^- beyond the fate of the microplot, plot and catchment boundaries. Such an approach requires a better understanding of the catchment's geochemistry and microbiology.

4.4 Depletion of Soil stocks in Specific Nutrients Due to Water Erosion

A study on the soil stocks of carbon and other nutrients was conducted within the 23 ha catchment by Dlamini (2010). The study had two main objectives: (a) to evaluate the spatial variations of soil organic carbon and nutrient stocks, under an overgrazed grassland; and (b) to quantify the impact of some of the controlling factors on the soil nutrient stocks within the 23 ha catchment. In the context of this current study there was not a detailed assessment of the controlling factors of nutrient losses, nutrient transport and nutrient transformations within the catchment, as was the case for the soil nutrient stocks. Such an objective requires a complete understanding of the carbon and nitrogen cycles in relation to the hydrological processes and pathways in conjunction with the biological activity within the catchment at the various hydrologically important areas (hillslopes, channel and dams *i.e.* where the water samples were taken in the catchment). This objective was beyond the scope of the research. In the

study of Dlamini (2010), the topsoil (0-0.05 m) of the 23 ha grassland catchment was sampled at the nodes of a 20×20 m grid. The average stocks were found to be 12.2 t/ha for OC and 0.7 t/ha for soil organic nitrogen (ON) (Dlamini, 2010). With the use of these figures, the percentage loss of 0-0.05 m soil stocks by water erosion during the 2010-2011 rainy season, would be as much as 2.8% for OC when microplot OC losses are considered, 3.4% for plots and 1.1% for the 23 ha catchment outlet. With reference to ON, the percentage of the soil Nitrogen stock lost during the 2010-2011 rainy season was 3.7% for 1 m^2; 4% for 10 m^2; and 0.6% for the 23 ha catchment outlet.

The percentage of the soil organic nitrogen stocks lost at the different scales for this study are comparable to studies that have been conducted in other parts of the world. For example, Vanni *et al.* (2001) found that for a 50 hectare agricultural catchment in Ohio the total soil organic nitrogen stock lost in runoff had a 5-year average of 1.1%, compared to 0.6% for the 23 ha catchment. However, the amount of soil organic nitrogen stocks lost from this study and the study of Vanni *et al.* (2001) are lower than those found in a study conducted in the sugarcane growing areas of tropical Mauritius by Ng Kee Kwong *et al.* (2002). Ng Kee Kwong *et al.* (2002) found that the mean percentage of soil organic nitrogen stocks lost for a 70 hectare catchment was 12.3% over a 3 year period.

The amount of organic Carbon lost at the 1m^2 (2.8%) microplot and 10m^2 plot (3.4%) scales is in the same range of sediment soil organic carbon (SOC) (2.4%<Sediment SOC<6%) (Mchunu *et al.*, 2011) lost from 22.1 m^2 runoff plots in the small-scale agricultural areas of the Potshini Catchment, where maize is grown. The results of this study and Mchunu *et al.* (2011) are in the same range (0 - 3.5%) of the soil organic carbon losses determined by Quinton *et al.* (2006) in a study conducted in the United Kingdom. However, the percentage of organic carbon lost at the different scales are much lower (0.09%<OC<0.6%) (Quinton *et al.*, 2006) and not within the range of OC losses reported by Mchunu *et al.* (2011). For both the results obtained in this study and the results of Mchunu *et al.* (2011), they are considerably lower than the losses of OC from runoff plots of 35 m^2 installed on different land management techniques found by Bertol *et al.* (2007) in a study conducted in the Santa Catarina Highlands of southern Brazil. Bertol *et al*. (2007) found that the OC in sediments lost from the soil ranged between 100% and 117%, depending on the land management practice. The soils of the study area used by Bertol *et al.* (2007) are of a similar soil type (Acrisols) to those of the ones found in the Potshini catchment. It is therefore apparent that

the organic carbon losses occurring within the Potshini catchment are within the range of particulate carbon lost in different parts of the world.

The question of whether or not these losses are higher than the natural replenishment of the soil OC and ON needs to be addressed. Moreover, the fate of the eroded and transported soil organic carbon between the different spatial scales of observation, as well as the composition of the sediments exported from the 1000 ha catchment needs to be further investigated. In a preliminary study conducted in the 23 ha catchment of the Potshini Catchment by Juarez *et al.* (2011), it was found that sediments with an OC enrichment factor of 1.8% were prone to high mineralization rates and CO_2 emissions to the atmosphere.

4.5 Landscape Connectivity for Runoff, Organic Carbon and Nutrients

The end member mixing analyses conducted, were an initial attempt to evaluate the contribution of the different water sources at the various spatial and temporal scales within the catchment. There was a general increase from the 23 ha catchment to the 1000 ha catchment in the contributions of soil water and decreased contributions from overland flow. Moreover, peak flows tended to be mainly composed of OF and SW, whilst low flows had a groundwater source. This result was surprising as groundwater was expected to continue to contribute some water to runoff during rainfall events. During periods of low flow, soil water, which has moved deeper into the soil profile and reached the soil/bedrock interface is expected to continue contributing to runoff (Lorentz, 2012). The isotopic and tracer signals of groundwater sourced water may have been weak when compared to that of the water sourced from overland flow and soil water (Lorentz, 2012). The results from the study were consistent with what has been found elsewhere. For example, Brown *et al.* (1999) found that, for different events, OF contributed between 21 and 53% and soil water between 10 and 31 % to catchment runoff in a 24ha catchment located in New York State. In a 109ha catchment, overland flow contributed between 15 and 51% to catchment runoff, whilst soil water contributions were between 18 and 46%, with groundwater having contributed some water to catchment runoff (Brown *et al.*, 1999). Ribolzi *et al.* (2000) in a 91ha Mediterranean catchment of Southern France found that the contribution of OF ranged between 12 and 82% during rainfall events. Groundwater contributions to catchment runoff was, in this study, high when compared to these international studies. However, the fact that soil water and OF contributions were the highest during rainfall events was consistent with the previous studies.

Groundwater contributions increased with increasing catchment size has also been found by Hunt *et al.*, (2005), Tetzlaff *et al.*, (2007), Tetzlaff and Soulsby (2008).

4.6 Impact of Soil Moisture and Antecedent Rainfall on Landscape Connectivity

The results of this study showed a sudden increase in the fluxes of water and nutrients during a specific period of the rainy season (as noticed in Figure 3.7). In relation to this, the temporal variations of soil water tension at different depths and landscape positions are shown in Figure 4.5. When comparing Figures 3.7 and 4.5, some noticeable trends can be identified. The spatial variations of soil moisture could explain the temporal variations of the fluxes of water and nutrients within the catchment.

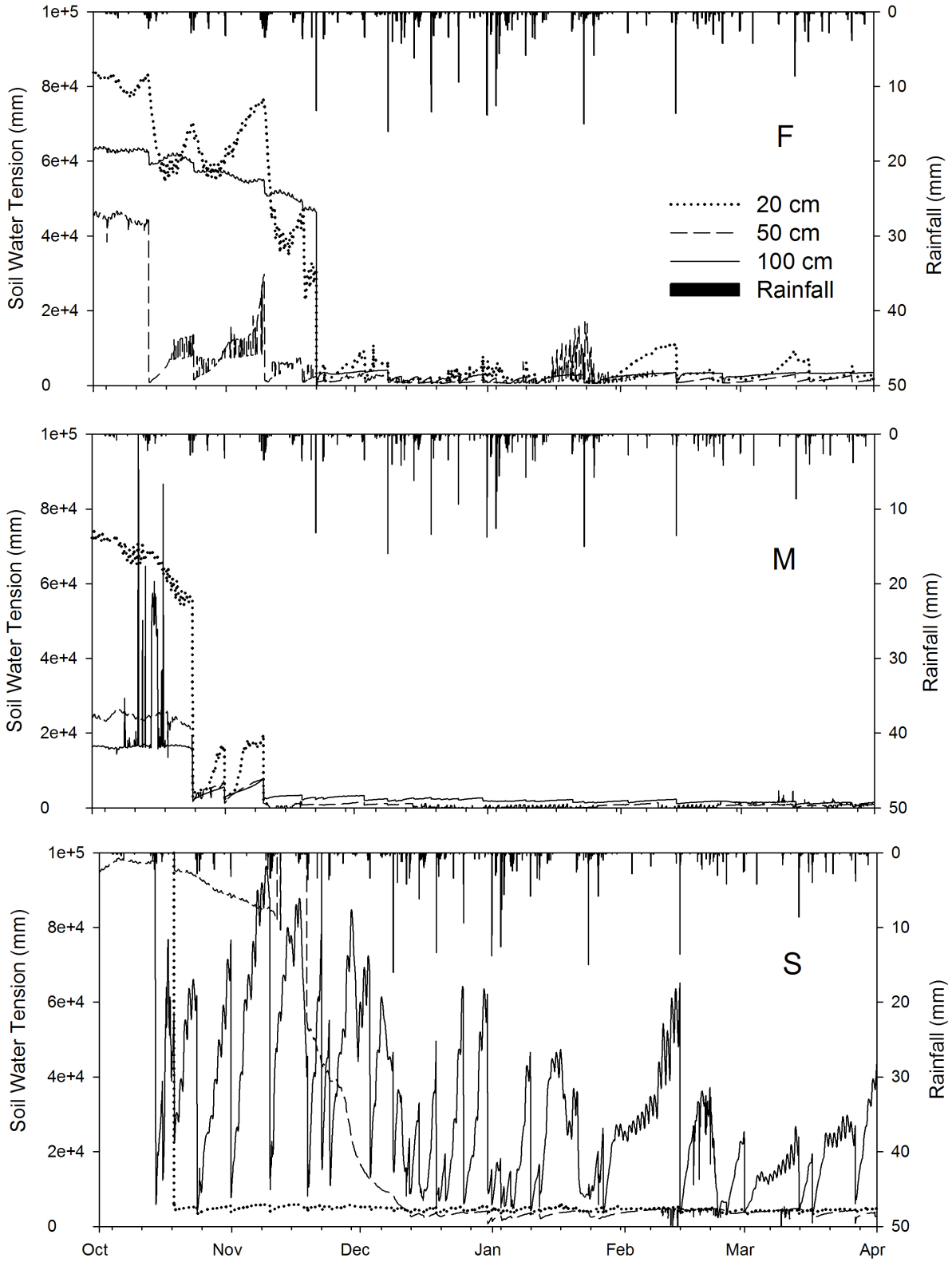

Figure 4.5 Temporal variations of soil water tension at different depths and landscape positions (2010-2011 rainy season). F for footslope, M for midslope and S for shoulder locations

The movement of water in the unsaturated zones of a catchment needs to be monitored to better understand the response of the catchment. To achieve this, the investigation of soil water tensions of different depths within the soil and at different landscape positions was conducted. When comparing the soil water tensions of the Footslope and Midslope locations to the cumulative flux of the different scales (Figure 4.5), the impact of the degree of catchment wetness on the catchment response to rainfall can be viewed. The cumulative volume curves generated at the $1m^2$ microplots, $10m^2$, and 100 ha catchment all showed a steep increase and change in the amount of water generated per unit area during the period of late November to December 2010 and late March 2011. This corresponded to the period in which the soil water tensions of all the monitored depths at the Footslope, Midslope and at the Shoulder were low. This was indicative of the soil having increased saturation by water. The 23 and 1000 ha catchment outlets showed cumulative volume curves indicative of consistent flow, but during some periods of the rainy season there were sudden and steep increases in the cumulative flux curves, which coincided with a period, in which there was consistent rainfall and decreased/lower soil water tensions. The amount of water generated at all the different nested scales increased during specific periods when the soils within the catchment increased in wetness. Thus, connectivity between the different nested scales was assumed to have occurred. Such a result highlights the important role that the wetness of the soils within a catchment have on the spatial and temporal variations of runoff generation.

In addition, these periods also occurred when the soil water tensions of the Footslope and Midslope positions were low, which was associated with increased soil water content (*e.g.* mid to late December 2010). The sudden changes in the behaviour and decrease of the soil water tension (*i.e.* when the soil went from being dry to being wet) corresponded to a certain amount of rainfall. This rainfall corresponded to the period since the start of the rainy season until the date at which the change in the soil water tension occurred. This can be viewed as a threshold amount of antecedent rainfall required to wet up the soil. The antecedent rainfall prior to the month of December 2010 was 226.2 mm. As the decrease in the soil water tensions corresponded to an increase in the water fluxes of the different scales, it is important to have an understanding of these thresholds to better understand and predict the behaviour of catchments with respect to periods of increased and rapid catchment runoff. The use of a simple method, such as a threshold amount of rainfall required to decrease the soil water tensions and increase the soil water content could prove to be valuable in predicting when there will be an increase in catchment runoff.

At the Footslope and Midslope positions a longer period of wetting up of the soil was observed. The Midslope position wetted up (and subsequently decreased soil water tensions) faster than that of the Footslope and Shoulder positions. This corresponded to the month of November. However, the Footslope location showed a delayed response (in comparison to the Midslope location), with the soil water tensions at 0.2 m and 1 m suddenly decreasing at the end of November. Thereafter, the soil water tensions for all depths for both these locations stayed low, with there being some increases during periods of little to no rainfall. However, when rainfall occurred, all 3 depths at both locations responded instantaneously. At the Footslope and Midslope, the soil profile for both locations stayed relatively constant and low in terms of soil water tension for the duration of the rainy season. The Shoulder of the hillslope showed, initially, that the soil at a depth of 0.2 m required less antecedent rainfall than the corresponding depths at the Midslope and Footslope positions for the soil water tensions to decrease. There was a great deal of variation in the soil water tension at the Shoulder location, with the soil at a depth of 100 cm showing a trend of responding rapidly (decrease in the monitored soil water tension) to rainfall and then subsequently drying rapidly (increase in the monitored soil water tension) when there was no rainfall.

5. CONCLUSION

In this study, the two main objectives were to:

a) To investigate the spatial and temporal variations of overland flow (OF) and its factors of control at the hillslope level; and
b) To evaluate runoff, organic carbon and nutrient fluxes at different scales.

There were two main findings on the spatial and temporal variations of OF. The first one was that OF had a high degree of spatial variation, with the fastest OF generation and highest amounts produced in areas that were either highly degraded or were saturated. Plots tended to produce more overland flow than microplots. The second main result was that OF was found to be either saturation excess overland flow in the bottomlands or Hortonian overland flow on the rest of the hillslope. In the bottomland, OF initiation and amounts were controlled by soil wetness in relation to soil saturation, while on the hillslope, OF variations were most affected by soil surface characteristics (mostly soil crusting and soil surface coverage) and soil clay content.

The main results on runoff, organic carbon and nutrient fluxes at the different scales are summarized in Figure 5.1, a schematic representation of the fluxes interpreted from field observations and tracer observations. The study landscape appeared to be constituted of three distinct compartments, each with a specific behaviour:

a) The study hillslope;
b) First order stream; and
c) Dam-impacted stream.

The hillslope experienced high water, SOC and nutrient fluxes, with most of the water infiltrating and replenishing the soil and groundwater stores. Sediments and SOC fluxes were the highest at the plot scale. Yields increased from the microplot to the plot scale. These yields increased, as interrill erosion mechanisms become more efficient. The loads decreased further to the 23 ha catchment outlet, as OF infiltration and sedimentation at footslopes occurred. Most of the water and nutrients exported from the hillslope have a shallow water table origin.

At the 23 ha catchment outlet, there was a steady decrease in the runoff and dissolved nutrient loads, whilst there was a sharp decrease for sediment and particulate nutrient fluxes. However, there was an increase in the fluxes of both DOC and NO_3^- that could be explained by the increased decomposition of the deposited organic matter. Such a process ultimately leads to the release and increase of DOC and dissolved species of N to the stream as well as increased emissions of CO_2 to the atmosphere. Temporally, water, sediment and nutrient fluxes at both the 23 ha catchment and 100 ha catchment outlets increased, as the soils of the catchment increased in saturation by water. There appeared to be an interaction, between both scales, with deep groundwater with some soil water and overland flow contributing to catchment runoff during events at both scales.

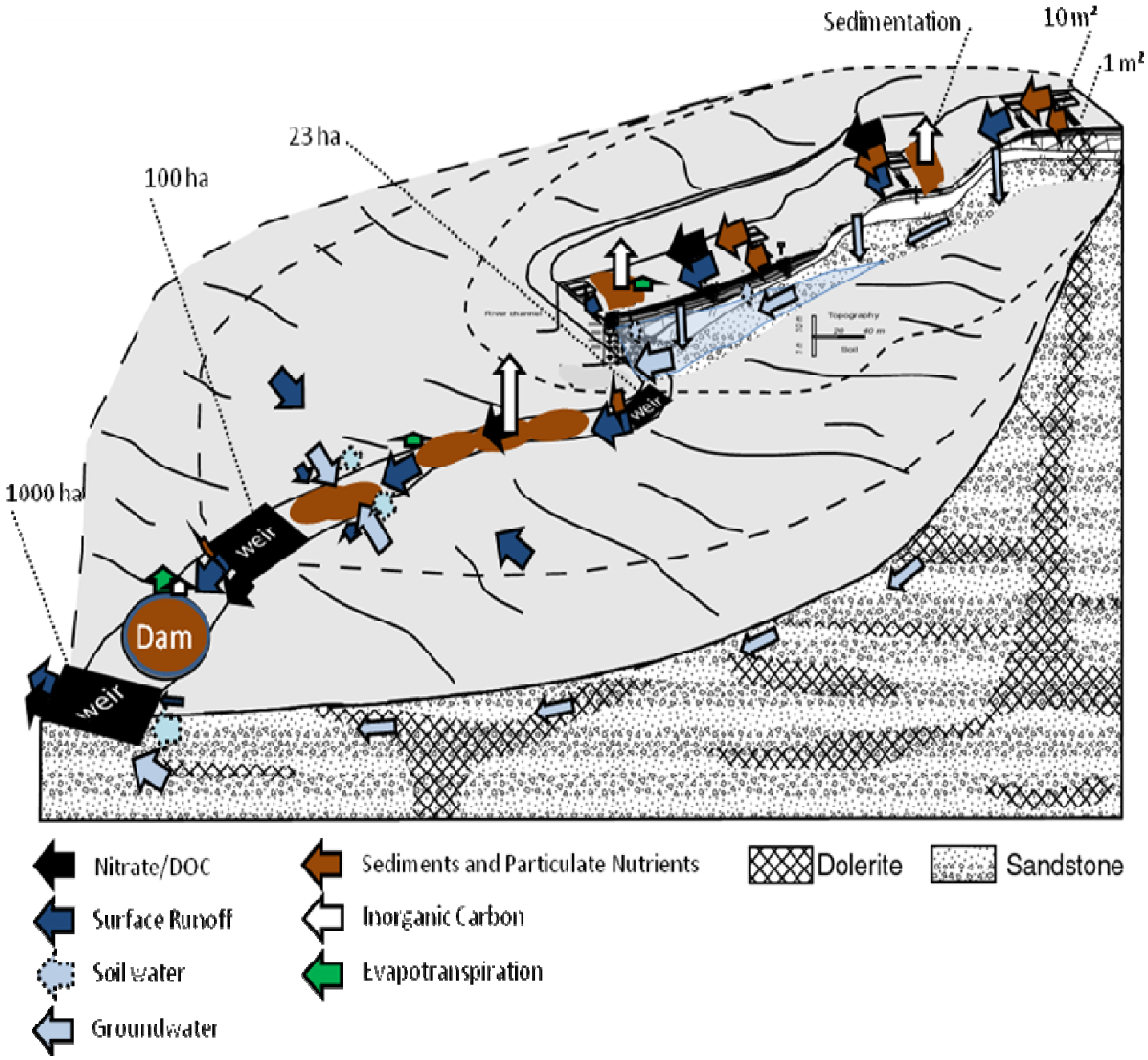

Figure 5.1 Schematic representation of the water, sediment, organic/inorganic carbon and nutrient fluxes at the catchment level and interpreted from fluxes and tracers evaluation

5.2 Future Perspectives

There was a sharp decrease in runoff, nutrients and sediment fluxes at the dam-impacted stream and the resulting exports from the 1000 ha catchment outlet were found to be considerably low for sediments, particulate nutrients and nitrate. This was accompanied by a

slight decrease in DOC, which probably reflects biochemical reactions within the dams. These biochemical reactions within the dams require further research. The decrease in water fluxes in this compartment is probably caused by dam extractions (for irrigation) and direct evaporation as evidenced by the evaporated isotopic signature of water sourced from the dams. In comparison, the catchment water outflows from the 1000 ha catchment outlet had a groundwater signature (data not presented).

Further understanding of the processes leading to changes of nutrient and carbon fluxes need to be performed in order to link this study with the overall ecosystem functioning of a landscape. Such a study requires more field observations and ultimately more data. A focus on the fate of the nutrients beyond the observed scales is required as well as larger scale observations. Such an approach can be used to extrapolate the results from this study to larger areas. The results of this study highlighted the decrease in particulate nutrient yields between the 23 ha catchment and 100 ha catchment outlets, whilst the yields of certain dissolved nutrients increased. If these particulate nutrients, especially particulate organic Carbon, are mineralized, then there would be implications for increased CO_2 emissions. With increased land degradation throughout the world, increased CO_2 emissions due to accelerated erosion of soils, which are enriched in Carbon, will have large implications for climatic change.

6. REFERENCES

Aitkenhead, JA, Hope, D and Billett, MF. 1999. The relationship between dissolved organic carbon in stream water and soil organic carbon pools at different spatial scales. *Hydrological Processes* 13:1289-1302.

Auzet, AV, Poesen, J and Valentin, C. 2004. Soil surface characteristics: dynamics and impacts on soil erosion. Editorial. *Earth Surface Processes and Landforms* 29:1063–1064.

Bartley, R, Roth, CH, Ludwig, J, McJannet, D, Liedloff, A, Corfield, J, Hawdon, A. and Abbot, B. 2006. Runoff and erosion from Australia's tropical semi-arid rangelands: influence of ground cover for differing space and time scales. *Hydrological Processes* 20:3317–3333.

Bautista, S, Mayor, AG, Bourakhouadar, J and Bellot, J. 2007. Plant Spatial Pattern Predicts Hillslope Runoff and Erosion in a Semiarid Mediterranean Landscape. *Ecosystems* 10:987-998.

Ben-Hur, M, Shainberg, I, Keren, R and Gal, M. 1985. Effect of water quality and drying on soil crust properties. *Soil Science Society of America Journal* 49:191-196.

Bergkamp, G. 1998. A hierarchical view of the interactions of runoff and infiltration with vegetation and microtopography in semiarid shrublands. *CATENA* 33(3-4):201-220.

Bertol, I, Engel, FL, Mafra, AL, Bertol, OJ and Ritter, SR. 2007. Phosphorus, potassium and organic carbon concentrations in runoff water and sediments under different soil tillage systems during soybean growth. *Soil and Tillage Research* 94:142-150.

Beven, K, Heathwaite, L, Heathwaite, L, Haygarth, P, Wailing, D, Braizer, R, Withers, P. 2005. On the concept of delivery of sediment and nutrients to stream channels. *Hydrological Processes* 19:551–556.

Bloschl, G and Sivapalan, M, 1995. Scale issues in hydrological modeling: A review. *Hydrological Processes* 9:251-290.

Bracken, LJ and Croke, J. 2007. The concept of hydrological connectivity and its contribution to understanding runoff-dominated geomorphic systems. *Hydrological Processes* 21:1749-1763.

Brown, VA, McDonnell, JJ, Burns, DA and Kendall, C. 1999. The role of event water, a rapid shallow flow component, and catchment size in summer stormflow. *Journal of Hydrology* 217:171-190.

Cammeraat, ELH. 2004. Scale dependent thresholds in hydrological and erosion response of a semi-arid catchment in southeast Spain. *Agriculture, Ecosystems & Environment* 104:317-332.

Casenave, A and Valentin, C. 1992. A runoff capability classification system based on surface features criteria in semi-arid areas of West Africa. *Journal of Hydrology* 130(1992):231-249.

Cerdan, O, Le Bissonnais, Y, Govers, G, Lecomte, V, van Oost, K, Couturier, A, King, A and Dubreuil N. 2004. Scale effect on runoff from experimental plots to catchments in agricultural areas in Normandy. *Journal of Hydrology* 299:4-14.

Chaplot, V, Khampaseuth, X, Valentin, C and Le Bisonnais, Y. 2007. Sheet erosion in the sloping lands of northern Laos submitted to shifting cultivation. *Earth Surface Processes and Landforms* 32:415–428.

Chaplot, V, Brown, J, Dlamini, P, Eustice, T, Janeau, J-L, Jewitt, G, Lorentz S, Martin, L, Mchunu, C, Oakes, E, Podwojewski, P, Revil, S, Rumpel C and Zondi, N. 2010. Rainfall simulation to identify the storm-scale mechanisms of gully bank retreat. *Agriculture Water Management* 98:1704-1710.

Chaplot, V and Poesen, J. 2012. Sediment, soil organic carbon and runoff delivery at various spatial scales. *Catena* 88(2012):46-56.

Cirmo, CP and McDonnell, JJ. 1997. Linking the hydrologic and biogeochemical controls of nitrogen transport in near-stream zones of temperate-forested catchments: a review. *Journal of Hydrology* 199:88-120.

Descheemaeker, K, Nyssen, J, Poesen, J, Raes, D, Haile, M, Muys, B and Deckers, S. 2006. Runoff on slopes with restoring vegetation: A case study from the Tigray highlands, Ethiopia. *Journal of Hydrology* 331:219-241.

Detty, JM and McGuire, KJ. 2010. Topographic controls on shallow groundwater dynamics: implications of hydrologic connectivity between hillslopes and riparian zones in a till mantled catchment. *Hydrological Processes* 24: 2222-2236.

Devaurs, M and Gifford, GF. 1984. Variability of Infiltration within Large Runoff Plots on Rangelands. *Journal of Range Management* 37:523-528.

De Vente, J, Poesen, J, Arabkhedri, M and Verstraeten, G. 2007. The sediment delivery problem revisited. *Progress in Physical Geography* 31:155–178.

Dexter, AR, 1988. Advances in characterization of soil structure. *Soil Tillage Research* 11:199–238.

Dexter, AR and Richard, G. 2009. The saturated hydraulic conductivity of soils with n-modal pore size distributions. *Geoderma* 154:76-85.

Dlamini, PE. 2010. An assessment of soil organic carbon and nutrient stocks in the Potshini catchment, KwaZulu-Natal, South Africa. Unpublished MSc Dissertation, School of Bioresources Engineering and Environmental Hydrology, University of KwaZulu-Natal, Pietermaritzburg, RSA.

Dlamini, P, Orchard, C, Jewitt, G, Lorentz, S, Titshall, L and Chaplot, V. 2011. Controlling factors of sheet erosion under degraded grasslands in the sloping lands of KwaZulu-Natal, South Africa. *Agricultural Water Management* 98(11):1711-1718.

ESRI, 2004. *Understanding GIS*: *The ArcView GIS 3.2*. ESRI, 380 New York Street, Redlands, CA, USA.

Fujimoto, M, Ohte, N and Tani, M. 2011. Effects of hillslope topography on runoff response in a small catchment in the Fudoji Experimental Watershed, central Japan. *Hydrological Processes* (2011):1-13.

Grimaldi, C and Chaplot, V. 2000. Nitrate depletion during within-stream transport: Effects of exchange processes between the streamwater, the hyporheic and riparian zones. *Water, Air, and Soil Pollution* 124: 95-112.

Heathwaite, AL and Johnes, PJ. 1996. Contribution of Nitrogen Species and Phosphorus Fractions to Stream Water Quality in Agricultural Catchments. *Hydrological Processes* 10: 971-983.

Hernandez, T, Nachabe, M, Ross, M and Obeysekera, J. 2003. Modelling runoff from variable source areas in humid, shallow water table environments. *Journal of American Water Resources Association* 39:75-85.

Hewlett JD and Hibbert AR 1967. Factors affecting the response of small catchment to precipitation in humid areas. In *Forest Hydrology*, Supper WE (ed). Pergamon: New York; 275–290.

Hooper, RP and Shoemaker, CA. 1986. A comparison of Chemical and Isotopic Hydrograph Separation. *Water Resources Research* 22 9(10): 1444-1454.

Hopp, L and McDonnell, JJ. 2009. Connectivity at the hillslope scale: Identifying interactions between storm size, bedrock permeability, slope angle and soil depth. *Journal of Hydrology* 376(2009):378-391.

Horton RE. 1933. The role of infiltration in the hydrologic cycle. *Transactions of American Geophysical Union* 14: 446–460.

Hunt, RJ, Coplen TB, Haas, NL, Saad, DA and Borchardt, M.A. 2005. Investigating surface water–well interaction using stable isotope ratios of water. *Journal of Hydrology* 302:154-172.

Huth, AK, Leydecker, A, Sickman, JO and Bales, RC. 2004. A two-component hydrograph separation for three high-elevation catchments in the Sierra Nevada, California. *Hydrological Processes* 18:1721-1733.

ISSS Working Group RB, 1998. World Reference Base for Soil Resources. In: Deckers, JA, Nachtergaele, FO and Spargaren, OC. (Eds.) *Introduction 1st edition*. ISSS.ISRC. FAO. Acco Leuven, Belgium.

Iwagami, S, Tsujimura, M, Onda, Y, Shimada, J and Tanaka, T. 2010. Role of bedrock groundwater in the rainfall–runoff process in a small headwater catchment underlain by volcanic rock. *Hydrological Processes* 24 (2010):2771-2783.

James, AL and Roulet, NT. 2009. Antecedent moisture conditions and catchment morphology as controls on spatial patterns of runoff generation in small forest catchments. *Journal of Hydrology* 377(2009):351-366.

Jencso, KG, McGlynn, BL, Gooseff, MN, Wondzell, SM., Bencala, KE and Marshall, LA. 2009. Hydrologic connectivity between landscapes and streams: Transferring reach- and plot-scale understanding to the catchment scale. *Water Resources Research* 45:pp16.

Jordán, A, Martínez-Zavala, L and Bellinfante, N. 2008. Heterogeneity in soil hydrological response from different land cover types in southern Spain. *CATENA* 74:137-143.

Joel, A, Messing, I, Seguel, O and Casanova, M. 2002. Measurement of surface water runoff from plots of two different sizes. *Hydrological Processes* 16:1467-1478.

Juarez, S. 2010. Carbon mineralization and lignin content of eroded sediments within a small-scale agricultural watershed of South-Africa. Unpublished MSc Dissertation, Department of Agronomy, AgroParisTech, Cedex, France.

Juarez, S, Rumpel, C, Mchunu, C and Chaplot, V. 2011. Carbon mineralization and lignin content of eroded sediments from a grazed watershed of South-Africa. *Geoderma* 167-168:247-253.

Koelle, W, Strebel, O and Boettcher, J.1985. Formation of sulfate by microbial denitrification in a reducing aquifer. *Water Supply* 3-26-35.

King, G.M., 2002. An explanation of the 1:500 000 general hydrogeological map, Dept. of Water Affairs and Forestry, Pretoria, Republic of South Africa.

Latron, J and Gallart, F. 2008. Runoff generation processes in a small Mediterranean research catchment (Vallcebre, Eastern Pyrenees). *Journal of Hydrology* 358(2008):206-220.

Li, XJ, Li, XR, Song, WM, Gao, YP, Zheng, JG and Jia, RL. 2008. Effects of crust and shrub patches on runoff, sedimentation, and related nutrient (C, N) redistribution in the desertified steppe zone of the Tengger Desert, Northern China. *Geomorphology* 96(2008):221-232.

Lorentz, S.A. 2012. Personal Communication, School of Bioresources Engineering and Environmental Hydrology, Pietermaritzburg, South Africa, 27 February 2012.

Los Gatos Research. 2007. DLT-100 Liquid-Water Isotope Analyzer Automated Injection: Manual Rev 07-C.

McBratney, AB and Webster, R. 1983. How many observations are needed for regional estimation of soil properties? *Soil Science* 135:177–183.

McGlynn. BL, McDonnell, JJ and Brammer, DD. 2002. A review of the evolving perceptual model of hillslope flowpaths at the Maimai catchments, New Zealand. *Journal of Hydrology* 257 (2002):1-26.

McGlynn, BL, McDonnell, JJ, Seibert, J and Kendall, C. 2003. Scale effects on headwater catchment runoff timing, flow sources and groundwater-streamflow relations. *Water Resources Research* 40:40 pp.

McGlynn, BL, and McDonnell, JJ. 2003a. Role of discrete landscape units in controlling catchment dissolved organic carbon dynamics. *Water Resources Research* 39(4):18 pp.

McGlynn, BL and McDonnell, JJ. 2003b. Quantifying the relative contributions of riparian and hillslope zones to catchment runoff. *Water Resources Research* 39(11):20 pp.

McGuire, KJ and McDonnell, JJ. 2010. Hydrological connectivity of hillslopes and streams: Characteristic time scales and nonlinearities. *Water Resources Research* 46:17 pp.

Mchunu, C, Lorentz, S, Jewitt, G, Manson, A and Chaplot, V. 2011. No-Till Impact on Soil and Soil Organic Carbon Erosion under Crop Residue Scarcity in Africa. *Soil Science Society of America Journal* 75(4):1502-1511.

McNamara, JP, Chandler, D, Seyfried, M, and Achet, S. 2005. Soil moisture states, lateral flow, and streamflow generation in a semi-arid, snowmelt-driven catchment. *Hydrological Processes* 19 (2005):4023-4038.

Mekki, I, Albergel, J, Ben Mechlia, N and Voltz, M. 2006. Assessment of overland flow variation and blue water production in a farmed semi-arid water harvesting catchment. *Physics and Chemistry of the Earth* 31(2006):1048–1061.

Meyles, E, Williams, A, Ternan, L and Dowd, J. 2003. Runoff generation in relation to soil moisture patterns in a small Dartmoor catchment, Southwest England. *Hydrological Processes* 17:251-264.

Meyles, EW, Williams, AG, Ternan, JL, Anderson, JM and Dowd, JF. 2006. The influence of grazing on vegetation, soil properties and stream discharge in a small Dartmoor catchment, Southwest England, UK. *Earth Surface Processes and Landforms* 31:622-631.

Miyata, S, Kosugi, K, Nishi, Y, Gomi, T, Sidle, RC and Mizuyama, T. 2010. Spatial pattern of infiltration rate and its effect on hydrological processes in a small headwater catchment. *Hydrological Processes* 24:535-549.

Murphy, SR, Lodge, GM and Harden, S. 2004. Surface soil water dynamics in pastures in northern New South Wales. 2. Surface runoff. *Australian Journal of Experimental Agriculture* 44:283-298.

Ng Kee Kwong, KF, Bholah, A, Volcy. L and Pynee, K. 2002. Nitrogen and phosphorus transport by surface runoff from a silty clay loam soil under sugarcane in the humid tropical environment of Mauritius. *Agriculture, Ecosystems and Environment* 91:147-157.

Oakes, EGM. 2012. Erosion Dynamics at the Catchment Level: Spatial and Temporal Variations of Sediment Mobilization, Storage and Delivery. Unpublished MSc Dissertation, School of Bioresources Engineering and Environmental Hydrology, University of KwaZulu-Natal, Pietermaritzburg, RSA.

Ocampo, CJ, Sivapalan, M and Oldham, C. 2006. Hydrological connectivity of upland-riparian zones in agricultural catchments: Implications for runoff generation and nitrate transport. *Journal of Hydrology* 331: 643-658.

Parsons, AJ,Wainwright, J, Brazier, RE and Powell,DM. 2006. Is sediment delivery a fallacy? *Earth Surface Processes and Landforms* 31:1325–1328.

Podwojewski, P, Janeau, J-L, Grellier, S, Valentin, C, Lorentz, S and Chaplot, V. 2011. Influence of grass soil cover on water runoff and soil detachment under rainfall simulation in a sub-humid South African degraded rangeland. *Earth Surface Processes and Landforms* 36:911-922.

Postma, D, Boesen, C, Kristiansen, H and Larsen, F. 1991. Nitrate reduction in an unconfined sandy aquifer: water chemistry, reduction processes, and geochemical modeling. *Water Resources Research* 27(8):2027.

Quinton, JN, Catt, JA, Wood, GA and Steer, J. 2006. Soil carbon losses by water erosion: Experimentation and modeling at field and national scales in the UK. *Agriculture, Ecosystems and Environment* 112:87-102.

Ribolzi, O, Andrieux, P, Valles, V, Bouzigues, R, Bariac, T and Voltz, M. 2000. Contribution of groundwater and overland flows to storm flow generation in a cultivated Mediterranean catchment. Quantification by natural chemical tracing. *Journal of Hydrology* 233:241-257.

Rommens, T, Verstraeten, G, Poesen, J, Govers, G, Van Rompaey, A and Peters, I. 2005. Soil erosion and sediment deposition in the Belgian loess belt during the Holocene: establishing a sediment budget for a small agricultural catchment. *The Holocene* 15: 1032–1043.

Sanjari, G, Yu, B, Ghadiri, H, Cielsiolka, CAA and Rose, CW. 2009. Effects of time controlled grazing on runoff and sediment loss. *Australian Journal of Soil Research* 47:796-808.

Sen, S, Srivastava, P, Dane, JH, Yoo, KH and Shaw, JN. 2010. Spatial - temporal variability and hydrologic connectivity of runoff generation areas in a North Alabama pasture - implications for phosphorus transport. *Hydrological Processes* 24(2010):342–356.

Schulze, R.E., 1997. South African Atlas of Agrohydrology and Climatology. TT82/96. Water Research Commission, Pretoria, RSA.

Shock, C, Barnum, JM, Seddigh, M. 1998. Calibration of Watermark soil moisture sensors for irrigation management, pp.139-146, Proceedings of the International Irrigation Show, San Diego, CA. Irrigation Association.

Sidle, RC, Tsuboyama, Y, Noguchi, S, Hosoda, I, Fujieda, M and Shimizu, T. 1995. Seasonal hydrologic response at various spatial scales in a small forested catchment, Hitachi Ohta, Japan. *Journal of Hydrology* 168(1995):227-250.

Soil Classification Working Group, 1991. Soil Classification. A Taxonomic System for South Africa. Department of Agricultural Development, Pretoria, South Africa.

Starr, GC, Lal, R, Kimble, JM and Owens, L. 2001. Assessing the impact of erosion on soil organic carbon pools and fluxes. In: Lal, R, et al. (Ed.), Assessment Methods for Soil Carbon. CRC Press, Boca Raton, pp. 417–426. Florida.

Tetzlaff, D, Waldron. S, Brewer, MJ and Soulsby, C. 2007. Assessing nested hydrological and hydrochemical behaviour of a mesoscale catchment using continuous tracer data. *Journal of Hydrology* 336:430-443.

Tetzlaff, D and Soulsby, C. Sources of baseflow in larger catchments – Using tracers to develop a holistic understanding of runoff generation. *Journal of Hydrology* 359:287-302.

Trimble, SW. 1983. A sediment budget for Coon Creek basin in the Driftless Area. *American Journal of Science* 283:1853–1977.

Uhlenbrook, S and Hoeg, S. 2003. Quantifying uncertainties in tracer-based hydrograph separations: a case study for two-, three- and five-component hydrograph separations in a mountainous catchment. *Hydrological Processes* 17:431-453.

Vanni, M.J, Renwich, WH, Headworth, JL, Auch, JD and Schaus, M.H. 2001. Dissolved and particulate nutrient flux from three adjacent agricultural watersheds: A five-year study. *Biogeochemistry* 54:85-114.

Van Es, HM, Cassel, DK and Daniels, RB. 1991. Infiltration Variability and Correlations with Surface Soil Properties for an Eroded Hapludult. *Soil Society of America Journal* 55:1346-1263.

van de Giesen, N, Stomph, TJ and de Ridder, N. 2005. Surface runoff scale effects in West African watersheds: modeling and management options. *Agricultural Water Management* 72:109-130.

van de Giesen, N, Stomph, T-J, Ajayi, AE and Bagayoko, F. 2011. Scale effects in Hortonian surface runoff on agricultural slopes in West Africa: Theory, models, and field data. *Agriculture, Ecosystems and Environment* 142(2011):1214-1220.

Wakindiki, IIC and Ben-Hur, M. 2002. Soil Mineralogy and Texture Effects on Crust Micromorphology, Infiltration, and Erosion. *Soil Society of America Journal* 66:897-905.

Vigiak, O., Ribolzi, O., Pierret, A., Sengtaheuanghoung, O., Valentin, C., 2008. Trapping efficiencies of cultivated and natural riparian vegetation of northern Laos. *Journal of Environmental Quality* 37:889–897.

Walling, DE, Collins, AL, Jones, PA, Leeks, GJL and Old, G. 2006. Establishing fine-grained sediment budgets for the Pang and Lambourn LOCAR catchments, UK. *Journal of Hydrology* 330:126–141.

Wang, Z, Govers, G, Steegen, A, Clymans, W, Van den Putte, A, Langhans, C, Merckx, R, and Van Oost, K. 2010. Catchment-scale carbon redistribution and delivery by water erosion in an intensively cultivated area. *Geomorphology* 124:65-74.

Wenninger, J, Uhlenbrook, S, Lorentz, S, and Leibundgut, C. 2008. Identification of runoff generation processes using combined hydrometric, tracer and geophysical methods in a headwater catchment in South Africa. *Hydrological Sciences Journal* 53(1):16 pp.

Williams, JR, Allmaras, RR, Renard, KG, Lyles, L, Moldenhauer, WC, Langdale, GW, Meyer, LD, Rawls, WJ, Darby, G, Daniels, R and Magleby, R. 1981. Soil erosion effects on productivity: A research perspective. *Soil Water Conservation* 36:82-90.

Williams, J and Bonell, M. 1988. The influence of scale of measurement on the spatial and temporal variability of the Philip infiltration parameters - an experimental study in an Australian savannah woodland. *Journal of Hydrology* 104:33-51.

Zehe, E and Bloschl, G, 2004. Predictability of hydrologic response at the plot and catchment scales: Role of initial conditions. *Water Resources Research* 40(W10202):1-21.